The Role of Apc in Medulloblastoma

Dennis McCaffery

Submitted for Degree of Doctor of Philosophy

University of Edinburgh

September 2007

Declaration

I declare that the work presented in this thesis is my own, except where otherwise stated. All experiments were designed by myself, or in collaboration with my supervisors Dr. John O. Mason and Professor Ian Whittle.

Dennis McCaffery, September 2007

Acknowledgements

Firstly I would like to thank my supervisors Dr. John Mason and Professor Ian Whittle who have guided me through this thesis. To John in particular for his advice, support and endless patience and encouragement.

Thanks to all the members of the Mason, Price, Kind and Spears labs for their help and advice. Particular thanks go to Vassiliki, Mike, Tom, Ben F, Dave T, Catherine, Mark B and Ian who have answered seemingly thousands of my dumb questions throughout the years. Thanks to my statistician Dave Thomas who is as good with numbers as I am bad. Thanks also must go to Duncan and John in the animal house for looking after my mice so well when everyone else's seemed to be going missing.

Thanks to all my good friends in the lab namely Mike, Natasha, Chris and Mark for allowing me to distract them with my bad chat and requests for coffee breaks.

To all the guys outside of work, namely Rob, Jason, Euan, Rad, Steve, Andy, Rob L, Al, Pete, James, for all the bad taste jokes, beer and general nonsense.

A huge thanks also goes to my parents Dennis and Jessie and my brothers Kevin, Brian, Magnus, and sisters, Margaret and Fiona for all their love and support.

And a special great big thank you to Simona who has helped me in every possible way over the past 3 years. I couldn't have done it without Yu.

Table of Contents

List of Abbreviations

AdCre	Adenovirus-cre mouse
AdCre	Adenovirus-cre mouse
AER	Apical Ectodermal Ridge
ALV-A	Avian Leukosis-A Virus
ANB	Anterior Neural Plate
APC	Adenomatous Polyposis Coli
ATRT	Atypical Teratoid/Rhabdoid Tumour
BCC	Basal Cell Carcinomas
BCNS	Basal Cell Nevus Syndrome
bFGF	basic Fibroblast Growth Factor
bHLH	Basic Helix Loop Helix
BrdU	5-bromo-2'deoxyuridine
CB	Cerebellum
Cer	Cerberus
CNS	Central Nervous System
CP	Choroid Plexus
CSF	Cerebrospinal Fluid
DAB	3,3'-diaminobenzidine
Dhh	Desert Hedgehog
Dkk	Dickkopf
dlg	Drosophila discs large
DMEM	Dulbecco/Vogt Modified Eagle's minimal essential Medium
DNA	Deoxyribonucleic Acid
dNTP	deoxynucleoside triphosphate

Dsh	Dishevelled
EB1	End-binding protein 1
ECM	extracellular matrix
EDTA	disodium ethylenediamine tetraacetate
EGF	Epidermal growth factor
EGL	External Germinal Layer of the cerebellum
En1	Engrailed 1
EtBr	Ethidium bromide
FAP	Familial Adenomatous Polyposis
FCS	Foetal Calf Serum
FG	First Generation
Fgf	Fibroblast growth factor
FISH	Fluorescent in situ hybridisation
Fmi	Flamingo
Frz	Frizzled
Fzd	Frizzled
GABA	γ-aminobutyric acid
GBP	GSK3b binding protein
GCP	Granule Cell Precursor
GFP	Green Fluorescent Protein
GLI	Glioma Associated oncogene homologue
GSK3b	Glycogen Synthase Kinase 3b
HCC	Hepatocellular Carcinoma
HCl	Hydrochloric Acid
HCMV	Human cytomegalovirus

HDLG	Human discs large
Hh	Hedgehog
hMCS	human mesenchymal stem cell
HRP	Horseradish Peroxidase
IddU	Iododeoxyuridine
IE	Immediate Early
IGF-1	Insulin-like growth factor-1
IGL	Internal Granule Layer
Ihh	Indian Hedgehog
IL-8	Interleukin-8
IO	Isthmus Organiser
JNK	c-Jun N-terminal Kinase
Kny	Knypek
LB	Luria broth
LDL	Low-density lipoprotein
LDLR	Low-Density Lipoprotein Receptor
LEF	Lymphoid Enhancer Factor
LEF	Lymphoid enhancer factor
LOH	loss of heterozygosity
LoxP	locus of crossover P1
LRP	Low-density lipoprotein-receptor related protein
LTR	Long Terminal Repeat
LV	Lateral Ventricle
MB	Medulloblastoma
MCMV	Murine cytomegalovirus

MCV	Mesencephalic Vesicle
MHJ	Mid-hindbrain Junction
MHO	Mid-Hindbrain Organiser
Min	multiple intestinal neoplasia
MMTV	Mouse Mammary Tumour Virus
NES	nuclear-export signal
NLS	nuclear-localisation signal
Ntv-a	Nestin tv-a mouse strain
O/N	Overnight
Otx	Orthodenticle homeobox gene
Pax	Paired box gene
PBS	Phosphate Buffered Saline
PCR	Polymerase Chain Reaction
PFA	Paraformaldihyde
PKC	Protein Kinase C
PLC	Phospholipase C
PLGF	Placenta-Like Growth Factor
PNET	Primitive Neuroectodermal Tumour
PNS	Peripheral Nervous System
PP2A	Protein Phosphatase 2A
PTC	Patched
R26R	ROSA-26 reporter mouse
RCAS	Replication competent ASLV long terminal repeat with splice acceptor
RSV-A	Rous sarcoma virus-A
RT	Room Temperature

RT-PCR	Reverse Transcription Polymerase Chain Reaction
SDS	sodium dodecyl sulphate
sFRP	Secreted Frizzled Related Protein
Shh	Sonic Hedgehog
SMOH	Smoothened
SS	Salmon Sperm
SSC	standard saline citrate
Stbm	Strabismus
SUFU	Suppressor of Fused
TBE	Tris-borate EDTA
TCF	T-Cell Factor
TE	tris EDTA
TGF-b	transforming growth factor-b
TTLB	Tail Tip Lysis Buffer
TUNEL	Terminal Deoxynucleotidyltransferase-Mediated dUTP Nick End Labeling
TVA	receptor for ALV-A
VEGF	Vascular Endothelial Growth Factor
wg	wingless
WT	wild-type

List of Figures

Abstract

Medulloblastomas represent the most frequent malignant brain tumour in children, and are thought to develop in the posterior fossa of the cerebellum. Some patients with medulloblastomas have a deficiency in the tumour suppressor gene *Apc* (Turcot's syndrome). Although the majority of medulloblastomas arise sporadically, people with *Apc* mutations are 92 times more likely to develop medulloblastomas. *Apc* encodes a very large protein known to function as a regulator of the Wnt signalling pathway. Activation of the canonical Wnt pathway leads to the stabilisation of β-catenin. In response to Wnt signals, β-catenin translocates to the nucleus where it interacts with the LEF/TCF family of transcription factors to activate transcription of target genes such as *c-myc* and *cyclinD1*. Mutations of *Apc* that cause an increase in β-catenin are found to be tumourgenic, whereas other mutations are not. Therefore it is thought that the main tumour suppression function of Apc is in its ability to destabilise and hence reduce cytoplasmic β-catenin.

The central hypothesis of this thesis is that the loss of *Apc* can lead to the development of medulloblastoma. Work from other groups has reported activation of Wnt signalling in a proportion of primary medulloblastomas. We undertook a study to assess this by using the cre-loxP recombination system to mutate *Apc* in a temporal and spatial manner. This approach is necessary as *Apc* has many functions in development and *Apc* mutant mice (Apc^{min}) do not develop past embryonic day 6.5 (E6.5). To date, there are no known cre-strains available to mutate *Apc* specifically in the cerebellum at early postnatal stages, so we combined the cre-*loxP* method with an avian retrovirus mediated method for tissue specific gene delivery (RCAS/tv-a system), in an attempt to create a strain of mice which carried the genotype $Ntv\text{-}a^{+};Apc^{LoxP/LoxP}$. This would allow us to infect an RCAS-cre virus directly into the hindbrain at

postnatal day 4 (P4). However subsequent genotyping of these animals showed that none carried the desired genotype of *Ntv-a*$^{+}$*;Apc*$^{LoxP/LoxP}$, making it impossible for both copies of *Apc* to be mutated in a mouse most likely because both the *Ntv-a* and *Apc* transgenes were located on the same chromosome. Consistent with this, out of a total of 265 mice none were found to have the *Ntv-a*$^{+}$*;Apc*$^{LoxP/LoxP}$ genotype.

We then adopted an alternative method for mutating *Apc* by infecting *Apc*$^{LoxP/LoxP}$ mice directly with an AdCre virus. PCR analysis showed that *Apc* was mutated, however the AdCre virus did not infect cells of the cerebellum, and instead only infected the choroid plexus. In these animals, 7 of 94 (7%) developed hydrocephalus indicating that losing *Apc* in the choroid plexus may promote hydrocephalus.

Finally, to address the role of Apc in normal hindbrain development, we crossed our *Apc*$^{LoxP/LoxP}$ mice to an *En1cre* strain which caused mutation in *Apc* from E8.5 in the mid-hindbrain region. The resulting *En1cre*$^{+}$*;Apc*$^{LoxP/LoxP}$ mutants displayed hydrocephalus in all ventricles and an in-growth of mesenchyme tissue at the mid-hindbrain border, closely associated with a tumour-like area of cells showing activated Wnt signalling. No mice were found to live past E18.5.

In conclusion, the role of Apc in medulloblastoma remains unclear. Future studies could use a different technique to mutate *Apc* such as crossing *Apc*$^{LoxP/LoxP}$ mice to the new *nestin-cre*^{ER} strain and inducting cre with administration of tamoxifen.

1. Introduction

1.1 Medulloblastomas

Central nervous system (CNS) malignancies are the most common solid tumours in childhood, and are the leading cause of cancer related death in this age group (Robertson 2006). There are five types of embryonic tumours that have been described in the CNS: medulloepithelioma, ependymoblastoma, medulloblastoma (MB), atypical teratoid/rhabdoid tumour (ATRT) and supratentorial primitive neuroectodermal tumour (PNET) (Ellison 2002). MBs are the most common type of malignant brain tumour that occur during childhood (Gilbertson 2004), and are classified as a malignant tumour of the cerebellum that preferentially occurs in children, and has the tendency to metastasise (Kleihues et al. 2002). Peak incidence of MB is in the eighth year, but while most cases present within the first 20 years, a significant proportion (30%) occurs in adulthood (Cervoni et al. 1994). MBs were originally identified by Bailey and Cushing (1925) when they were creating the first comprehensive classification of CNS tumours. They recognised similarities between its cytological features and those of the embryonic medullary velum (Bailey 1925; Rorke 1994). Other CNS tumours composed of blast-like cells with a high nuclear : cytoplasm ratio, with little cytological differentiation and a high mitotic count have since been classified as embryonal tumours with the MB (Ellison 2002).

Five different variants of MB have been described: Melanotic MB and medullomyoblastoma are very rare, accounting for around 1% of MBs (Dolman 1988). Melanotic MB are distinguished from other variants by the presence of melanin in cells, clusters of which may occasionally have an epithelioid appearance

and a tubular or papillary architecture (Dolman 1988). Medullomyoblastomas show degrees of rhabdomyoblastic differentiation (Smith & Davidson 1984). Because of their rarity, the biological behaviours of the melanotic MB and medullomyoblastoma have not been established as significantly different from that of the classic MB (Ellison 2002). Large cell MB is an aggressive variant of MB with a poor prognosis. These are also rare, making up only 4% of MBs (Brown et al. 2000), and are described as containing large tumour cells with prominent nucleoli and abundant cytoplasm, and also characterised by anaplasia (Gilbertson 2004). The desmoplastic variant of MB accounts for around 15% of MBs (Giordana et al. 1997). They contain nodules of tumour cells that commonly show neurocytic differentiation and are surrounded by collagen rich tissue (Gilbertson 2004). And lastly, the classic variant of MB (accounting for around 80% of MBs), tend to grow as sheets of cells with a high nuclear : cytoplasm ratio with the capacity to invade adjacent brain tissue. They lack the nodular / desmoplastic architectural features of desmoplastic MBs, but can display Homer-Wright rosettes or palisades (Ellison 2002). All of these variants are graded as grade IV by the World Health Organisation (WHO).

Classic symptoms of MB occur as a result of increased intracranial pressure, including headache, vomiting, irritability or lethargy, and sometimes with symptoms due to involvement of local structures, such as ataxia, head tilt or cranial nerve palsies (Robertson 2006).

1.1.1 Medulloblastoma treatment

MBs represent a significant challenge in the field of neuro-oncology due to their highly aggressive nature and sequelae from the tumour and treatment. There are 3

main prognostic markers for a patient with MB: patient's age at diagnosis, the extent of postoperative residual disease, histological subtype of MB, and tumour metastasis.

MB in infants (children under 3 years of age), is twice as likely to progress within 5 years of diagnosis than MB occurring in older children (Zeltzer et al. 1999). Before the1980's, the treatment of infants was the same as that of older children, but their survival and subsequent standard of life was significantly worse. One of the main reasons for this is due to the use of radiation treatment. Radiation is a highly effective treatment for MB, however it can also cause severe damage to the developing brain. Therefore, treatment of MB in infants is generally restricted to surgery and chemotherapy alone (Gilbertson 2004). Another reason why young patients seem to have a higher mortality rate than those over 3 years at age of diagnosis, is due to inherent differences in disease biology. ATRTs are highly aggressive tumours that are distinct from MBs, but share similar characteristics clinical signs and symptoms and radiological features (Rorke et al. 1996). They are more common in infants, and cause a much higher mortality rate than MB. ATRTs were in previous years not differentiated from MBs, so an infant with an ATRT would have been included in MB clinical trials (Gilbertson 2004). This would contribute to the very high mortality seen in very young children.

MBs have a tendency to metastasise, with around a third of patients showing signs of metastasis within the CNS at diagnosis (Zeltzer et al. 1999), and a small proportion of MBs have also been seen to metastasise to extraneural areas such as the bone, bone marrow, lungs, liver, and lymph nodes (Eberhart et al. 2003). MB is staged according

to Chang's criteria (Chang 1969) for classifying tumour and metastasis stage in MB, and metastases remain one of the most important prognostic markers of MB.

Lastly, a large volume of postoperative residual tumour (≥1.5cm^2 on a postoperative MRI (Gilbertson 2004) is a very strong indication of a poor clinical outcome for the patient.

1.1.1.1 Surgery

Surgery is the initial treatment for most children with brain tumours. With surgical resection, it is essential to extract as much of the tumour as possible as this will increase the patients chance of survival. However, the extent of resection must be a balance between the benefit of taking as much tumour material as possible, and the risk of damaging adjacent neuroanatomical structures.

1.1.1.2 Radiation Therapy

Radiation therapy is usually the first adjuvant treatment after surgery for MB. It was initially developed in the early 1900's for the treatment of adult gliomas and pituitary tumours (Robertson 2006). Radiation therapy is normally applied to the primary tumour site, or in the case of a tumour with a tendency to metastasise (ie. MB), it is applied to the entire craniospinal axis.

1.1.1.3 Chemotherapy

Chemotherapy is defined as the treatment of disease with chemical substances, and in particular, the treatment of cancer with cytotoxic and other drugs. Broadly, most chemotherapeutic drugs work by impairing mitosis, effectively targeting fast-dividing

cells. As these drugs cause damage to cells they are termed cytotoxic. Unfortunately, chemotheraputic drugs cannot differentiate between cancer cells and normal cells. The normal cells will grow back once the treatment stops, however during the treatment regimen, side effects occur. The normal cells most commonly affected by chemotherapy are rapidly dividing cells such as blood cells, epithelial cells in the mouth, stomach and bowel, and the hair follicles; resulting in low blood counts, mouth sores, nausea, diarrhoea, and/or hair loss. Different drugs may affect different parts of the body.

Chemotherapy was initiated for the treatment of paediatric brain tumours such as MB in the 1970's. Studies carried out by the Childrens Cancer Group (CCG) and the International Society for Paediatric Oncology (SIOP) have demonstrated the efficiency of post-irradiation chemotherapy in children with high-stage disease, although, trials have failed to show the same efficiency in low-stage disease (Evans et al. 1990; Tait et al. 1990).

New chemotherapeutic strategies are being developed that specifically focus on targeting tumour cells to reduce side effects of conventional chemotherapeutic drugs. Identification of molecular differences between brain tumour cells and normal healthy cells has opened the way for a number of therapeutic strategies that take advantage of these differences. Targeted therapies take advantage of these differences to inhibit growth of tumour cells, for example, by inhibiting growth of blood cells (anti-angiogenic therapy), inhibiting signal transduction pathways, using immunotherapy, and regulating gene expression (Robertson 2006).

1.1.1.3.1 Anti-angiogenic Therapy

Tumour growth depends on the recruitment of blood vessels, a process called angiogenesis. Angiogenesis occurs during development, however, it also important later in tissue regeneration (Kerbel & Folkman 2002). Cancer cells create an "angiogenic switch" to promote angiogenesis in early tumour development. This involves turning on genes involved in the growth of new blood cells such as vascular endothelial growth factor (VEGF), basic fibroblast growth factor (bFGF), interleukin-8 (IL-8), placenta-like growth factor (PLGF), transforming growth factor-β (TGF-β) and others (Fukumura et al. 1998; Relf et al. 1997). Fibroblasts in or near the tumour bed begin to produce these pro-angiogenic factors and tumours also recruit progenitor endothelial cells from bone marrow (Fukumura et al. 1998; Shi et al. 1998). The angiogenic switch also involves the down-regulation of angiogenic suppressor proteins such as thrombospondin (Dameron et al. 1994).

Anti-angiogenic drugs can either act directly on the tumour cells to inhibit synthesis of proteins such as bFGF, VEGF and TGF-α or other receptors on the endothelium that are expressed by the tumour cells. An example of such a drug is ZD1839 (Iressa) (Kerbel & Folkman 2002). Direct angiogenesis inhibitors, such as endostatin, target the microvascular endothelial cells that are recruited to the tumour bed and prevent them from responding to various endothelial mitogens (Kerbel & Folkman 2002).

1.1.2 What factors lead to Medulloblastoma development?

Understanding the biology of MBs will be a key factor in future treatment strategies. It is unlikely that current methods of combating MBs can significantly increase survival rate among patients, and also decrease the serious long-term side effects that

affect survivors' lives. The aberrant activation of several cell-signalling pathways have been implicated in MB formation, and investigation of these pathways should lead to the development of new treatments and risk-stratification tools for MB in the near future. Two of these pathways, the hedgehog and Wnt pathways, where aberrant signal transduction in MBs are thought to occur are discussed below.

1.1.2.1 Sonic Hedgehog (Shh)

The *Drosophila melanogaster* gene *hedgehog (hh)* and its mammalian homologues *Shh*, *Desert hedgehog (Dhh)*, and *Indian hedgehog (Ihh)* are secreted glycoproteins that have key roles in tissue patterning acting as morphogens involved in patterning many systems, including the limb and midline structures in the brain and spinal cord. The loss or reduction of Hh signalling is associated with numerous developmental deficits or malformations, one of the most striking of which is the cyclopia associated with loss of Shh signalling (Muenke 2001). The Shh pathway acts through patched 1(Ptc1), a 12-pass transmembrane receptor that represses the activity of the protein smoothened. Smoothened is a 7-pass transmembrane associated protein which is closely related to the frizzled family of Wnt receptors (discussed below). Ptc1 is thought to suppress smoothened indirectly, resulting in GLI (glioma-associated oncogene homologue) transcription factors to be bound to microtubules in the cytoplasm. This is done by a complex which includes fused and suppressor-of-fused. GLI 1 is sequestered into this complex, preventing it from activating gene transcription, while GLI 2 and GLI 3 are cleaved to produce truncated transcriptional repressors. The binding of Shh to Ptc1 inhibits Ptc1's suppression of smoothened, which in turn disrupts the complex containing fused and suppressor-of-fused.

Subsequently, GLI 1 is released and activates gene transcription, whereas GLI 2 and GLI 3 cleavage is blocked (McMahon et al. 2003) (Figure 1.1).

The involvement of the Hh pathway in human cancer was first appreciated upon the identification of *Ptch* as the tumour suppressor in Gorlin's syndrome (also known as basal cell nevus syndrome (BCNS)). Sufferers of Gorlin's syndrome can display a variety of abnormalities such as craniofacial and rib alterations, polydactyly, syndactyly, and spina bifida as well as a multitude of tumour types such as fibromas of the ovaries and heart, cysts of the skin, meningiomas, basal cell carcinomas (BCCs) and medulloblastomas (Johnson et al. 1996). A study by Johnson *et al* (1996) found altered *Ptch* sequences in germline DNA from BCNS individuals and also in BCCs. Supporting this, is a study by Hahn *et al.,* (1996) found *smoothened* (*SMOH)* mutations in 20% of sporadic BCCs. Shh signalling was first linked to MB through studies of the human *PATCHED1 (PTCH1)* gene. 10-20% of sporadic MBs have been found to carry mutations at the *PTCH1* locus (Pietsch & Wiestler 1997; Raffel 1997b; Xie et al. 1997), which suggests that defects in Shh/Ptc signalling can contribute to the development of MBs. *PTCH1* mutations are not the only mutations of the Shh pathways found in MBs. Activating mutations of *SMOH* have been detected in up to 5% of sporadic MBs (Reifenberger et al. 1998), and a study by Taylor et al. (2002) showed somatic mutations of *SUFU (Suppressor of Fused)* in 9% of children with MB.

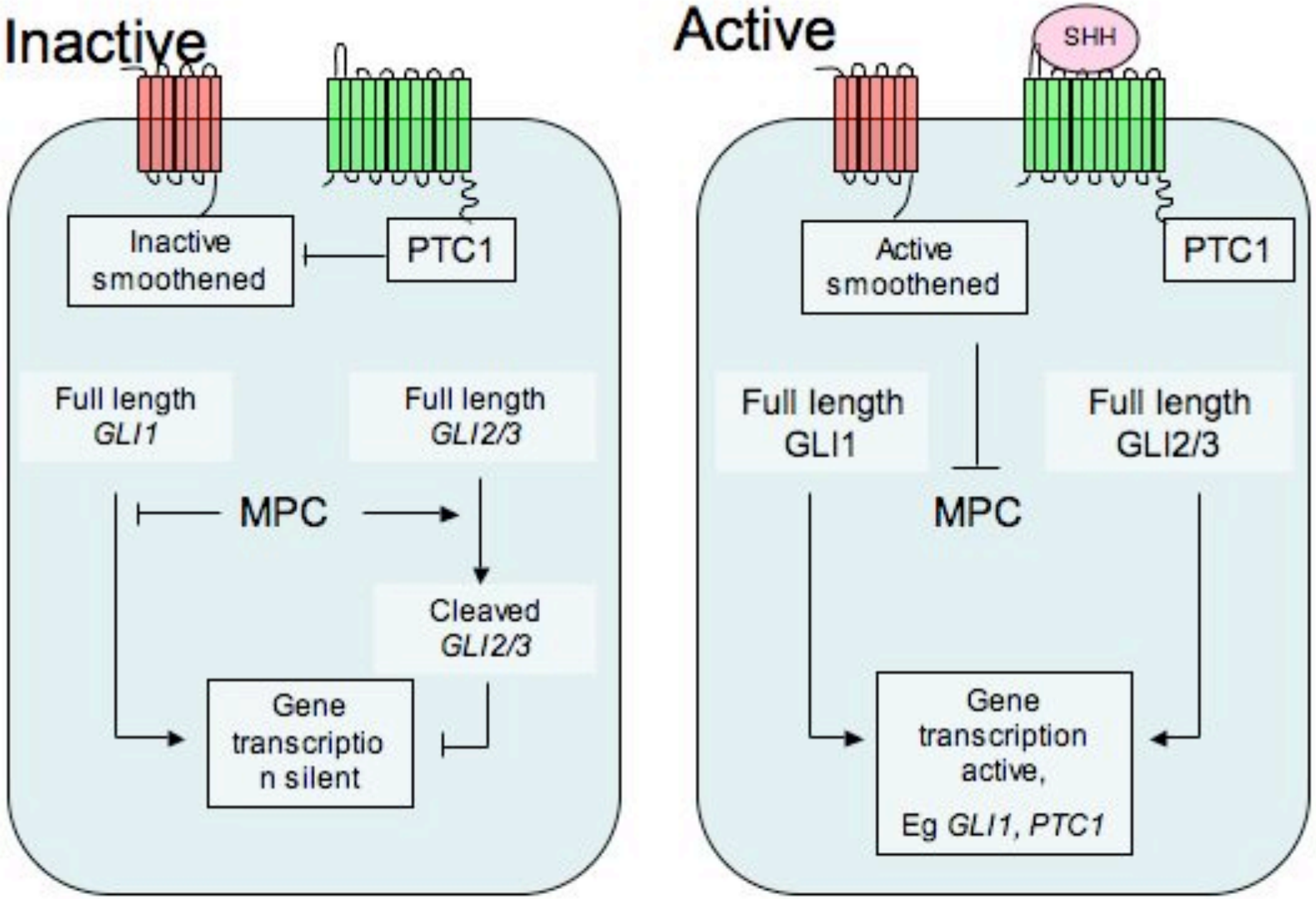

Figure 1.1: Simplified diagram of the Sonic Hedgehog (SHH) pathway.

When SHH is absent, the pathway is inactive, as PTC represses smoothened. When SHH binds to PTC, this repression stops and smoothened is able to repress the multi-protein complex (MPC),which contains fused and suppressor of fused. This in turn allows GLI 1 is released and activates gene transcription, whereas GLI 2 and GLI 3 cleavage is blocked.

The first unconditional proof showing that mutations in the Hh pathway can lead to MB development came from the study of *Ptc1*$^{+/-}$ mice (Goodrich et al. 1997; Hahn et al. 1998) which have had one copy of *Ptc* deleted. Homozygous *Ptc1*$^{-/-}$ mice die at E9.5 with severe defects in the cardiovascular and nervous systems, but heterozygotes are viable and initially the only phenotypes are increased body size and a low incidence of polydactyly (Goodrich et al. 1997). However, at around 5 months of age, between 15% and 25% of mice develop aggressive cerebellar tumours with the characteristic small, round cells on the surface of the cerebellum that MB possess (Goodrich et al. 1997; Wetmore et al. 2000). Studies trying to determine whether the second allele of *Ptc1* must be lost to induce tumourigenesis have been contradictory with studies by Wetmore et al. (2000), Zurawel et al. (2000) and Romer et al. (2004) all detecting wild type *Ptc1* RNA in tumours from *Ptc1*$^{+/-}$ mice (Raffel 1997a; Romer et al. 2004; Wetmore et al. 2000). However, contradicting this is a report from Berman et al. (2002) who found that wild type *Ptc1* may be silenced possibly through DNA methylation (Berman et al. 2002). Although this study was conducted using autografted cell lines, and the Hh pathway has been shown to undergo silencing when primary cell lines are cultured *in vitro* (Romer et al. 2004).

The mechanism by which dysregulation of Hh signaling leads to MB formation is still unclear, however there is evidence to suggest a close connection between activated Hh signaling and impaired cell-cycle control. Studies by Pomeroy et al. (2002) and Lee et al. (2003) which looked at the gene expression in MBs using microarrays, found elevated levels of *Gli1, N-Myc, C-Myc, CyclinD1 and CyclinD2*. These genes were also found to be expressed in the developing cerebellum (Lee et al. 2003; Pomeroy et al. 2002) which implies that MB cells may be similar to granule cell

precursors (GCPs). Shh has been linked to cell-cycle control from a study by Kennedy and Rowitch (2000) which showed that Shh could induce expression of the G1 cyclin genes (Kenney & Rowitch 2000). Shh stimulation has also been shown to hamper exit from the cell-cycle, in part through blocking cell-cycle arrest induced by the cyclin-dependent kinase inhibitor $p21^{CIP1}$ (Fan & Khavari 1999).

1.1.3.2 Wnt Signalling

Along with the hedgehog proteins and other families of secreted factors, Wnt proteins have been implicated in a wide range of biological processes. Wnt1, the first Wnt protein, was discovered in 1982 in a study by Nusse and Varmus. This study looked at whether the mouse mammary tumour virus (MMTV), an oncogenic retrovirus, integrated into a certain region of the host genome. The study showed that the MMTV integrated into the *Wnt1* locus, and *Wnt1* was subsequently cloned (Nusse & Varmus 1982). From this landmark discovery, the role of *Wnt* genes in cancer was the main area of research in the 1980's in this field (reviewed by Nusse and Varmus 1992). The focus of Wnt research changed when the *Drosophila* orthologue of Wnt1 (*wg)* was discovered (Cabrera et al. 1987; Rijsewijk et al. 1987), and with the phenotypic analysis of *Wnt1* mutations in mice (McMahon & Bradley 1990; Thomas & Capecchi 1990), Wnt research largely changed focus to now study their effects in development. The discovery that *wg* was a *Wnt* family member allowed the powerful genetics of Drosophila to be applied to understanding *Wnt* gene function. More recently, with the discovery that Apc is the tumour suppressor involved in familial adenomatous polyposis, Wnt research has come full circle and many researchers are looking at components of the Wnt pathway in cancer.

To date, in vertebrates, 16 *Wnt* genes have been identified in *Xenopus*, 11 in chick, and 12 in zebrafish. Humans have 19 *Wnt* genes and there are also 19 in the mouse. These are highly conserved between species, especially between vertebrates, and only slightly less conserved between vertebrates and invertebrates. A comprehensive list of Wnt genes can be found at the Wnt homepage at http://www.stanford.edu/~rnusse/wntwindow.html, maintained by Roel Nusse.

Wnt signals are transduced through at least three distinct intracellular signalling pathways including the canonical 'Wnt/β-catenin' pathway, the 'Wnt/polarity' pathway and the 'Wnt/$Ca2^{+}$' pathway (Adler & Lee 2001; Kuhl et al. 2001; Miller et al. 1999). Each of these pathways can be activated by distinct sets of Wnt and Frizzled receptor pairs which achieve alternative cellular responses.

The main known function of the Wnt/polarity (also known as the Wnt/JNK pathway) is for specifying cell polarities in epithelial cells (Adler 2002). This pathway involves the cadherin-related transmembrane molecule flamingo (Fmi), the proteoglycan knypek (Kny), and the PDZ molecule strabismus (Stbm) and branches at the level of Dsh from the canonical pathway. Frizzled, which with the help of protein kinase C (PKC), activates c-Jun N-terminal kinase (JNK) (Kinoshita et al. 2003). In vertebrates, this pathway controls cell movements during gastrulation (Tada & Smith 2000; Wallingford & Harland 2001). In Drosophila, this pathway has many developmental roles such as regulating asymmetric cell divisions in neuroblast populations, and ensuring the appropriate orientation of the hairs on the adult wing (Adler & Lee 2001; Adler & Taylor 2001)

Little is known about biological function of the Wnt/$Ca2^{+}$ pathway. The Wnt $Ca2^{+}$ pathway leads to the release of intracellular calcium, possibly via G-proteins. Phospholipase C (PLC) and PKC are activated causing increased Ca^{2+} which leads to dephosphorylation of the transcription factor NF-AT. NF-AT accumulates in the nucleus and, in xenopus embryos, NF-AT suppresses canonical Wnt signals during axis formation (Huelsken & Behrens 2002).

1.1.3.2.1 The canonical Wnt signalling pathway

The β-catenin-dependent, or canonical, Wnt signalling pathway was the first to be discovered and is best understood Wnt pathway. During the remainder of this thesis, any reference to the 'Wnt pathway' will be referring to the canonical pathway. This pathway acts through β-catenin to activate specific target genes, which in turn, are able to modulate cell fate, apoptosis and proliferation (Cadigan & Nusse 1997; Miller et al. 1999; Wodarz & Nusse 1998).

The canonical Wnt signalling pathway is activated by a Wnt protein binding to its receptor, Frizzled. Frizzled has seven-transmembrane spanning receptors, which may be coupled to heterotrimeric G proteins. Various secreted factors, such as cerberus (Cer) and FrzB, can bind to Wnts and block the interaction with frizzled proteins. Dickkopf (Dkk) antagonises Wnt action by blocking access to the LRP co-receptor.

The binding of Wnt to Frizzled recruits Dishevelled (Dsh) to the membrane and negatively regulates GSK-3β, causing the complex between Apc, Axin and GSK-3β to lose its ability to bind and cause the phosphorylation β-catenin via a ubiquitin-

ligase complex. This leads to a build-up of stabilised intracellular β-catenin in the cytoplasm (Fearnhead et al. 2001). β-catenin then translocates to the nucleus where it acts as a transcriptional co-activator by associating with members of the T cell factor (TCF) and lymphoid enhancer factor (LEF) family of transcriptional activators (Roose & Clevers 1999). This β-catenin – transcription factor complex regulates transcription of target genes such as c-myc and cyclin D1, which are regulators of cell growth and proliferation (Nathke 1999) (Figure 1.2).

In the absence of a Wnt signal, β-catenin is sequestered in the cytoplasm and destabilised by a complex containing Axin, GSK3β, and Apc which phosphorylates β-catenin by GSK3β (Behrens et al. 1998; Hart et al. 1998). Phosphorylated β-catenin becomes ubiquitylated and is targeted for degradation by the proteasome via a ubiquitin ligase complex (Zeng et al. 1997). Hence β-catenin cannot translocate to the nucleus and turn on transcription of target genes. Both Apc and Axin are key negative regulators of the Wnt signalling pathway. Axin binds to Apc forming a complex which in turn binds both GSK3β and β-catenin. This is important not only as GSK3β requires both Apc and Axin to bind β-catenin, but also because both Apc and Axin are phosphorylated by GSK3β, which strengthens the binding of β-catenin (Ikeda et al. 1998). Axin was once thought to be merely a scaffold protein linking other members of the complex, however, it is now thought to play a more dynamic role in the degredation of β-catenin by binding to the tail of LRP in response to a Wnt signal (Mao et al. 2001). Membrane tethering of Axin to LRP is thought to be enough to activate signalling (Brennan et al. 2004) possibly by titration of Axin away from the Apc/Axin/GSK3β complex. GSK3β phosphorylates three conserved residues in the amino-terminal region of β-catenin, Ser 33, Ser 37, and Thr 41. However, studies

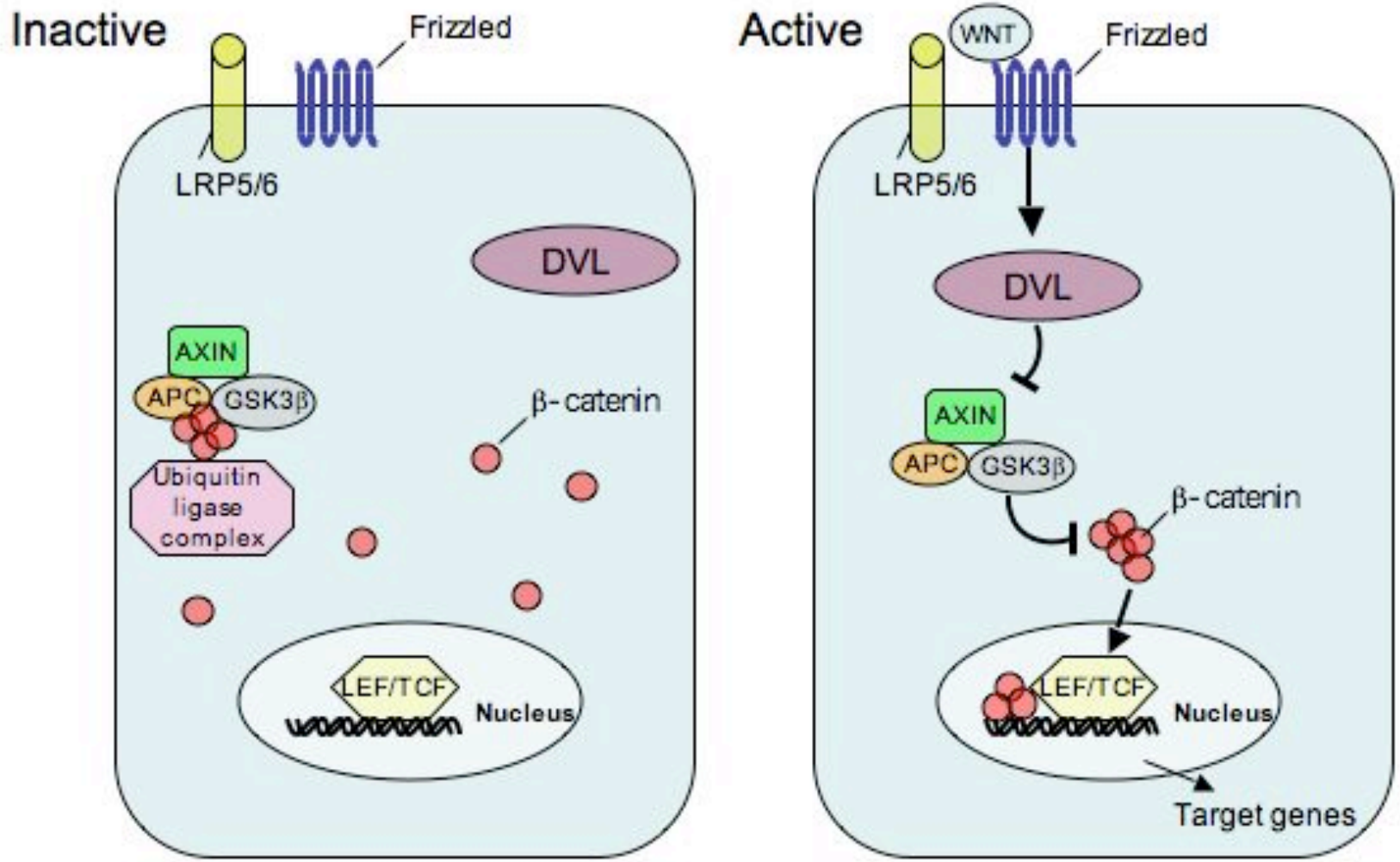

Figure 1.2: Simplified diagram of the canonical Wnt signalling pathway.
In the absence of a Wnt signal β-catenin is targeted to the proteasome for degradation via a ubiquitin ligase complex. Wnt signalling is activated by Wnt binding to Frizzled which stabilises β-catenin which in turn translocates to the nucleus, interacts with LEF/TCF family members and results in transcription of target genes such as *c-myc* and *cyclinD1*.

have shown that for efficient phosphorylation casein kinase 1 (CK1) should phosphorylate β-catenin at Ser 45. This then serves as a priming site for GSK3β phosphorylation (Amit et al. 2002; Liu et al. 2002; Yanagawa et al. 2002). This explains why many human tumours carry mutations of Thr 41 and Ser 45 of β-catenin (Polakis 2000).

β-catenin has another main function outside the Wnt pathway. β-catenin has been shown to interact with other proteins such as E-cadherin and α-catenin (Hulsken et al. 1994), and play a critical role in cellular adhesion. The cytoplasmic domains of E-cadherin, a calcium ion dependent cell adhesion molecule, bind either β-catenin or γ-catenin (plakoglobin) (Aberle et al. 1996). These catenin proteins then complex with α-catenin which acts as a bridge to bind actin molecules making up the cytoskeleton (Aberle et al. 1996).

The deregulation of Wnt signalling has emerged to be an important step in human oncogenesis (Polakis 2000). Mutations of proteins in the Wnt pathway occur in around 15% of sporadic MBs (Baeza et al. 2003; Eberhart et al. 2000; Huang et al. 2000; Koch et al. 2001), and can cause heritable forms of the disease when transmitted through the germline (Robertson et al. 2004). In the majority of cases, mutations that cause aberrant Wnt signalling block the breakdown of β-catenin in the cytoplasm of the cell, allowing it to translocate to the nucleus and turn on transcription of Wnt target genes such as *c-myc* and *cyclin D1*. The Wnt/β-catenin pathway will be discussed in more detail in a later section.

Most of the mutations of the Wnt pathway that have been reported in sporadic MBs have targeted residues S33 and S37 of β-catenin and account for between 5-10% of cases, however, less common mutations have been described in the *Apc* tumour suppressor gene at a frequency of around 4% (Huang et al. 2000).

1.1.4 Familial Adenomatous Polyposis (FAP)

The *Apc* gene encodes a large, multi-domain protein that was initially identified by positional cloning of the Familial Adenomatous Polyposis (FAP) locus (Groden et al. 1991; Kinzler et al. 1991) following mutational analyses of unrelated families with FAP. FAP is a dominantly inherited colorectal cancer syndrome which is characterised by multiple (potentially thousands) of colorectal adenomas throughout the colorectum and duodenum (Galiatsatos & Foulkes 2006).If left untreated, this will progress to colorectal cancer within the third to fourth decade of life (Bisgaard et al. 1994). To date, there have been over 700 disease causing Apc mutations identified (Galiatsatos & Foulkes 2006)leading to the introduction of a premature stop codon leading to truncation of the protein product in the C-terminal region. Of these, 68% are frameshift mutations, 30% are nonsense mutations, and 2% are large deletions (Beroud & Soussi 1996). There is also an association between tumours of the CNS and multiple colorectal polyps in some FAP patients, a condition known as Turcot's syndrome. Patients suffering from this condition have mutations in *Apc*. Although brain tumours arise sporadically in the general population, patients with a germline mutation in *Apc* are 92 times more likely to develop MB (Raffel 2004).

1.2 Adenomatous Polyposis Coli (Apc)

Apc encodes a large multidomain protein that plays an integral role in Wnt signalling and cell adhesion (Fearnhead et al. 2001), as well as being implicated in apoptosis (Morin et al. 1996) and neuronal cell migration (Munemitsu et al. 1994). The *Apc* gene is located at human chromosome 5q21 spanning 8535bp, with 21 exons (Thliveris et al. 1996), and encoding a predicted 2843 amino acid polypeptide in its commonest isoform (Santoro & Groden 1997). Exon 10A is the subject of alternative splicing and adds an additional 18 amino acids to the Apc protein when it is spliced in (Xia et al. 1995). Exon 15 comprises over 75% of the coding sequence and is the most common target for both germline and somatic mutations (Beroud & Soussi 1996). Originally *Apc* was thought to comprise of 15 exons (Groden et al. 1991), however, studies such as the one by Bardos *et al* (1997), showed by using RT-PCR that alternative mRNA isoforms exist that encode unique Apc proteins. This study indicates that the *Apc* gene codes for a complex pattern of gene products that are generated on the basis of alternative splicing (Bardos et al. 1997).

The Apc protein contains an armadillo region in the N-terminus, an oligomerisation domain, a number of 15-and 20- amino acid repeats in its central portion, and a C-terminus that contains a basic domain and binding sites for EB1 and the human discs large (HDLG) protein. These multiple domains of the Apc protein allow it to interact with numerous protein partners (Fearnhead et al. 2001) (Figure 1.3).

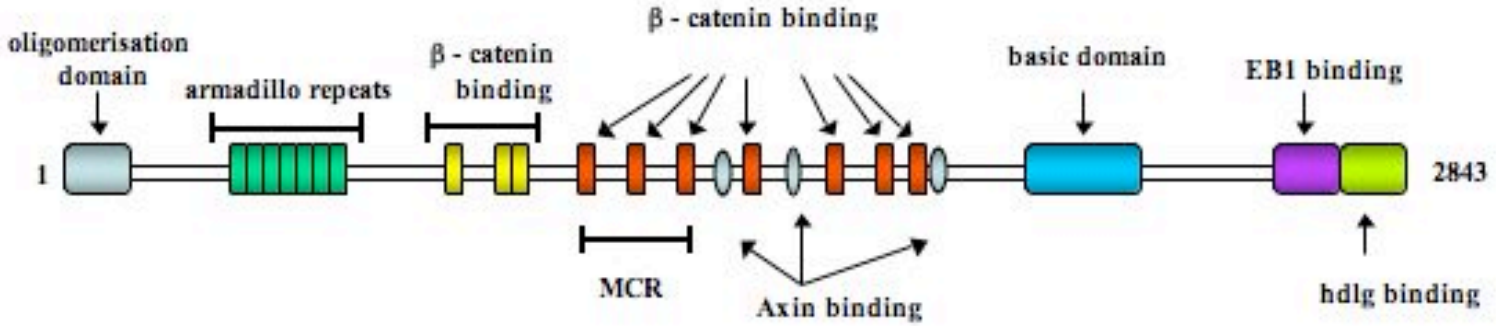

Figure 1.3: Linear representation of the APC protein. Functional domains include the oligomerisation domain, the β-catenin binding domain, the basic domain, and the EB1 and human discs large binding domain.

The armadillo region consists of seven repeats which bear a high degree of homology to β-catenin and its Drosophila homologue, armadillo (Kinzler et al. 1991). The armadillo region has been shown to bind the regulatory subunit B56 of protein phosphatase 2A (PP2A) (Seeling et al. 1999),which is an enzyme which can also bind axin. Indeed, the findings from a study by Hsu et al. (1999) indicated that PP2A might interact with the Apc/Axin/GSK3β/β-catenin complex and antagonise the GSK3β phosphorylation of β-catenin (Hsu et al. 1999).

The oligomerisation domain in the Apc protein, located in the N-terminus, allows Apc to form homo-dimers (Su et al. 1993). This domain makes it possible for Apc to form dimers with both wild-type and truncated mutant forms of Apc.

There are three 15 and seven 20 amino acid repeats located in the central portion of the Apc protein. These are areas which bind β-catenin (Fearnhead et al. 2001), however, β-catenin binding at these sites can only occur after phosphorylation of each site by GSK3β (Munemitsu et al. 1995; Rubinfeld et al. 1996). Downregulation of β-catenin is dependent on the presence of at least three of the seven 20 amino acid repeats in Apc (Rubinfeld et al. 1997). The majority of truncated mutant proteins lack all or most of the 20 amino acid repeats, suggesting that these are targets for elimination during tumourigenesis (Polakis 1997).

The basic domain is situated between amino acids 2200 and 2400 in the C-terminus (Groden et al. 1991). It derives its name from the high proportion of (basic) arginine and lysine residues, however this domain also contains a very large number of proline residues. Studies by Smith et al. (1994) and Munemitsu et al. (1994) have shown that

Apc binds microtubules at the C-terminal (Munemitsu et al. 1994; Smith et al. 1994a). Taking this further, in the study by Munemitsu et al. (1994), they show that mutant Apc fragments only associate with cytoplasmic microtubules if they contain the C-terminal portion. Moreover, a recent study by Moseley et al. (2007) showed that actin not only binds to the basic region of Apc, but also competes with microtubules for binding to this domain. Tumour formation and metastasis involve coordinated changes in the actin and microtubule cytoskeletons (Moseley et al. 2007), so it is of note that truncated Apc proteins found in colorectal tumours rarely retain the basic domain (Fearnhead et al. 2001). The ability of Apc to assemble and/or associate with microtubules may in part explain the localisation of Apc to the leading edge of migrating cells, a region where microtubule assembly is required, and in addition may lend itself to the observations of disordered cell migration in models of Apc overexpression and in animal models of FAP (Mahmoud et al. 1997; Mahmoud et al. 1999; Nathke et al. 1996; Wong et al. 1996).

The C-terminus region contains the binding site for end binding protein 1 (EB1) and Human Disks Large (hdlg). EB1 is a microtubule plus-end tracking protein that binds to and partially co-localizes with Apc *in vivo* (Kita et al. 2006). The presence of EB1 at the plus ends of microtubules occurs independently of Apc (Berrueta et al. 1998; Morrison et al. 1998). In fact, if the EB1 binding domain is deleted from Apc, then Apc is still able to bind microtubules (via its basic domain), however, the study by Askham et al. (2000) suggest that the interaction between Apc and EB1 targets Apc to microtubule tips, and without this interaction, Apc binds microtubules randomly (Askham et al. 2000).

The final 72 amino acids of Apc are necessary for hdlg binding (Matsumine et al. 1996). The hdlg protein is the human homologue of the *Drosophila* Discs Large (dlg) tumour suppressor protein which when lost in *Drosophila* results in neoplastic growth in the imaginal disc of the developing embryo (Bryant et al. 1993). Overexpression of Apc can halt progression of the cell cycle from G_0/G_1 to S phase (Baeg et al. 1995), with a study by Ishidate et al. (2000) showing that an Apc-hdlg complex is crucial for this cell cycle blocking ability of Apc (Ishidate et al. 2000).

1.2.1 Functions of Apc

Possibly the best understood function of Apc is in its role as a negative regulator in the Wnt signalling pathway. As discussed earlier, Apc forms a complex with GSK3β and Axin to bind β-catenin which leads to its breakdown in the cytoplasm. Truncation mutations of Apc that render it unable to form this complex with GSK3β and axin, leads to an accumulation of β-catenin which causes changes in the transcriptional activation of Wnt target genes such as *c-myc*, *cyclin D1*, *ephrins* and *capsases* (Chen et al. 2003; Fodde 2002; van de Wetering et al. 2002). These genes are known to have the ability to change the proliferation and differentiation state of cells (Nathke 2004). Therefore, Apc is thought of a negative regulator of the Wnt signalling pathway by binding to and, hence, down-regulating free cytoplasmic β-catenin. This was shown experimentally by Munemutsu et al. (1995) who demonstrated a dramatic reduction in intracellular β-catenin by transiently transfecting SW480 colorectal cancer cells with wild type Apc protein. These colorectal cancer cells have a mutated Apc protein and are unable to mark β-catenin for degradation, and hence have very high β-catenin levels (Munemitsu et al. 1995). Therefore, by adding wild type Apc protein, they were

able to re-establish a functional Wnt pathway. In summary, losing Apc function in the canonical Wnt signalling pathway has the same result as constantly stimulating the pathway.

The other main function of Apc lies in its ability to interact with the cytoskeleton. Apc is highly expressed in the peripheral ends of some microtubules in migrating epithelial cells (Nathke et al. 1996). In polarised cells, the majority of Apc expression can be seen at the basal surface where the plus ends of microtubules terminate (Mogensen et al. 2002). Apc has also been linked to some aspects of formation and/or maintenance of mitotic spindles. Apc can associate with the cytoskeleton in at least two ways. It can either directly bind to microtubules (Munemitsu et al. 1994; Smith et al. 1994b), or indirectly connect with the actin cytoskeleton (Townsley & Bienz 2000). As stated previously, Apc can bind microtubules directly at the C-terminal via the basic domain and the EB1 domain. However, as shown by Zumbrunn et al. (2001), Apc can still associate with microtubules even in mutated forms of Apc lacking the basic domain (Zumbrunn et al. 2001).

Apc is found in the nucleus as well as the cytoplasm, and contains several nuclear import and export signals (Henderson & Fagotto 2002). It is possible that Apc may play a role in the shuttling of β-catenin in the nucleus, however, the shuttling of β-catenin from the cytoplasm to the nucleus can take place in the absence of Apc (Henderson & Fagotto 2002). That leaves the possibility that Apc may play a role in shuttling β-catenin out of the nucleus and into the cytoplasm for subsequent degradation. Along the length of the Apc protein are nuclear export sequences (NES). Indeed, a paper by Henderson (2000) showed that mutating NESs on Apc causes a

build up of β-catenin in the nucleus, and conversely, overexpression of wild-type Apc in Apc deficient colon cancer cells has been shown to increase nuclear export and degradation of β-catenin (Henderson 2000).These findings suggest that wild-type Apc controls the nuclear accumulation of β-catenin by a combination of nuclear export as well as cytoplasmic degradation.

1.2.2 The role of Apc in cancer

As discussed earlier, abberant Wnt signalling is thought to be involved in medulloblastoma. However, dysregulation of the Wnt pathway is thought to play a role in other types of cancers. Indeed, 20% of gastric carcinomas screened have activating mutations in β-catenin (Clements et al. 2002). In melanomas, when pulling the results of various screening studies, it appears that 5% of all melanomas have either a mutation of Apc or β-catenin (Giles et al. 2003). Hepatoblastomas represent the most frequent liver cancer in children, and although most cases are sporadic, there is a greatly elevated incidence in patients with FAP (Giles et al. 2003). When hepatoblastomas were screened for mutations in either Apc or β-catenin, 51% were found to carry a mutation in exon 3 on β-catenin, which affected the ability of GSK3β to bind and phosphorylate β-catenin (Blaker et al. 1999; Jeng et al. 2000; Koch et al. 1999; Park et al. 2001; Taniguchi et al. 2002; Wei et al. 2000). Therefore, since dysregulation of the Wnt pathway can lead to various types of cancers, and that Apc plays a key role in the Wnt pathway, it is easy to see how mutations of Apc can lead to cancer development.

However, this model is complicated when you consider that there are pathways outside the Wnt signalling pathway which have the ability to regulate levels of β-

catenin. These include the p53-inducible Siah-1 protein (Liu et al. 2001), and retinoid X receptor (Xiao et al. 2003). This makes it difficult to establish how mutations in Apc can lead to colon cancer through the de-regulation of β-catenin. This lends weight to the idea that Apc's other functions such as its role in the cytoskeleton also play a role in its role in cancer. Indeed, in early mitosis, Apc localises to the end of microtubules that are embedded in kinetochores, but Apc is also present in spindle microtubules and centrosomes (Dikovskaya et al. 2004; Louie et al. 2004). Indeed, mutations in APC have been in the development of chromosomal instibility early in tumour formation (Shih et al. 2001). To investigate further Apc's role in microtubules, Dikovskaya et al. (2004) conducted a study using *Xenopus* egg extracts which were arrested in metaphase of meiosis II (referred to as cytostatic factor extracts). Their results showed that a lack of Apc leads to defects in the structure of mitotic spindles including a general loss of mictrotubule mass and redistribution of microtubule density from the centre of spindles towards the poles. The resulting phenotype could only be rescued by Apc protein containing intact microtubule binding site (Dikovskaya et al. 2004). Other effects such as changes in asters formed in the absence of chromatin indicate that changes in cytostatic factor extracts' spindle structure that result from Apc depletion can be at least partially attributed to direct effects on microtubule network removal (Dikovshaya et al. 2004). The study then went on to show that loss of Apc leads to chromosome mis-segregation suggesting that mutations in Apc could lead to cancer by causing aneuploidy (Dikovskaya et al. 2004). This reinforces other studies by Fodde et al. (2001), and Green and Kaplan (2003) who reported aberrant spindle structures in cells expressing mutant Apc.

There is a strong relationship between the functions of Apc and colorectal cancer. In the gut, all cells except stem cells have a very short lifespan. Epithelial cells differentiate and migrate out from the base of the crypts of Lieberkühn and are usually exfoliated within 3-5 days. A very strict balance must be maintained between differentiation, proliferation, cell adhesion and migration to ensure healthy gut maintenance. Mutations in Apc can affect the process of cell migration through its interactions with microtubules and the actin cytoskeleton causing cells to move less efficiently leading them to spend more time in the toxic environment of the gut which could in turn lead to further mutations. Also, defective mitotic spindles can cause genetic instability (Fodde et al. 2001) which would have major consequences as possibly lead to tumour formation if the mutation happened in a gut stem cell. Further, mutations of Apc would lead to abnormal β-catenin regulation which could lead to abnormal cell differentiation. All these factors may explain why a mutation in a single gene can have such severe consequences and lead to malignancies.

A study by Sansom et al. (2004) looked at the role Apc plays in the small intestine conditionally mutated *Apc* in this area which lead to altered crypt-villus architecture and morbidity after five days (Sansom et al. 2004). The study showed that the loss of *Apc* activated nuclear β-catenin which was seen by immunohistochemistry. They observed that differentiation, migration, proliferation and apoptosis were perturbed such that Apc-deficient cells maintain a crypt progenitor-like phenotype. To follow up this study, the same group created a double mutant for *Apc* and *Myc* (Sansom et al. 2007). In this double mutant, the changes conferred by Apc deficiency are rescued by Myc deficiency even in the presence of elevated nuclear β-catenin. A previous study showed that *Myc* deficient stem cells are selected against with the wild-type

surrounding cells outcompeting the mutant cells (Muncan et al. 2006), and this was found to be the case in Samson et al.'s $Apc^{LoxP/LoxP};Myc^{LoxP/LoxP}$ mice. Therefore, one can conclude that Myc is essential for the cellular and molecular changes which occur following loss of Apc in the murine small intestine.

1.2.3 Expression of Apc

Previous expression studies have provided conflicting results as to where Apc is expressed in the embryonic brain. Particularly confusing are studies which predict neuronal expression of Apc protein using *in situ* hybridisation (Bhat et al. 1994), and immunohistochemical studies that found intense labelling of oligodendrocytes without discernible neuronal staining (Bhat et al. 1996). A subsequent study was carried out by Brakeman et al. (1999) to try to clarify the Apc expression pattern. They found that *Apc* is expressed at high levels in neuronal cell bodies, dendrites and axons. The staining was particularly intense in neuronal layers of the hippocampus, olfactory bulb and cerebellum (Brakeman et al. 1999). This result is again controversial as another group (Senda et al. 1998) reported Apc expression in astrocytes as well as neurons.

1.2.4 Apc 2

A second Apc protein called Apc2 (previously known as ApcL), has been identified and is closely related to Apc. Since its discovery in by Nakagawa et al. (1998), Apc2 has been shown to be broadly expressed throughout embryonic development in Drosophila (McCartney et al. 1999; Yu et al. 1999), as well as in humans (Nakagawa

et al. 1998) and rodents (Yamanaka et al. 2001). Like Apc, Apc2 has been shown to function within the Wnt signalling pathway to deplete levels of β-catenin (Nakagawa et al. 1998), as well as being involved in actin-associated events to influence cell motility or adhesion (Jarrett et al. 2001). A study by Yamanaka et al. (2002) showed that in the mouse, *Apc2* is expressed strongly not only in the CNS, but also in the peripheral nervous system (PNS). Expression was first detected by northern blot at E10 in the brain and high expression levels continue until P10, at which point levels decrease through to adulthood. Using in situ hybridisation, *Apc2* was found to be predominantly expressed in postmitotic neurones of the cerebral cortex, the retina, and the cerebellum at embryonic stages. By early postnatal stages, expression had reduced significantly in the cortex and the retina, however, in the still developing cerebellum, there is still relatively high levels of expression in the external and internal germinal layers. In the adult mouse brain, there are many regions which express *Apc2*. Expression was detected in the hippocampus, the cerebral cortex, the midbrain, and the cerebellum (Yamanaka et al. 2002).

The expression pattern of Apc2 is important in relation to this project as our aim was to mutate *Apc* in the brain and observe the effects this has. It is possible that Apc2 could assume Apc's role in areas where we have mutated Apc. For example, in Drosophila, Apc and Apc2 have been shown to play redundant roles in larval brain development through the Wg (Drosophila Wnt) pathway and outside the Wg pathway (Ahmed et al. 2002; Akong et al. 2002; Hamada & Bienz 2002). Akong et al. (2002) showed by using an Apc2 mutant, that although Apc2 is strongly expressed throughout the CNS in normal flies, it is not essential for brain development. The most likely explanation for this is that Apc, which is also expressed throughout the

larval nervous system, can compensate for the loss of Apc2. To test this, Akong et al. studied both Apc and Apc2 mutants individually, and then created a double mutant. They found that individually, mutations of *Apc* and *Apc2* were not lethal and that the only noticeable abnormality was in the Apc mutants photoreceptors in the eyes which displayed inappropriate apoptosis. However $Apc^{-/-};Apc2^{-/-}$ double mutants were zygotically lethal, which lends weight to the hypothesis that when mutated individually, they can compensate for each other in cells where expression overlaps (Akong et al. 2002).

Further, a study by Hayashi et al. (1997) found that mutant Drosophila embryos that lacked D-APC (Drosophila homolog of mammalian Apc) showed a wild type cuticle pattern. Failure to downregulate Arm (β-catenin homologue) normally results in a uniform 'naked cuticular' pattern, hence implying that D-Apc may not be an essential component of the wingless (Wnt homolog) pathway (Hayashi et al. 1997). Since Apc2 seems to have areas of overlapping expression with Apc in rodents (Brakeman et al. 1999; Yamanaka et al. 2002), and that D-Apc2 has been shown to have the ability to interact directly with Arm and negatively regulate wingless signalling in the embryonic epidermis (McCartney et al. 1999), it is therefore very likely that Apc2 can substitute for Apc where there is loss of function of Apc.

1.3 Wnt Signalling

1.3.1 Wnt signalling in CNS Development

Wnt signalling has been implicated in all the crucial stages in CNS development: induction, patterning, expansion/proliferation, differentiation/migration, and synaptogenesis. For reviews, see Ciani & Salinas (2005); Kiecker & Niehrs (2001) and Stern et al. (2001).

1.3.1.1 Induction and Patterning

A study by Ikeya et al. (1997) looked at Wnt1 and Wnt3a signalling in the developing CNS. They did this by generating compound mutant mice lacking *Wnt1* and *Wnt3a*. Briefly, their results demonstrate that in the absence of Wnt1 and Wnt3a, there is a marked deficiency in neural crest derivatives, and a pronounced reduction in dorsolateral neural precursors within the neural tube. This study suggests that Wnt signalling regulates dorsoventral patterning in the mammalian CNS through the control of cell proliferation (Ikeya et al. 1997).

Further, a study by Houart et al. (2002) suggests that local antagonism of Wnt signalling in the anterior ectoderm of the anterior neural plate (ANB) is required to establish the telencephalon of zebrafish (Houart et al. 2002). This study ties in with a more recent one by Lagutin et al. (2003) who inactivated Six3 (a direct inhibitor of Wnt1 transcription), and found that the resultant mice had no forebrain. It could be concluded from this study that a Wnt signal gradient specifies posterior fates in the ANB (Lagutin et al. 2003).

1.3.1.2 Expansion/Proliferation and Differentiation/Migration

A study by Chenn and Walsh (2002) indirectly shows that disrupting Wnt signalling by overexpressing β-catenin in mice causes grossly enlarged brains with a considerable increase in surface area and thickness of the cerebral cortex. The main conclusion drawn form this paper is that β-catenin can function in the decision of precursors to proliferate or differentiate during mammalian neuronal development (Chenn & Walsh 2002). However, this is not direct evidence that Wnt signalling is involved in these stages of CNS development as: 1) β-catenin has other functions outside the Wnt pathway, so the overproliferation observed in the mutant mice may not be caused by β-catenin signalling through the Wnt pathway. 2) They created a mutant form of β-catenin which cannot be marked for destruction by the Apc/GSK-3β/axin complex, therefore it is very possible that this has disrupted some of β-catenin's other functions outside the Wnt pathway. However, since β-catenin (acting in the Wnt pathway) regulates genes known to be responsible for cell growth and differentiation (ie *c-myc* and *cyclinD1*) it is very possible that the mutant β-catenin is acting through the Wnt signalling pathway to cause gross overproliferation in the cerebral cortex of these mutant mice.

1.3.1.3 Synaptogenesis

A study by Hall et al. (2000) demonstrated that Wnt-7a was responsible for synaptogenesis in the cerebellum. Briefly, when they introduced a Wnt antagonist to cultured granule cell axons they found that the axon remodelling ability of granule cells was lost. They then added sFRP-1 (secreted frizzled related protein, a Wnt7a antagonist) found that simpler, less mature glomerular rosettes formed. The main

conclusion drawn from this study is that Wnt-7a, produced by granule cells, acts as a synaptogenic factor in vivo by regulating axon morphology and the accumulation of synaptic proteins (Hall et al. 2000).

1.4 Development of the cerebellum

To understand how medulloblastomas form in the cerebellum, and from what cell type, first we need to understand how the cerebellum forms during development (For review, see Wang & Zoghbi (2001). The cerebellum develops from the dorsal region of the posterior neural tube. The embryonic cerebellum begins as symmetric bulges into the fourth ventricle: cerebellar hemispheres arise as buds from laminae on either side of the rhombencephalic midline, and the most rostral segment of the metencephalon provides outgrowths that form the first elements of the cerebellum. These lateral sections develop towards the midline and fuse, forming the superior and inferior vermis. The lateral elements from this fusion develop into the cerebellar hemispheres.

The cerebellum is made up of various cell types: granule, purkinje, stellate, basket and golgi cells and glia. The granule cells are glutamate – releasing, excitatory neurones, whereas the purkinje cells are inhibitory cells, using as their transmitter. The other three are interneurons, found in the molecular layer of the cerebellum, which have a modulatory action on the purkinje cells and granule neurones (Wang & Zoghbi 2001).

The cells of the cerebellum arise from two different germinal matrices. The ventricular zone (also known as the ventricular germinal matrix) firstly gives rise to cells that radiate laterally and evolve into the deep cerebellar nuclei and purkinje cells of the cerebellum. The interneurons (stellate, basket and golgi cells) are born in the ventricular zone after the purkinje cells. These neurones migrate to the molecular layer of the cerebellum. The second germinal matrix that gives rise to cerebellar cells is an area called the rhombic lip. The rhombic lip arises relatively late in development at the interface between the neural tube and the roofplate of the fourth ventricle (Wingate 2001). The rhombic lip produces granule cell precursors which migrate away from the rhombic lip and populate the EGL. From the EGL, a second zone of proliferation, the granule cell precursors migrate deeper into the cortex where they differentiate into mature granule cells.

Once developed, the cerebellum's main role is to control the execution of smooth coordinated movements. The cerebellum is composed of predominantly purkinje cells and granule cells which are arranged in a laminar array (Palay et al. 1974). Granule cell parallel fibre excitation and ascending axonal inhibition of purkinje cells are the principal elements of cerebellar circuitry (Bower 2002). The Purkinje cells communicate with the thalamus, brainstem and spinal cord by projecting efferent fibres which act as the sole output of the cerebellar cortex (Cholley et al. 1989; Teune et al. 2000).

1.4.1 Genes involved in development of cerebellum

Patterning of the mid/hindbrain region from the neural tube is largely controlled by the isthmus organiser (IO) which is located at the border between these two regions. The IO is set up in a large part by the reciprocal expression of the genes *Gbx2* and *Otx2*. *Otx2* is expressed form E7.5 in the mesencephalon with its posterior boundary at the rostral metencephalon, whereas *Gbx2* is expressed in the caudal mesencephalon. In addition to helping form the IO, *Otx2* and *Gbx2* regulate expression of *Fgf8*, with *Otx2* repressing *Fgf8* and Gbx2 maintaining it (Broccoli et al. 1999; Wassarman et al. 1997). *Fgf8* is essential for normal midbrain development as Meyers et al. (1998) showed by creating a hypomorphic allele of *Fgf8*, which displayed severe patterning defects in the mid/hindbrain region which also affected the cerebellum (Meyers et al. 1998). *Fgf8* is known to lie upstream of the Wnt signalling pathway, and in this mid/hindbrain region, it induces expression of *Wnt1*. Wnt1 in turn maintains expression of *En1* which completes a feedback loop by positively regulating expression of *Fgf8* (Simeone 2000). Other genes which are important for patterning this mid/hindbrain region are *Pax2* and *Pax5*. *Pax5* mutants only show a mild phenotype (Urbanek et al. 1997), however, *Pax2*-null mutant mice do not develop a posterior mesencephalon or cerebellum (Favor et al. 1996). A recent study by (Gao et al. 2007) showed the importance of *Lim1b* in patterning of this area by creating *Lim1b*$^{-/-}$ mutant embryos which displayed abnormal Wnt1, Fgf8, En1, and Gbx2 expression patterns. As a result of this, development of the cerebellum and tectum were severely impaired.

At the rhombic lip, the bHLH transcription factor *Math1* plays an important role in patterning. Indeed, a null mutation of *Math1* in this area halts both precursor

differentiation and migration leading to a complete loss of the cerebellar granule cell layer and hindbrain mossy fibre afferent nuclei (Wingate 2005).

In the cerebellum itself, there is a zone of proliferation in the EGL which has similar characteristics to the proliferative neural crest cells. Proliferation in these cells is known to be regulated by Wnts (Garcia-Castro et al. 2002), coupled with the fact that Wnt1 is expressed in precerebellar progenitor cells of the rhombic lip (Rodriguez & Dymecki 2000), it is very possible that Wnt signalling is plays a role in proliferation in these granule cell precursor cells.

Shh (acting through Ptch) is also thought to play a vital role in normal cerebellar development, and in particular, in regulating EGL progenitor cells (Wechsler-Reya & Scott 2001). Purkinje cells are the main producers of Shh during cerebellar development (Marino 2005), and if Shh is blocked by using antibodies against Shh, then numbers of differentiated granule cells are reduced (Dahmane & Ruiz i Altaba 1999). This effect of Shh on granule cell precursors is thought to be mediated through Shh's role in cell cycle control. Shh induced *cyclinD1* and *cyclinD2* expression during development (Ciemerych et al. 2002) through N-myc (Kenney & Rowitch 2000). Mice lacking either N-myc or cyclinD2 display disorganised cerebellums and fewer cells in the IGL (Huard et al. 1999; Knoepfler et al. 2002).

1.5 Conditional gene targeting of Apc in the brain

Conditional gene targeting is a method for mutating a gene of interest *in vivo*. This approach is very useful, for example in the case of Apc, where a constitutive knockout approach causes embryonic lethality, as well as evaluating the effects of mutating a gene in a specific tissue at a specific time. One of the most widely used methods of conditional gene targeting is the Cre/*loxP* recombination system (Stricklett et al. 1999).

1.5.1 The Cre/*loxP* system

The Cre/*loxP* system allows for the inactivation of the target gene in a single cell type, thereby allowing the analysis of physiological and pathophysiological consequences of the genetic alteration in mature animals. Cre recombinase is a 38-kDa protein encoded by bacteriophage P1. Its roles in the life cycle of P1 are thought to include cyclisation of the linear genome and resolution of chromosomes following DNA replication. A single Cre protein is sufficient to catalyse the recombination between two *loxP* (locus of X-over in P1) sites, each of which is a 34bp DNA sequence containing two 13bp inverted repeats and an asymmetric 8pb spacer region (Stricklett et al. 1999). Cre recombinase expressed ectopically in mammalian cells can cause either deletion or inversion of the sequences which are flanked by *loxP* sites, depending on the orientation of the *loxP* sites (Sauer & Henderson 1988). The main advantage of this system lies in its simplicity. For example, no cofactors are required for Cre activity because the Cre/*loxP* complex forms phosphotyrosine intermediates at the point of strand exchange which provides the necessary energy (Abremski & Hoess

1984). Another advantage is that the *loxP* target sites are small and easily synthesised and Cre recombinase is a stable protein (Stricklett et al. 1999). Finally, a great advantage of the system is that it is relatively easy to generate DNA constructs with a promoter of interest to drive the Cre expression. This last advantage however, can also lead to the main disadvantage of the Cre/*loxP* system. For example, in the case of this project, we wanted to mutate Apc specifically in the EGL of the cerebellum at P4 of development. We had a floxed Apc mouse which expressed *loxP* sites flanking exon 14 of Apc, however, we were unable to identify a suitable gene to act as a promoter for Cre which was expressed specifically at our desired time and place. This led us to look for alternative ways to use the Cre/*loxP* system to mutate Apc.

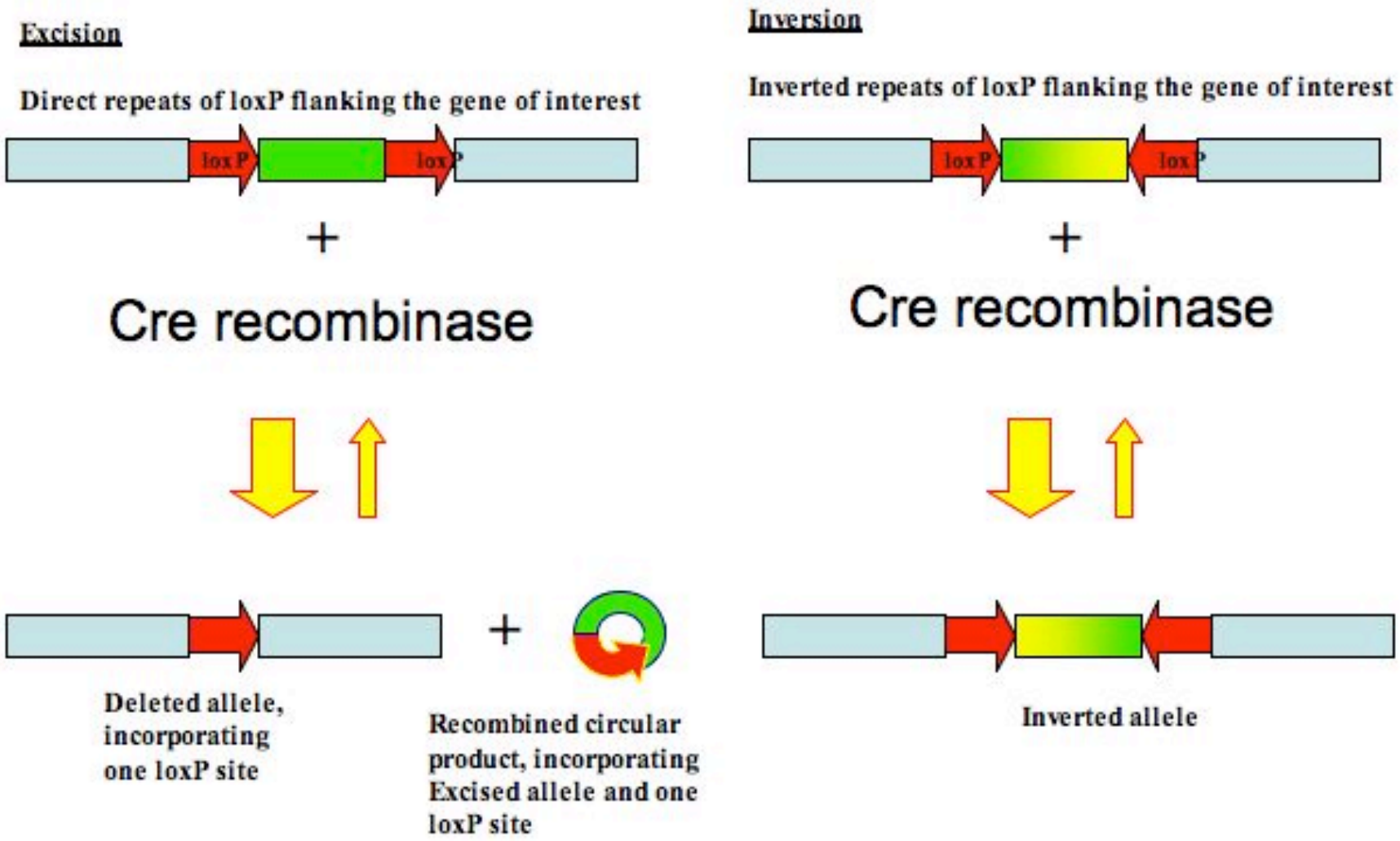

Figure 1.4 The Cre-lox system of site directed recombination.
Recombination of loxP sites is mediated by Cre recombinase. Excision of the floxed allele is energetically favourable over the reverse reaction. Inversion is reversible in the continued presence of Cre.

1.5.2 The Adenovirus-Cre system

Adenoviral vectors have been used for some time for introducing heterologous gene expression in mammalian cells (Berkner 1992; Prevec et al. 1991). They have many advantages, for instance, they can infect a wide variety of dividing or non-dividing cells, they can be purified to high titres, they can accommodate up to 36 kb of foreign genetic material (Parks et al. 1996), to name a few. An adenovirion is a non-enveloped icosahedral capsid with an approximate size of 700nm (Graham 2000) (Figure 4.1A). They contain protein and linear double-stranded DNA of around 30-40kb in size. DNA replication and virion assembly takes place inside the nucleus, producing many thousands of virion before exiting and killing the host cell.

For the transduction of mammalian cells, viral vectors under the control of promoter elements derived from viruses have been commonly used to date. One of the most frequently used promoters in these expression cassettes is that of the human cytomegalovirus (HCMV) immediate early (IE) gene. The HCMV enhancer/promoter directs high levels of transgene expression in a wide variety of cell types (Schmidt et al. 1990). More recent adenovirus vectors have been produced which used the murine cytomegalovirus (MCMV) IE promoter element. Indeed, Addison et al (1997) created such an adenovirus which when compared to an adenovirus driven by the HMCV promoter, was shown to drive higher transgene expression *in vivo* in mice and rats (Addison et al. 1997), indicating that Ad vectors carrying the MCMV IE promoter may be more effective than those with the HCMV IE promoter for transgene expression in animal models.

Adenoviral vectors are commonly created with deletions of the early regions 1 and 3 (E1 and E3) (Danthinne & Imperiale 2000). The E3 region is not essential so can be deleted without hindering the virus's ability to replicate, however E1 region is essential for replication so if deleted, can only be propagated in vitro in cells that express E1 (Graham 2000). Such adenoviruses produced by deleting regions E1 and or E3 are known as First Generation (FG) vectors. FG vectors are useful for applications that require transient gene expression, however are not suitable for long-term expression since they retain most of their viral genes and express them at low levels causing host immune response in vivo.

Cre-expressing adenoviral vectors have been extensively used in the mouse for targeting a variety of tissues such as the intestine (Shibata et al. 1997), the liver (Akagi et al. 1997; Chang et al. 1999; Stec et al. 1999; Wang et al. 1996), the brain (Wang et al. 1996) and in tumours (Sato et al. 1998). These studies have shown that this system for delivering Cre-recombinase in a spatial and temporal manner is very effective. However, there are drawbacks to the system. The main drawback is that adenoviruses, once injected into an area will infect all cells in that area. This is a problem for studies that require delivery of Cre-recombinase directly to specific cell types in, for example, the CNS. Further, adenoviruses are known to be able to infect many different cell types, however not all are equally well infected by the vector (Wang et al. 1996). Another drawback is that complications can arise from using E1 deleted adenoviruses from the expression of viral functions on the vector genomes resulting in host immune response and loss of transduced cells (Badorf et al. 2002). Moreover, incorporation of tissue-specific promoters in first generation adenoviral vectors often results in loss of specificity because of viral elements influencing the

promoter activity (Badorf et al. 2002). Lastly, as will be discussed in a later chapter, delivery of the adenovirus can be problematic. For example, in the case of delivery of an adenovirus to the CNS, one must be very careful not to damage the brain through careless injection technique.

1.5.3 The RCAS/*tv-a* system

Retroviruses are capable of infecting target cells and introducing new genetic information into the chromosomes of these cells. Thus they can be used as vehicles for the delivery of genes into cells. A commonly used retrovirus is the avian leukosis-A virus, RCAS (replication competent ASLV long terminal repeat with splice acceptor). RCAS was derived from RSV-A (Rous sarcoma virus-A) by the replacement of the *src* gene with a multicloning site that stably accommodates inserts of up to 2.5kb (Boerkoel et al. 1993; Greenhouse et al. 1988). These vectors are very widely used for gene transfer because they are replication competent viruses only in avian cells, and high titre viral stocks can be produced without a helper component (Orsulic 2002).

The cloning of the *tv-a* gene in 1993, which encodes for the receptor for ALV-A, called TVA (Bates et al. 1993), has made it possible for RCAS vectors to be used in mammalian hosts such as mice. The receptor is a membrane-associated protein with homology to the ligand-binding repeat of the low-density lipoprotein receptor (LDLR). It was demonstrated that the ectopic expression of *tv-a* in mammalian cells, allows for entry and chromosomal integration by ALV-A (Bates et al. 1993). Without the expression of *tv-a* in the host, the ALV-A viruses would not be able to enter cells.

The advantage that the RCAS/*tv-a* transgenic system in mice has over avian uses of the RCAS virus is that the TVA receptor can be expressed under the control of a cell or tissue specific promoter. For example, only mouse cells that have been manipulated to express the TVA receptor can be infected; whereas mouse cells that do not express *tv-a* are resistant to RCAS infection. Once inside the cell, RCAS virus synthesises a DNA copy of the viral genome and integrates this into the host DNA. Once integrated, the expression of the inserted gene is driven by the viral long terminal repeat (LTR), giving a high level of transcription of the integrated provirus (Orsulic 2002). Further, the lack of viral protein production prevents cell-to-cell spreading of infection, thus reducing any host immune response (Pinto et al. 2000).

There are a few disadvantages however to using this avian system for genetic manipulation. For example, when introducing the RCAS virus into an appropriate *tv-a* expressing host, one has no control over the site at which integration of viral DNA occurs. In a worst-case scenario, the viral DNA could integrate in the proximity of an oncogene and lead to oncogenesis. Another issue is that the efficiency of the infection is dependent upon the accessibility of the organ and the proliferation rate of the target cells, as cell division is required for efficient viral integration (Orsulic 2002). A further disadvantage of using this method over traditional adenovirus methods is the necessity of producing a line of mice expressing the *tv-a* gene. This process adds considerable time and cost to the experiment.

1.6 Aims of thesis

The central aim to this thesis was to assess the role of Apc in the development of medulloblastoma. Our goal was to create a mouse model for medulloblastoma by conditionally inactivating *Apc* specifically in the cerebellum of P4 mice firstly by using the Cre/LoxP systen in combination with the RCAS/*tv-a* to administer Cre-recombinase, and then when that method was unsuccessful, we used an alernative method of administering cre to $Apc^{LoxP/LoxP}$ mice using an adenovirus. A secondary aim of this thesis was to study the role of Apc in normal development in the mid-hindbrain region, an area from which cells migrate from to populate the cerebellum. We did this by crossing the $Apc^{LoxP/LoxP}$ mouse to the *En1-cre* mouse. This was addressed as medulloblastoma is thought of as an embryonal tumour, which arises from cerebellar granule cell precursors, and that dysregulation of normal developmental pathways are involved in medulloblastoma development.

2. MATERIALS AND METHODS

2.1 Methodology for Basic Cloning

2.1.1 Agarose gel electrophoresis using DNA

Agarose gel concentrations used varied from 0.5% to 2% w/v in Tris-borate EDTA (TBE) depending on the size of the DNA molecules. An appropriate mass of agarose powder was boiled (BioWhittaker Molecular Applications) in TBE buffer until dissolved and 0.1mg/ml ethidium bromide (EtBr)(Fisher Scientific) was added. DNA samples (volumes ranged from 2-50µl) were mixed with one-sixth volume of type III loading buffer (see Appendix for all solutions and reagents) and loaded onto the gel. Molecular weight markers were run adjacent to DNA samples. They comprised of 1Kb or 100bp (New England Biolabs) and were diluted in loading buffer. Electrophoresis was carried out in 1X TBE at 50-100V for periods of 25 minutes to 3 hours, with the exception of genomic DNA which was performed at 40 Volts for 12 hours. Gels were visualised using UV light on a transilluminator.

2.1.2 Restriction endonuclease digestion of DNA

Plasmid DNA (1µg-5µg) was mixed with 0.1 volumes of 10X reaction buffer, 0.1 volumes of appropriate restriction endonuclease, and the volume made up to 20-50µl with ddH_20. The digests were incubated in a shaking water bath set to 37°C for 90 minutes. Genomic DNA was digested as above except that digests were incubated at 37°C overnight to allow for complete digestion of genomic DNA. All restriction endonucleases were purchased from New England Biolabs, Promega Ltd., or Roche.

2.1.3 Extraction of DNA fragments from agarose gels

The QIAquick^{TM}Gel Extraction Kit (Quiagen) was used for the extraction of DNA fragments from agarose gels. DNA was digested with restriction endonucleases and electrophoresed on an agarose-TBE gel stained with ethidium bromide. A clean scalpel was then used to excise the DNA from the gel. The gel slice was weighed and 3 volumes of Buffer QG were added (eg. 100µl of buffer QG per 100mg of gel). The solution was heated to 50°C until the gel had dissolved completely. One gel volume of isopropanol was added to the solution, mixed, and applied to a Quiaquick spin column and centrifuged for 1 minute at 13 000rpm. To wash the DNA, 0.75ml of buffer PE was added to the column, centrifuged for 1 minute at 13 000rpm and the flow-through again discarded. To remove the last traces of buffer PE, the column was centrifuged once more then placed in a 1.5ml eppendorf tube. 30µl of water was then added to the centre of the column and the column allowed to stand at room temperature for 1 minute. The DNA was eluted by centrifugation at 13 000rpm for 1 minute and the elute then transferred to a fresh 1.5ml eppendorf tube. DNA concentration could then be determined by electrophresis and either used immediately or stored at -20°C.

2.1.4 DNA ligation

DNA to be used as an insert in a ligation reaction was first purified by agarose gel electrophoreses and quantified on an agarose gel. An approximate 3-5 fold molar excess of insert DNA was added to vector DNA (10-15ng/µl) and diluted to 8µl with

water. 1μl of 10 ligation buffer was added to the solution followed by 1μl T4 DNA ligase (1 U/μl; Boehringer Mannheim). The solution was then incubated at 4^0C overnight.

2.1.5 Transformation of competent bacteria

For routine transformations DH5α *E.coli* cells were used. 200μl aliquots were removed from -80^0C storage and thawed on ice in a 12ml snap top Falcon 2059 tube. 5μl of plasmid DNA was added directly to the cells and then the tube was tapped gently to mix. The cells and DNA were incubated on ice for 30 mintes, then heat-shocked in a water bath set to 42^0C for 60 seconds, and returned straight onto ice. 500μl of room temperature 2XTY media was added before shaking the tubes at 37^0C for 1 hour in a shaking incubator at 225rpm. The transformed bacteria were plated onto LB-agar plates containing appropriate antibiotics to select for transformants. Plates were inverted and incubated overnight at 37^0C. For all other transformation reactions, aliquots of JM109 competent *E.coli* cells (Promega) were used. Transformation protocol was as above except that the heat-shock duration was 30 seconds followed by the addition of 500μl of preheated SOC medium.

2.1.6 Mini and Midipreps

For small scale preparations of plasmid DNA, a QUIAGEN QIA prep Spin Miniprep kit was used to purify the plasmid DNA from the transformed bacterial cells. A single bacterial clone was picked using a sterile yellow pipette tip. The clone was transferred to a falcon 2059 tube containing 1.5ml of LB medium supplemented with appropriate

antibiotics. This was then incubated overnight at 37^0C in a shaking incubator (225rpm). The next day, the bacterial culture was poured into a 1.5ml eppendorf microcentrifuge tube and spun at 13,000 rpm for 1 minute. The supernatant was discarded and the bacterial pellets were resuspended in 250µl of resuspension buffer (50mM Tris-HCl pH7.5, 10mM EDTA, 100g/ml RNase A). 250µl of bacterial lysis solution (0.2M NaOH, 35mM SDS) was added, and mixed by inversion to lyse the cells. The reaction was then neutralised by adding 350µl of neutralisation buffer (1.32M potassium acetate pH4.8) and mixed by inversion. The protein precipitate which subsequently forms was removed by centrifugation for 10 minutes at 13 000 rpm. The supernatant was transferred to a QIASpin filter tube and placed in a collection tube and the liquid was passed through the filter by centrifugation for 1 minute at 13 000 rpm. 750µl of wash buffer (80mM potassium acetate, 8.3mM Tris-HCl pH 7.5, 40M EDTA, 55% (v/v) ethanol) was added to the QIASpin filter tube and then centrifuged for 1 minute at 13 000 rpm. To remove all the wash buffer, the collection tube was emptied and the filter tubes spun again for 1 minute at 13 000 rpm. The filter tube was then placed in a fresh 1.5ml eppendorf before adding 50µl of water. The tube was incubated at room temperature for 1 minute and then spun for 1 minute at 13 000 rpm. The eluted DNA was either used immediately or stored at -20^0C.

To achieve greater quantities of DNA than could be produced by the miniprep method, midipreps were carried out using the Quiagen Plasmid Midi Kit. A conical flask containing 50ml of LB or 2XTY medium, supplemented with appropriate antibiotics, was inoculated with bacteria created from a suitable miniprep culture. The bacteria was shaken at 225 rpm at 37^0C for 12 – 16 hours. The culture was then

centrifuged at 6 000g for 5 minutes at 4^0C, and the supernatant removed. The cells were re-suspended, lysed and neutralised using the same solutions as for the miniprep method. The protein precipitate was removed by centrifugation at 20 000g for 30 minutes at 4^0C. Supernatant was removed and re-centrifuged at 20 000g for 15 minutes at 4^0C, then added directly to equilibrated QIAGEN-tips, and allowed to pass through the DNA binding resin by gravity flow. Columns with bound DNA were washed with the supplied wash buffer (as above) twice prior to elution of the DNA. DNA was removed from the column using the supplied elution buffer (as above) before the addition of 0.7 volumes of isopropanol. The DNA was collected by centrifugation at 15 000g for 30 minutes at 4^0C. 70% ethanol was used to wash the DNA pellet before re-centrifugation for 1 minute at 13 000 rpm. The DNA pellet was re-suspended in 100µl of water and either stored at -20^0C or used immediately.

2.2 Dissecting mouse tissue for histological analysis

2.2.1 Harvesting embryos

The mother was humanely killed by cervical dislocation and the embryos were dissected out in ice cold PBS before being placed directly into 4% PFA overnight. For embryos older than E15.5, the heads were removed and the bodies discarded to ensure that the PFA could penetrate the brain tissue more effectively. After fixation, the embryos were washed 3 times in PBS for 5 minutes each with shaking before being placed in 50% ethanol ready for processing and embedding in paraffin blocks. The processing and embedding was carried out by our histological technicians.

2.2.2 Harvesting postnatal mouse brains

Mice were perfused with 4% PFA and the skulls removed before removing the brain from the head. Depending on what the tissue was for, either the whole brain was placed into 4% PFA overnight, or the cerebellum was removed and placed into 4% PFA fix overnight. The tissue was then washed and processed as above.

2.3 Histological analysis

10μm sections were cut from paraffin embedded tissue and floated onto Poly-L-Lysine (Sigma) coated slides in a water bath set to 42^0C. Slides were then stained with haematoxylin and eosin for histological analysis.

2.4 Immunohistochemistry

Immunohistochemistry was carried out using the DAKO envision plus system (cat. # K4006 for mouse kit and K4010 for rabbit kit) and performed using the manufacturers guidelines. β-catenin was detected using a mouse monoclonal antibody (BD Biosciences cat. # 610154) (see appendix for protocol) using the mouse DAKO envision kit. These kits come with a peroxidase blocking solution, and a peroxidase labelled polymer conjugated to goat anti-mouse immunoglobulins. Staining is visualised with 3,3'-diaminobenzidine (DAB) + substrate-chromagen which results in a brown-coloured precipitate forming at the antigen site.

Slides were dewaxed in xyline and rehydrated in an alcohol series before being placed in ddH_2O. Antigen retrieval was carried out in 10mM Na-Citrate buffer, pH 6, and the slides were microwaved three times at 700W for 5 minutes each and cooled on ice for 20 minutes. The slides were washed in ddH_2O, incubated in peroxidase block for 5 minutes before being rinsed in ddH_2O and then placed into PBS for 5 minutes. Slides were incubated in antibody buffer (1 in 5 dilution of goat serum in PBS) for 10 minutes before the addition of primary antibody at an optimal concentration of 1 in 100 dilution for 1 hour at room temperature. Slides were thoroughly rinsed in ddH_2O and incubated in HRP anti-mouse secondary antibody for 30 minutes at room temperature. Slides were thoroughly washed in ddH_2O before the addition of DAB solution. Once appropriate staining had occurred, the DAB solution was washed off with ddH_2O, counterstained with haematoxylin and then dehydrated through an alcohol series, cleared in xyline and mounted using DPX mounting media (Sigma). See appendix (Section 8.2.2) for a detailed protocol.

Apc was detected using an Apc C-terminal rabbit polyclonal primary antibody (Santa Cruz cat. # sc896) (see appendix for protocol), and the DAKO envision plus rabbit kit. The protocol was as above except all washes were carried out three times for 5 minutes each with PBSTx in an effort to reduce background staining. Antigen retrieval was carried out in10mM Na-citrate 4 times for 5 minutes in a 700W microwave. The primary antibody was titrated and used at an optimal concentration of 1 in 500 dilution overnight at 4^0C. See appendix (section 8.2.1) for a detailed protocol.

Nestin immunohistochemistry was carried out using identical conditions to those of the β-catenin immunohistochemistry (see appendix for protocol, section 8.2.2) except a Nestin antibody was used at a concentration of 1:200 in antibody buffer.

Pax 3 immunohistochemistry was carried out using identical conditions to those of the Apc immunohistochemistry (see appendix for protocol, section 8.2.1) except a Pax 3 antibody was used at a concentration of 1:100 in antibody buffer.

2.5 Tissue Culture

2.5.1 DF-1 cells

DF-1 cells were stored at -80^{0}C in CryoTube^{TM} vials (Nunc) and were thawed with gentle agitation in a water bath prewarmed to 37^{0}C. The cell suspensions were then dispersed into 25ml of DMEM culture media (Gibco. Cat # 11960-044) supplemented with 10% (w/v) foetal calf serum (FCS), 20mM L-Glutamine (Sigma), 20U/ml Penicillin (Sigma) and 20μg/ml Streptomycin (Sigma). Cells were incubated at 37^{0}C in an atmosphere of 5% CO_2 in Sanyo CO_2 incubators. Cells were cultured in disposable sterile plasticware flasks and petri dishes (either Nalge-Nunc or Greiner). All media added to cells was sterile and prewarmed in a water bath to 37^{0}C.

2.5.2 Trypsinisation of cells in a T75 flask

The medium was aspirated off and the cells washed twice with 5 ml of PBS buffer to remove all the old media. The PBS was aspirated off before the addition of 1 ml

Trypsin solution. The flask was gently rocked so the typsin covered all the cells before being incubated at 37^0C for 2-3 minutes (or until cells started to come off the culture flask when gently tapped). 2 ml of culture medium was added to the flask using a pasture pipette and the solution drawn up and down the pipette several times to break up the clumps of cells and remove all the cells from the side of the flask. The liquid transferred to a 15ml centrifuge tube and made up to a volume of 10 ml by adding 8 ml fresh culture medium. The tube was centrifuged at 1000 rpm for 5 minutes to create a pellet of cells at the bottom of the tube. The media was aspirated off and 10ml of PBS added before further centrifugation at 1000rpm for 5 minutes. The PBS was aspirated off and the bottom of the tube tapped to loosen the cells. The cells could either be re-suspended in fresh media and plated at a density of 2 x 10^6 cells/ml or resuspended in freezing media to a concentration of 4 x 10^6 cells/ml and stored at -80^0C.

2.5.3 Transfecting cells using GeneJuice transfection reagent

Stably transfecting RCAS-cre and R26R plasmids into DF-1 cells was carried out using GeneJuice transfection reagent (Merck). 45µl of GeneJuice reagent was added to 800µl of serum free DMEM media in a sterile 1.5ml eppendorf. The contents were mixed by inversion and incubated at room temperature for 5 minutes. 15µl plasmid DNA was added and the contents mixed again and incubated for 15 minutes. This mix was then added evenly over sub-confluent DF-1 cells in a 10cm tissue culture petri dish containing DMEM supplemented with 10% FCS. The cells were then incubated for 5 hours at 37^0C. The transfection mix was then aspirated off and replaced with complete growth medium (lacking antibiotics). Cells were incubated for 2 days until confluence was reached. The virus was then titred by extracting the supernatant and

making a series of 10-fold dilutions of the viral supernatant (from 10^o to 10^9) in growth medium. 1ml of each dilution was added to a 60 mm TC dish containing DF-1 cells. Dishes were then incubated for 3 hours at 37^oC. 2 ml of growth medium was added to each dish. Cells were allowed to grow for 4 to 7 days and assayed for gene expression by plating cells on a glass coverslip and viewing under a fluorescent microscope.

2.5.4 Preparing RCAS containing DF-1 cells for injection into mice

On day of experiment, RCAS containing DF-1 cells where trypsinised from T75 flask and a cell count was carried out to determine the number of cells in the flask. The cells were then resuspended in an appropriate volume of DMEM (lacking antibiotics) so that 1μl contained $1x10^4$ RCAS containing DF-1 cells. This virus preparation was then aliquoted into eppendorfs. From this, 1μl containing $1x10^4$ RCAS containing DF-1 cells was injected into the hindbrain region of 127 postnatal day 4 (P4) mice.

2.6 Isolating stably transfected clones

Cells which were successfully transfected with R26R plasmid carried antibiotic resistance so could be separated from non transfected clones by adding Geneticin (G418) Sulphate (Invitrogen). G418 was added at an optimal concentration of 400μg/ml and incubated at 37^0C. Cells were checked each day and single colonies of cells were picked by applying 2μl of trypsin directly onto the colony and then

immediately drawing the cells into the pipette tip. The cells were transferred into a 96 well tissue culture plate in 200µl complete growth media. Once confluent, cells were transferred into a T25 and then again into a T75 flask once confluence had been achieved.

2.7 Isolating genomic DNA from mouse ear or tail biopsies

For genotyping purposes, DNA was extracted from either ear clips or tail tips. 500µl of lysis buffer (TTLB) was added to the ear clips in a 1.5 ml eppendorf tube and incubated overnight at 55^0C in a shaking water bath. 300µl phenol chloroform was added and the mixture vortexed to mix before being incubated at room temperature for 5 minutes. The tubes were centrifuged at 13,000 rpm for 1 minute to leave an upper aqueous phase which was subsequently removed into a fresh 1.5ml eppendorf containing 2.5 volumes of 100% ethanol and 0.1 volumes of 3M NaOAc. The tubes were vortexed to mix and incubated for 30-60 minutes at -20^0C to allow the DNA to precipitate. The tubes were centrifuged at 13,000 rpm for 15 minutes to pellet the DNA and 200µl of ddH_2O added to re-suspend the DNA if using ear clips. When using tail tips, 400µl ddH_2O was used to re-suspend DNA. In order to remove all residual traces of ethanol, the tubes were incubated at 55^0C for 45 minutes on a PCR block with the caps left open to allow ethanol to evaporate. The samples were then vortexed and briefly centrifuged to collect the entire sample at the bottom of the tube.

The DNA could then be used directly in a genotyping PCR reaction, or stored at -20^{0}C.

2.8 Southern Blot

2.8.1 Making Probe

Probe used was designed based on Probe C described by Shibata et al. (1997) and is a 1kb Hind III – Xba I fragment derived from exon 15 of *Apc*. Using primers which flanked the 1kb Hind III – Xba I fragment of *Apc*, PCR was used to create the desired probe from genomic DNA. The probe was then transformed in *E.coli* and purified with a midiprep.

A restriction digest was then set up using 40µl of midiprep DNA with 5µl of EcoR1 and 5µl of enzyme buffer and incubated at 37^{0}C overnight. The digest DNA was then run on an agarose gel before being cut out and gel purified.

2.8.2 Making Southern quality DNA

Tissue (eg half of cerebellum) was digested overnight at 55^{0}C in 500µl of TTLB with proteinase K. Equal volumes of phenol chloroform (500µl) was added to DNA and mixed by inverting for 10 minutes. The tubes were centrifuged at 13,000 rpm for 1 minute to leave an upper aqueous phase which was subsequently removed into a fresh 1.5ml eppendorf containing 2.5 volumes of 100% ethanol and 0.1 volumes of 3M NaOAc. Eppendorfs were shaken hard for a few seconds until a white precipitate formed. This precipitated DNA was removed from the solution and dipped in 70%

EtOH to clean before being put in a clean eppendorf. DNA was then left for 2-3 hours to dry before addition of 20µl of buffer TE. DNA was then re-suspended in a 37^0C shaking water bath overnight. Once the DNA had re-suspended, it was cut using a restriction digest containing 40µl DNA, 5µl 10x buffer, 2µl spermidine, and 2µl Sac I restriction enzyme. Digest was incubated overnight at 37^0C before the addition of 10µl loading buffer. Samples were then run on an 0.8% maxi gel (containing no ethidium bromide) for 16 hours at 40V.

The gel was ethidium bromide stained and images of the electrophoresed DNA were captured on a UV transilluminator for later comparison. Transfer of the DNA to the nylon membrane was improved by partial depurination ('acid nick') of the DNA prior to transfer. Partial depurination was achieved by soaking the gel for 30 minutes in 0.2M HCI. The gel was then soaked in 500ml of southern denaturation buffer for 30 minutes to denature the DNA. After a brief rinse with water the gel was submerged in 500ml of southern neutralisation buffer for 30 minutes. Meanwhile a sheet of Hybond®-N nylon membrane (Amersham Pharmacia Biotech) was briefly equilibrated in transfer buffer (10X SSC). DNA was transferred from the gel onto the membrane overnight. The membrane was subsequently rinsed in 2XSSC, UV cross linked and baked at 120°C for 20 minutes. Membranes were stored between sheets of Whatman 3MM paper at room temperature until ready to probe.

2.8.3 Prehybridisation

The prepared membrane was rolled between two hybridisation meshes in a hybridisation tube (Hybaid) and 25mls of Church Hybridisation buffer, preheated to 65°C, was added. Salmon sperm DNA was denatured for 5 minutes in a water bath set to 100^0C and added to a final concentration of 0.1mg/ml to reduce background hybridisation. Membrane and buffer were incubated with rotation at 65°C for 3 hours in a hybridisation oven (Hybaid) to allow the membrane to equilibrate.

2.8.4 Making radiolabelled probe

25ng of clean probe DNA was made up to 45µl with buffer TE and added on top of the labelling mix (Rediprime II Random Probe Labelling System, Amersham Pharmacia). 5µl of ^{32}P-dCTP was added and mixed by pipetting, and incubated at 37°C for 10 minutes. The reaction was stopped by the addition of 5µl 0.2M EDTA (pH8). Labelled probe was separated from unincorporated nucleotides using a Sephadex G50 column (Amersham Pharmacia Biotech). The column is equilibrated by centrifugation at 3000rpm for 1 minute. The radiolabelled probe solution was added to the column, centrifuged at 3000rpm for 2 minutes and the elute containing the radiolabelled probe was collected in a 1.5ml Eppendorf tube. Unincorporated nucleotides remained in the column and it was discarded. The radiolabelled probe was denatured by placing in a hot block at 100°C for 10 minutes, and placed on ice.

2.8.5 Hybridisation

Following prehybridisation, the Church buffer was removed and 10mls of fresh church buffer, preheated to 65°C and containing salmon sperm DNA, was added to

the hybridisation tube. The radiolabelled probe was then added and the membrane was incubated with rotation overnight at 65°C. The membrane was washed four times for 30 minutes each in Church Wash at 65°C. Following these washes the membrane was removed from the hybridisation tube, sealed in Saran wrap and exposed to MR X-ray film (Kodak) in an autoradiography cassette. Autoradiography cassettes were stored at -70°C for 1-5 days, depending on signal strength. Autoradiography films were then developed (Hyperprocessor, Amersham).

3. Deleting Apc in the early postnatal hindbrain using the RCAS/*tv-a* system

3.1 Background

With this experiment, our aims were to test the hypothesis that the loss of *Apc* on both chromosomes leads to MB development in mice. We used a variation of the Cre-loxP method of selectively mutating genes in a spatial and temporal manner.

In an attempt to deliver Cre-recombinase, stage- and site- specifically, we utilised retroviruses. We decided on this approach because there was not an appropriate Cre strain of mouse available at that time. Ideally, we wanted a strain of mouse that expressed Cre-ER under the control of the nestin promoter and enhancer. Cre-ER is a fusion of Cre and the mutated ligand-binding domain of the human oestrogen receptor α. Upon administration of tamoxifen, the Cre-ER is turned from an inactive state to an active one, which is capable of recombination (Imayoshi et al. 2006). Unfortunately, there was not an ideal Cre mouse strain available at the time, so we decided to use a retroviral method. Since the time of this experiment, Imayoshi et al. (2006) have generated a Nestin-CreER strain of mouse.

To mutate *Apc* specifically in the hindbrain at early postnatal stages to create a mouse model for MB, we used the RCAS/*tv-a* system with an RCAS virus which expressed Cre-recombinase and green fluorescent protein (GFP) (Gift from Eric Holland, MSKCC) in infected cells, and a mouse strain which expresses the *tv-a* gene under the nestin promoter. Nestin is an intermediate filament protein, expression of which is

extensively used as a marker for CNS progenitor cells (Dahlstrand et al. 1995). The nestin promoter was deemed to be the best promoter to drive expression of the *tva* gene, as it has been shown to be expressed in proliferating neural precursor cell populations with very high expression from E7.75 to E15.5, and reducing in its expression during the later part of neural development until P0 stage where its expression is restricted to the developing CB and the ventricular and subventricular areas of the telencephalon (Dahlstrand et al. 1995). From the literature, we would expect that MBs form in proliferating cells of the EGL of the postnatal cerebellum, and since these cells are neural precursor cells, we would expect them to express nestin. However, to date the expression of nestin has not been published in enough detail for us to be sure of its exact expression pattern at postnatal day 4, when we ideally wanted to mutate *Apc*. Therefore, immunohistochemistry for the nestin protein was carried out to ascertain the exact expression of nestin in the CB at P4.

3.2 Results

3.2.1 Nestin expression

We removed the brains from P4 wild-type CBAxBl 6 F1 mice and fixed them in paraformaldehyde. They were embedded in wax and cut in a sagittal plane. Immunohistochemistry was then performed using the nestin primary antibody as described in the materials and methods section. Figure 3.1 shows nestin expression in the filaments of these proliferating EGL cells of the cerebellum. No nestin expression was observed anywhere else in the CNS at this stage of development.

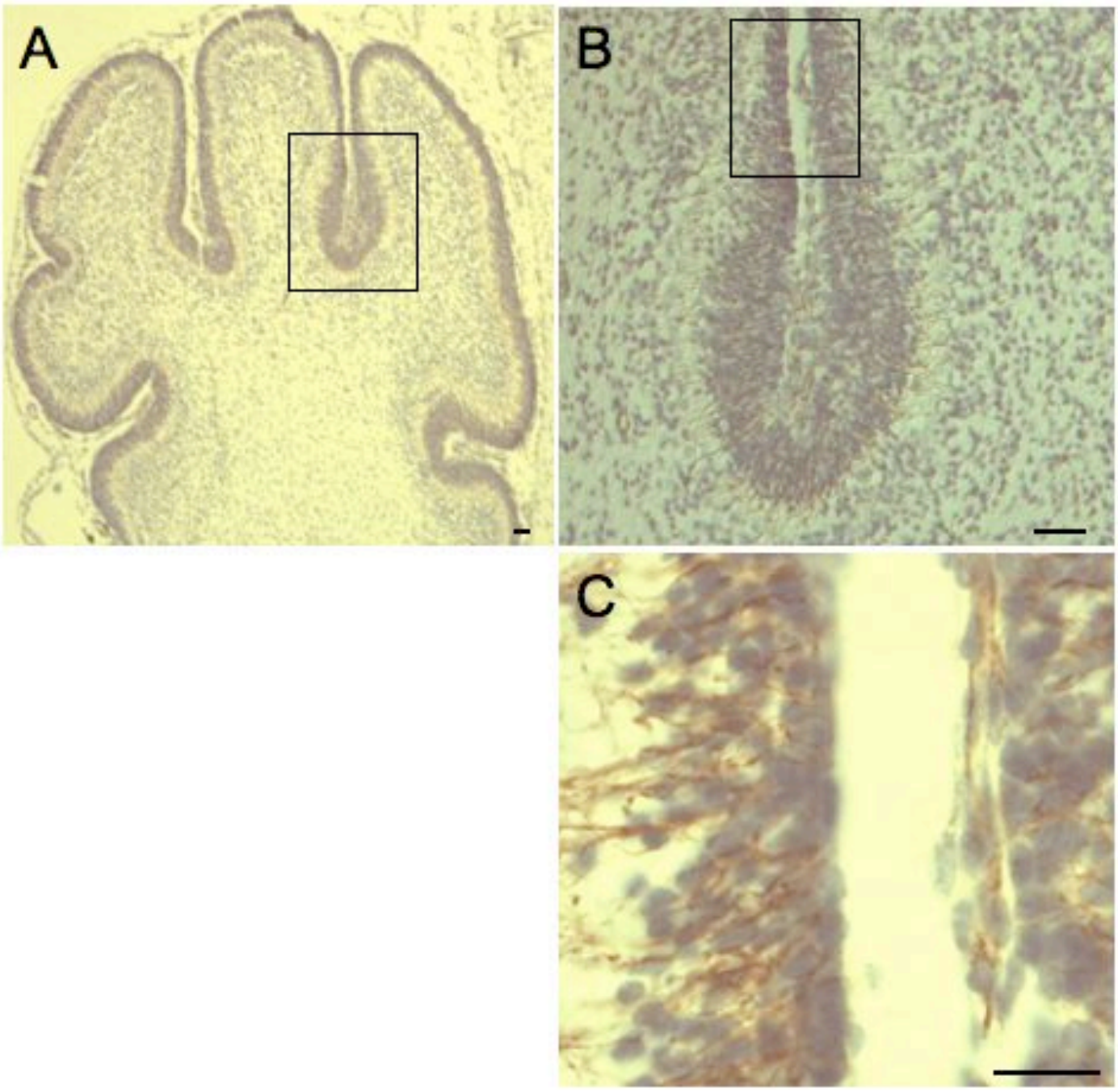

Figure 3.1: Immunohistochemistry showing nestin expression in the developing postnatal day 4 cerebellum. Sections cut in the sagittal plane. Figure A shows a P4 CB with brown nesting staining localised to the external germinal layer. Figures B and C show higher magnifications of the same section. Scale bars: A and B = 40 μm, C=20 μm.

3.2.2 Apc expression

For *Apc* to be mutated in the EGL of the cerebellum, it must be expressed in the EGL of the cerebellum. Therefore, we carried out immunohistochemistry using an Apc primary antibody. This experiment was necessary because previous studies of Apc expression in the CNS were not conclusive (see introduction section 1.2.3) and did not show a detailed expression pattern of Apc in the CB at P4 stage of development. The results of our Apc immunohistochemistry show that Apc is strongly expressed in the GCPs and throughout the cerebellum. (Figure 3.2)

3.2.3 RCAS-Cre virus preparation

Once it was established that both Apc and nestin were expressed in the expected patterns, we obtained an aliquot of the RCAS-Cre plasmid. This had to be propagated in *E. coli* to produce a large midi prep stock. This DNA was then transiently transfected into DF-1 (chicken fibroblast) cells. Since the RCAS virus has the ability to replicate and infect other DF-1 cells, any successfully transfected DF-1 cell will produce RCAS-Cre virus and within a few days, will infect all the cells in the dish. The RCAS-Cre plasmid also carries GFP in the insert. This made it easy to test the trasfection efficiency as a sample of transfected cells could be grown on a poly-L-lysine coated coverslip and observed under a fluorescent microscope. Under fluorescent light, cells expressing RCAS-Cre appear green and non-infected cells will be invisible. Figure 3.3 compares a white light picture to a fluorescent picture of transfected DF-1 cells. Although the picture quality is not perfect, when looking down the microscope, it could be observed that 100% of cells fluoresced green and therefore carry the RCAS-Cre virus.

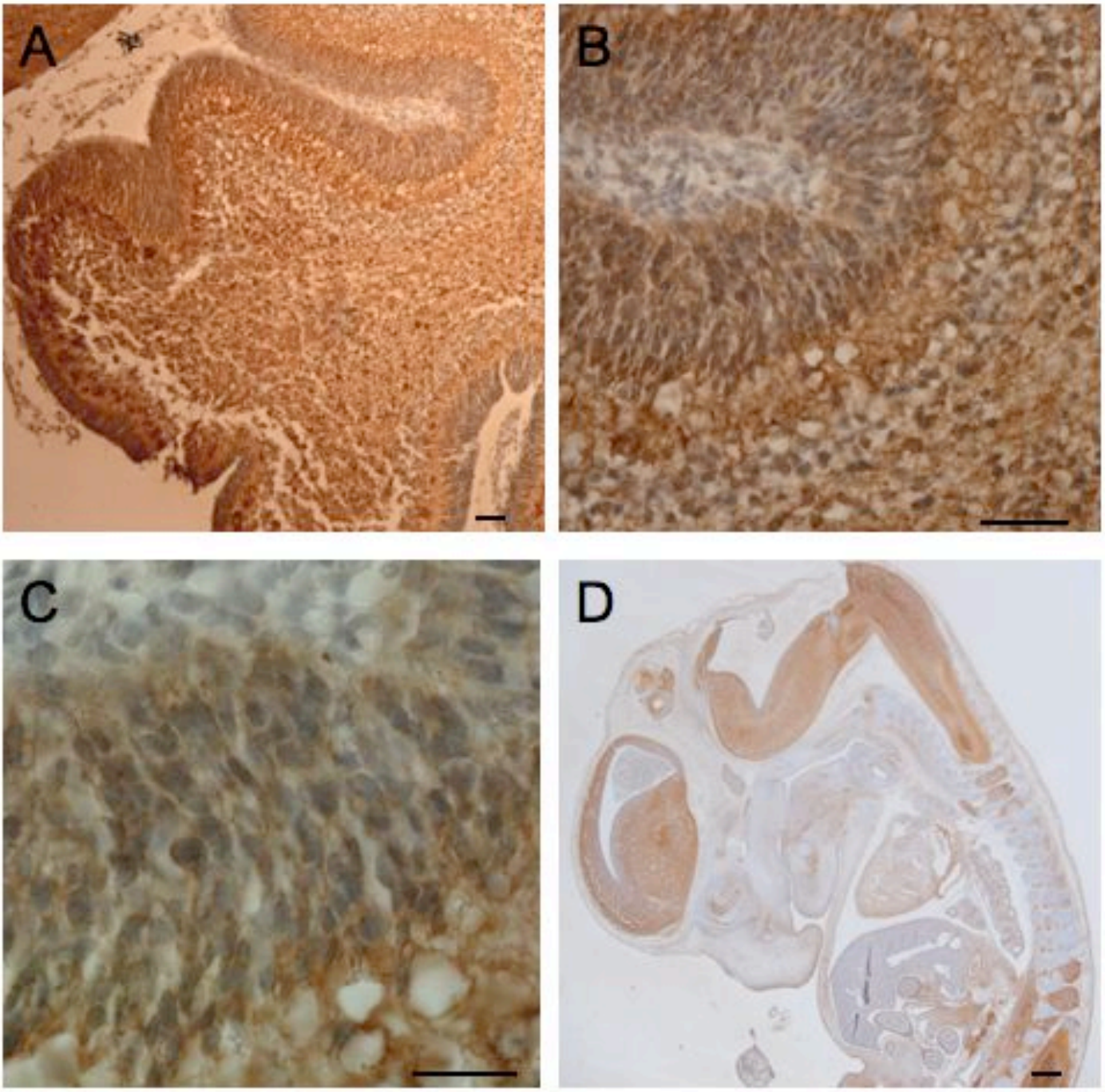

Figure 3.2: Immunohistochemistry showing Apc expression in the developing postnatal day 4 cerebellum. Sections cut in the sagittal plane. Figure A shows a P4 CB with brown Apc staining throughout the cerebellum and notably in the external germinal layer. Figures B and C show higher magnifications of the same section. Figure D shows a control mouse embryo illustrating tissue specificity of the antibody. Scale bars: A and B = 40 μm, C=20μm, D=10μm.

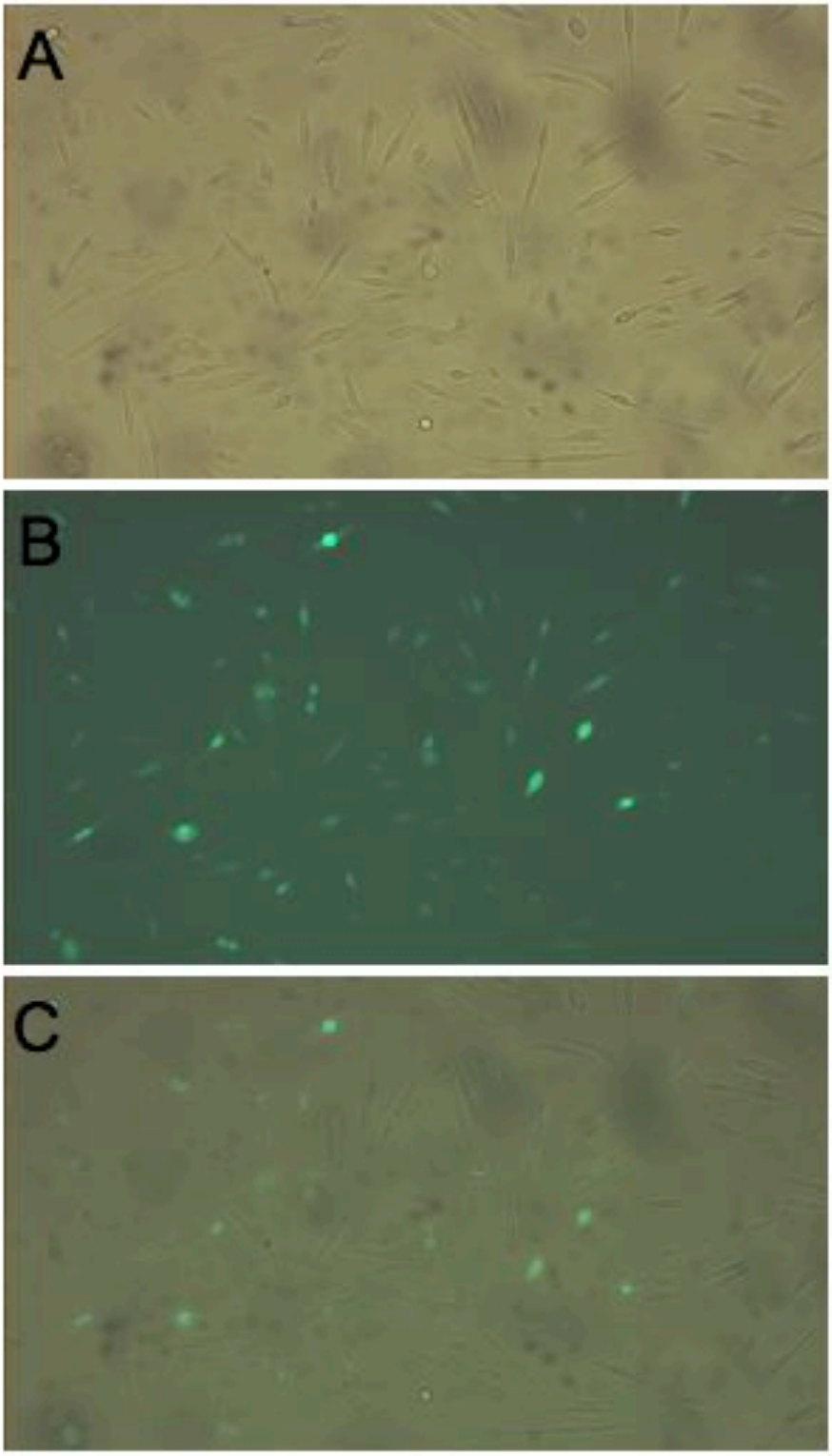

Figure 3.3: Figure showing transient transfections of RCAS-Cre into DF-1 cells. A, shows cells under white light. B shows same cells fluorescing green due to expression of GFP. Figure C shows previous figure merged. All cells were observed to be expressing GFP therefore must be expressing RCAS-Cre

3.2.4 Generation of experimental animals

Mouse crosses were set up to create animals of the desired genotype (*Ntv-a* $^{+}$*;Apc*$^{LoxP/LoxP}$*).* A diagram of how the crosses were set up can be seen in Figure 3.4. 1μl containing 1x10^{4} RCAS containing DF-1 cells was injected into the hindbrain region of 127 postnatal day 4 (P4) mice. These mice were the progeny of a cross between an *Ntv-a*$^{-}$*;Apc*$^{LoxP/LoxP}$ male and a *Ntv-a*$^{+}$*, Apc*$^{LoxP/+}$ female. The resultant progeny were expected to follow Mendelian genetics giving us 1 out of 4 animals of the desired genotype. 2 weeks after injection, the animals could be ear-punched for genotyping. Results of genotyping showed no animals of the desired genotype. The PCR genotyping was repeated with the same result. Our conclusion from this was that *tv-a* and *Apc* must be located on the same chromosome. This would necessitate a recombination event taking place for us to see our desired genotype (Figure 3.4B). If this recombination took place, then the reciprocal recombination genotype to *Ntv-a*$^{+}$*;Apc*$^{LoxP/LoxP}$*,* which is *Ntv-a*$^{-}$*;Apc*$^{LoxP/+}$*,* would also not be observed in any of the injected animals.

Animals with the genotype is *Ntv-a*$^{-}$*;Apc*$^{LoxP/+}$*,* would have been uninfectible with RCAS-Cre, and so were classed as a control. Mice with the genotype *Ntv-a* $^{+}$*;Apc*$^{LoxP/LoxP}$*,* we called our experimental group as these are the ones which would be infectible with RCAS-Cre, and were homozygous for the floxed Apc allele. The genotyping results showed that 4 out of the 127 RCAS-Cre injected animals had the control genotype (*Ntv-a*$^{-}$*;Apc*$^{LoxP/+}$*)* implicating that a recombination event had taken place. This gave us hope that the transgenes were relatively far apart on the chromosome making it possible for recombination events to take place. We reasoned that if we set up many crosses of animals with the genotypes as follows; *Ntv-a* $^{+/-}$*,*

$Apc^{LoxP/+}$ X $Apc^{LoxP/LoxP}$, we would eventually get an animals with the desired experimental genotype (*Ntv-a* $^{+}$;$Apc^{LoxP/LoxP}$). An additional advantage of creating such a recombinant mouse is that it would generate large numbers of suitable mice because the *tv-a* transgene would be fixed on the same chromosome as the floxed allele and would therefore be co-inherited at a high frequency.

In total, 15 crosses were set up which produced 138 pups. When genotyped, no animals were found to have either of the recombinant genotypes. From this result, the validity original genotypes of the four recombinant animals were brought into question. When re-genotyped, the animals were found to actually have the genotype *Ntv-a* $^{+}$;$Apc^{LoxP/+}$ (not recombinants) (Figure 3.5). Therefore, out of 265 mice, none were found to have either the experimental or control recombinant genotypes. The null hypothesis would state that the resultant progeny were expected to follow Mendelian genetics giving us one out of four animals of the desired genotype (Figure 3.4D). To test whether there was a high probability that our results could be due to chance, a chi-squared test was performed to compare the observed results against the expected result. The result of this test showed $p< 0.001$, hence we can reject the null hypothesis that the observed values of our cross are the same as the theoretical distribution of a 3:1 ratio.

To approximately determine the distance between the *Ntv-a* and Apc^{LoxP} alleles we can use the technique devised by T.H. Morgan, who was the first person to discover linkage. Indeed, the ratio of recombinants to non-recombinants can give an indication of the genetic distance between two loci. If 1 centimorgan equals 1% of recombination events which take place, and if 1 centimorgan also equals 1000 kilo

base pairs (kbp) in the mouse, we can work out that since we saw 0 recombination events in 265 mice, then the genetic distance between alleles must be less than 1000kbp.

A $Ntv\text{-}a^{+};Apc^{+/+}$ X $Ntv\text{-}a^{-};Apc^{LoxP/LoxP}$

B $Ntv\text{-}a^{+};Apc^{LoxP/+}$ X $Ntv\text{-}a^{-};Apc^{LoxP/LoxP}$

Ntv-a+; APC loxP/+

C

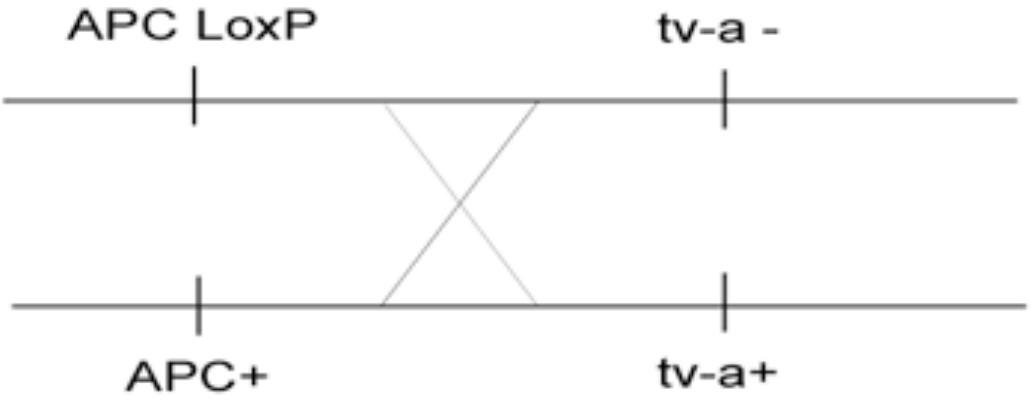

D

Genotypes	No. of mice expected	No. of mice observed
$Ntv\text{-}a^{+};Apc^{LoxP/+}$	64	136
$Ntv\text{-}a^{-};Apc^{LoxP/LoxP}$	64	129
$Ntv\text{-}a^{-};Apc^{LoxP/+}$	64	0
$Ntv\text{-}a^{+};Apc^{LoxP/LoxP}$	64	0

Figure 3.4: Breeding strategy for $Ntv\text{-}a;Apc^{LoxP/LoxP}$ mice. A,*Nestin tv-a* (*Ntv-a*) mice were crossed with homozygous $Apc^{loxP/LoxP}$ mice. B: The resulting progeny of this cross with the genotype $Ntv\text{-}a^{+};Apc^{LoxP/+}$ were again crossed to $Apc^{LoxP/LoxP}$ mice. C: Diagram of the recombination even that would have to take place to produce mice of the desired genotype of $Ntv\text{-}a^{+};Apc^{LoxP/LoxP}$.D, table of mice expected of each genotype against observed results.

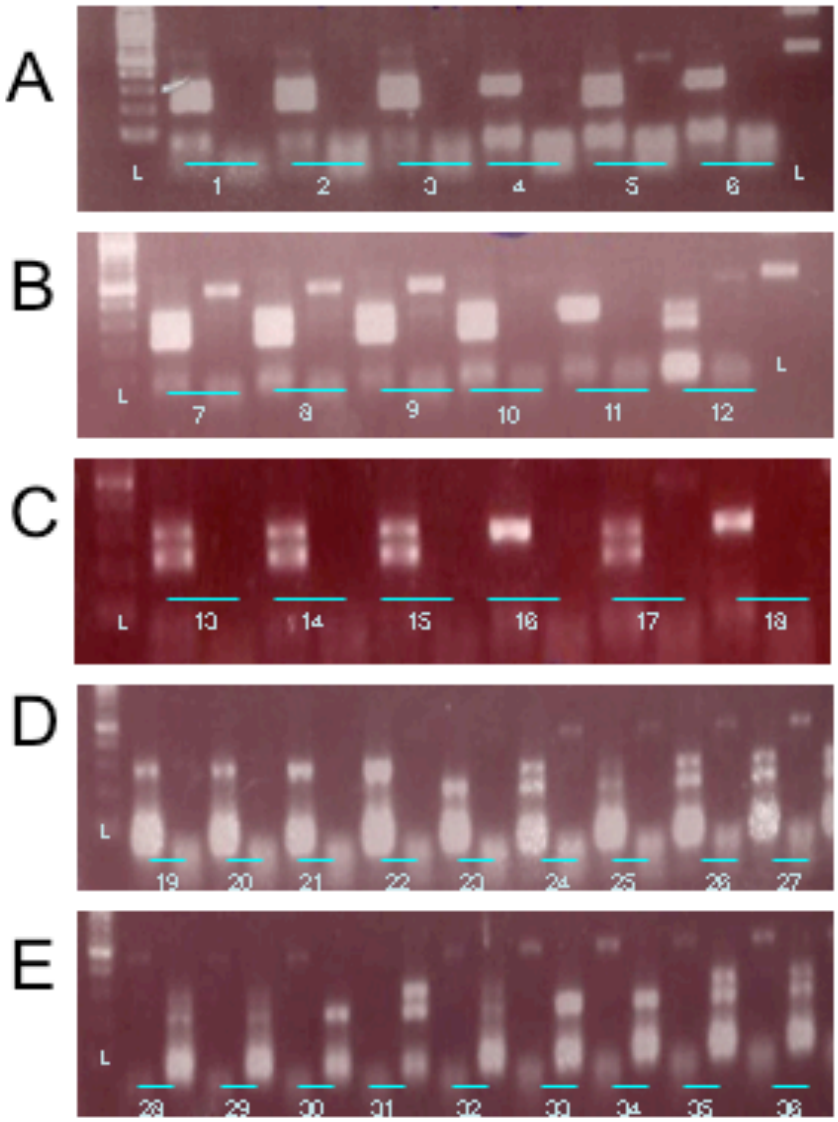

Figure 3.5: Examples of PCR screening to look for recombinant *Ntv-a*$^{+}$;*Apc*$^{LoxP/LoxP}$ mice. Figures A-D show the *Apc* lane followed by *tv-a* genotype on its right for each mouse, while figure E shows *tv-a* lane to the left of the *Apc* lane Apc WT band is 200bp and the LoxP band is 300bp. The *tv-a* band is 500bp. The ladder on the leftmost lane is a 500bp ladder. No *Ntv-a*$^{+}$;*Apc*$^{LoxP/LoxP}$. Some PCRs are not very clear with the *tv-a* band being very faint compared to the *Apc* band, with the pictures often having to be oversaturated to reveal any *tv-a* band.

3.2.5 Analysis of RCAS/*tv-a* infected animals

All of the 127 RCAS-Cre infected animals were left for a period of between 10 and 20 weeks with no animals showing signs of brain tumours, such as lack of appetite, sluggish movement, swollen head etc. We let the animals live for as long as possible even though we knew that none had the desired genotype as there was a slight chance that one could spontaneously loose the second *Apc* allele and develop a tumour as we would expect to happen in the human condition. Eventually, all the animals had to be sacrificed as the animal unit they were housed in was closing. For each animal, the cerebellum was removed, cut in half along the midline with half being fixed with PFA, embedded in wax and a random selection of 10 brains were cut sagittally. DNA was extracted from the other half of the cerebella for use PCR analysis to test for loss of *Apc.* Of note, none of the mice showed any external signs of abnormalities before they were culled.

Upon haematoxylin and eosin histological examination, the cerebella of the RCAS-Cre infected animals were no different to that of wild-type control animals. (Figure 3.6). With regard to the PCR analysis, none of the 127 mice showed any sign of cre-mediated deletion of *Apc* (Figure 3.7)

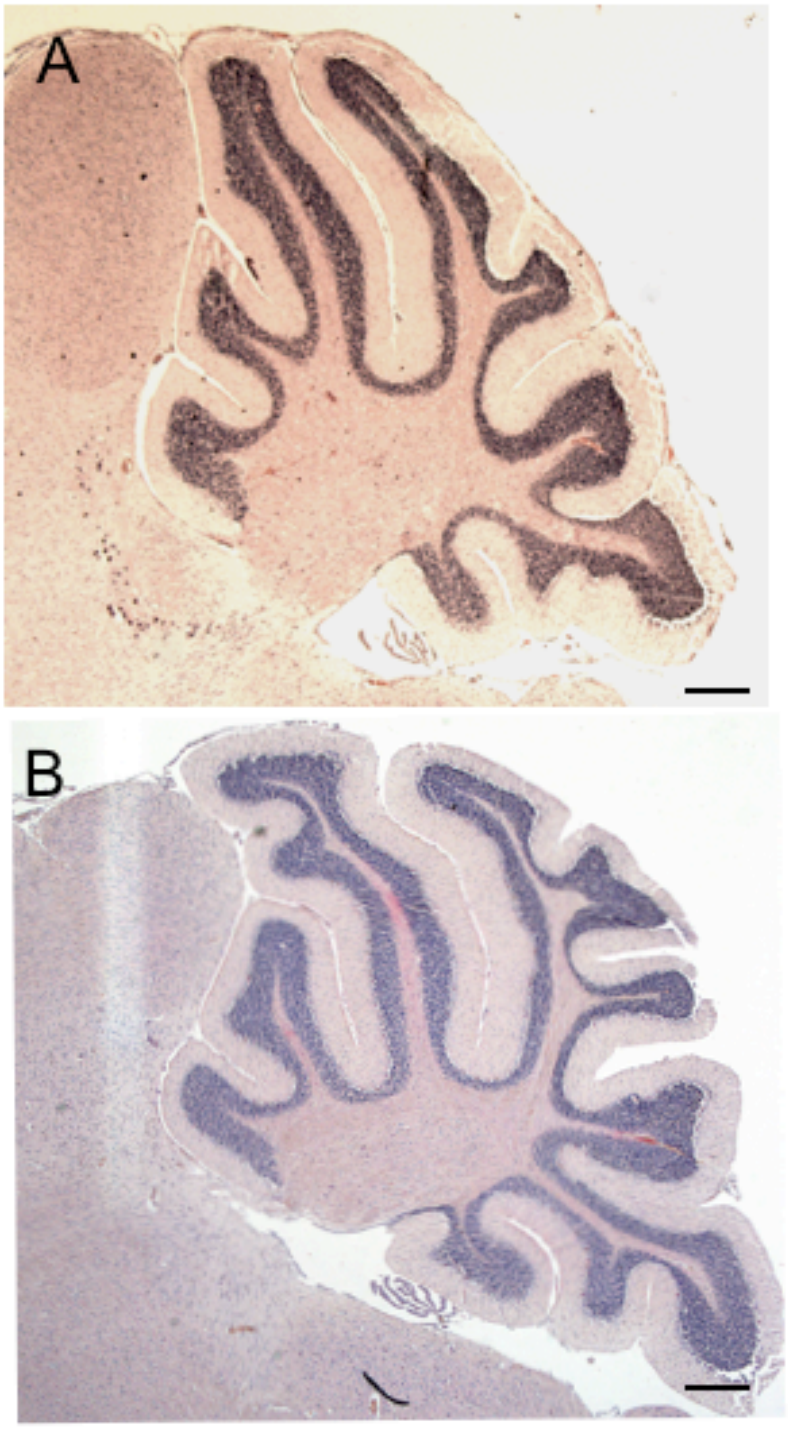

Figure 3.6 Histological analysis of RCAScre infected mouse cerebella. A, *Ntv-a*$^{+}$; *Apc* $^{LoxP/+}$ mouse. B, (*Ntv-a*$^{-}$; *Apc*$^{LoxP/LoxP}$) control injected animal. Injected mice displayed no histological difference to control animals. Scale bar=200 μm

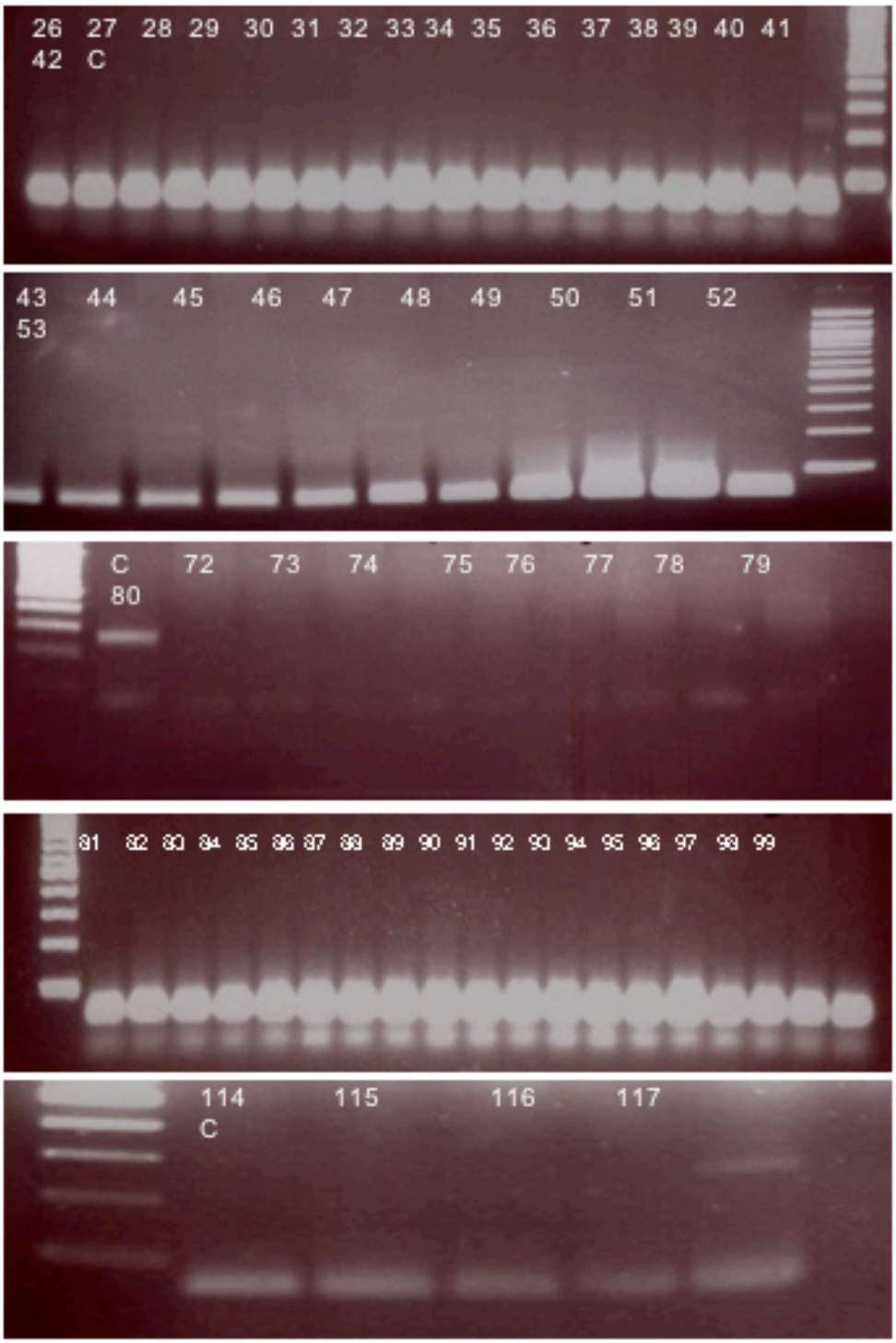

Figure 3.7: Sample PCRs showing RCAScre injected animals showing no of *Apc* deleted band. Top line of numbers indicate mouse number. Positive controls were performed to ensure the PCR had worked and are marked with a "C". Deleted *Apc* band = 250bp. Ladder (marked "L") was 500bp ladder.

3.3 Discussion

In conclusion, this experiment did not give us the expected result because we were unable to produce mice with the genotype (*Ntv-a* $^{+}$*;Apc*$^{LoxP/LoxP}$) necessary to cause the deletion of both alleles of *Apc* when mice were infected with RCAS-cre. Our conclusion was that both *Apc* and *tv-a* must be on the same chromosome. We believed that we had four mice with the reciprocal recombinant genotype, which gave us hope that the *Apc* and *tv-a* were far enough apart on the chromosome to produce a recombination again. However, after an extensive breeding program we were unable to produce any more recombinant animals. When the original recombinant mouse DNA was retested, it was concluded that the mice were miss-genotyped. This was a problem as at the time, the PCR protocol for detecting *Ntv-a* was unreliable.

We looked at the infected mice for histological abnormalities and found none compared to wild-type infected controls. When we also tested the DNA of infected *Ntv-a* $^{+}$*;Apc*$^{LoxP/+}$ heterozygotes, we did not detect any cre-mediated deletion of Apc via PCR. We would have expected to see a deleted band in RCAS-cre infected *Ntv-a* $^{+}$*;Apc*$^{LoxP/+}$ heterozygotes as one of the chromosomes should have been deleted. However, a possible explanation for this is that as only one chromosome would have been deleted, perhaps this was below the level of detection of the PCR.

If more time had permitted, we would have conclusively tested whether *Apc* and *tv-a* were on the same choromosome by performing fluorescent in situ hybridisation (FISH). Apc and β-catenin immunohistochemistry could also be carried out to assess in more detail whether any cre mediated deletion of *Apc* had occurred and wheter the Wnt pathway was over stimulated. However, since so much time had been spent on

this project, we had to push ahead with an alternative strategy which is outlined in the next Chapter.

4. Deleting Apc in the early postnatal hindbrain using Adenovirus-Cre

4.1 Background

Once it became clear that we could not inactivate *Apc* in the granule cell precursor cells of the cerebellum using the RCAS/tv-a method, we switched an alternative strategy of using an adenovirus which expresses cre-recombinase (AdCre) and injecting it directly into the developing cerebellum of postnatal day 4 (P4) $Apc^{LoxP/LoxP}$ mice. The main downside to using an adenovirus was that the virus was expected to infect all cells around the injection site so would not be nearly as specific as the RCAS-cre virus. The advantage of the AdCre method over the RCAS/tv-a method was that we could inject the virus directly into our floxed Apc mice without the need for complicated, time-consuming and expensive breeding steps. We decided to purchase for our experiment the AdCreM2 adenovirus from Microbix. The AdCreM2 vector carries the cre recombinase encoding gene under the control of the murine cytomegalovirus (MCMV) immediate early gene promoter (Figure 4.1B). This first generation type of AdCre was selected for our use as the MCMV promoter has been shown to produce higher expression levels in almost all cells in the mouse compared with adenoviruses whose gene expression is driven by the human cytomegalovirus (HCMV) (Addison et al. 1997). From published work by Wang et al. (1996), we estimated that we needed to inject a very small volume (1μl) of highly concentrated ($1x10^8$pfu per μl) adenovirus. We could not find any supplier who could deliver AdCre at such a high concentration, so we bought a low concentration aliquot from Microbix and sent it to another company (Virapur) to be concentrated.

4.2 Results

To test whether the AdCre was infecting Apc expressing cells and that the cre-recombinase was able to delete the floxed region of the Apc gene, we conducted a small-scale pilot experiment. Eight $Apc^{LoxP/LoxP}$ postnatal day 4 mice (the progeny of a male $Apc^{LoxP/LoxP}$ crossed to an $Apc^{LoxP/LoxP}$ female) were anaesthetised and injected with adenovirus-cre (AdCre) as with the RCAS/*tv-a* experiment. Infected mice were sacrificed at 3 days, 21days, and 5 weeks post infection. The cerebella were removed and the DNA was extracted to perform a PCR using primers that identified whether the exon 14 of the Apc gene had been deleted (Figure 4.1B). Figure 4.2 shows DNA from eight AdCre infected animals at various time points after infection, and two RCAS-cre infected animals as controls. From the gel, it is clear that deletion of exon 14 of *Apc* to generate $Apc^{LoxP\Delta}$ can be detected 3 days, 21 days, and 5 weeks post infection. No cre-mediated deletion was observed in the RCAS infected animals. Thus, the AdCreM2 virus is able to promote cre-mediated inactivation of the conditional Apc^{LoxP} allele in early postnatal hindbrain. $Apc^{LoxP\Delta}$ was detected as soon as three days post infection and was still detectable five weeks later, suggesting that loss *Apc* is not necessarily fatal to the cells.

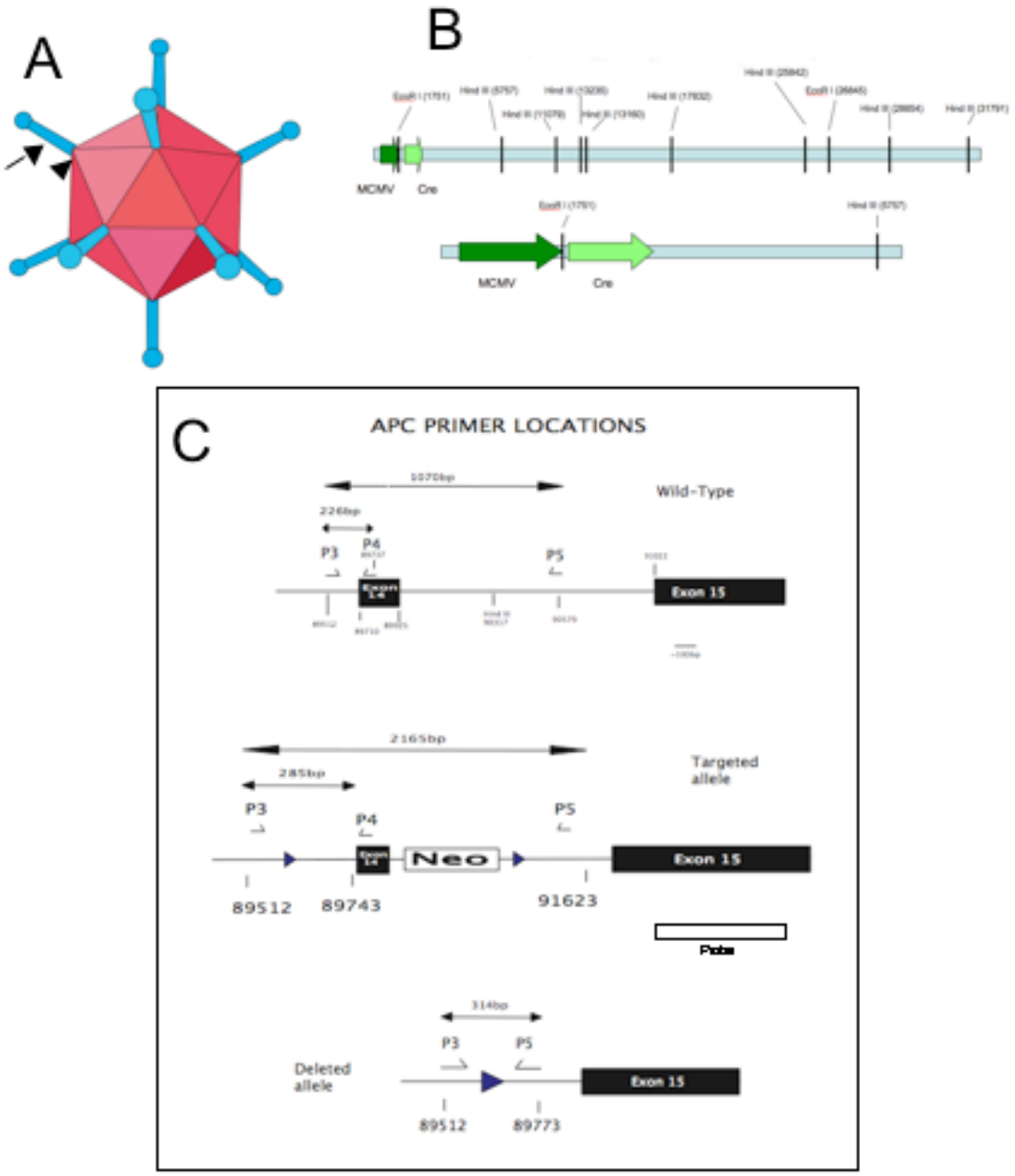

Figure 4.1 Adenovirus diagram and Apc primer locations. A: Adenovirus virion is an icosahedron with fibres (arrow) attached to a penton base (arrowhead) at each of the 12 vertices. B: Diagram of AdCreM2 vector with fragment of AdCreM2 underneath. C: Structure of the conditionally targeted allele of Apc (Apc^{LoxP}) and the mutated Apc allele ($Apc^{LoxP\Delta}$) resulting from cre-loxP mediated recombination. Shown are positions of PCR primers used to detect each allele. Southern blot probe is also shown and is a 1kb Hind III-Xba I fragment derived from exon 15.

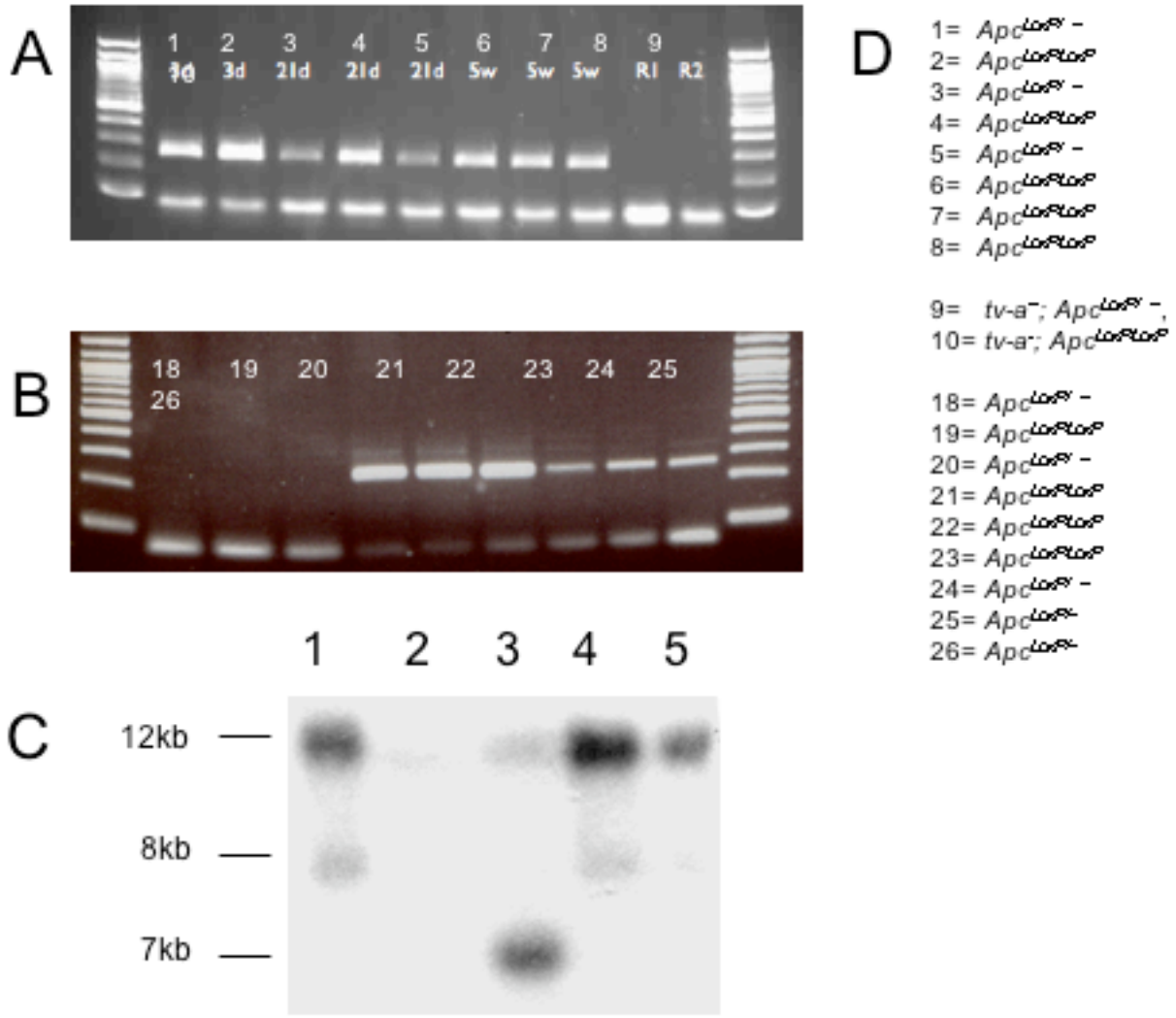

Figure 4.2: Adenovirus samples showing deletion using PCR and Southern blot. A: Adenovirus injected samples showing deletion of Apc with a band of 250bp. Top line of numbers indicate mouse number with second line showing time of sacrifice following AdCre infection. Mice 9 and 10 were RCAS-Cre infected animals, showing no cre-mediated deletion of Apc. B: PCR showing mice 18-26 as an example of the large-scale screening of adult AdCre infected mice. C: Southern blot showing samples 1-5. 12kb band shows floxed band, 8kb indicates deleted band, and 7kb shows the WT band. From this Southern blot, only samples 1, 4 and possibly 5 display a deleted band. D: genotypes for all mice displayed .

From here we set up a larger scale experiment using a total of 94 mice injected with AdCre. Infections were carried out as with the RCAS/*tv-a* experiment, and culled at set time intervals (Figure 4.3) Animals were watched closely for any evidence of brain tumour formation such as lack of appetite, circling movements, lack of movement, swelling of the head etc. Seven mice out of the 94 infected showed these symptoms so were culled immediately and examined. All seven mice were found to be suffering from hydrocephaly and none had any evidence of brain tumour formation. The brains were fixed and embedded in wax to be cut for histological analysis and an example of one can be seen in Figure 4.4 which shows a hydrocephalic brain with characteristically enlarged ventricles and an enlarged fluid filled cerebellum.

When mice were sacrificed the cerebella were bisected along the midline, with half being used for histological analysis, ie. stained with haematoxylin and eosin, and the DNA was extracted from the other half of the cerebellum for either Southern blots or PCR to identify whether or not *Apc* was successfully deleted. Samples shown by PCR to have strong *Apc* deletion were cut and stained for histological analysis. Figure 4.2B shows an example of the large scale PCRing that was carried out to determine which AdCre infected animals showed evidence of deletion of exon 14 of *Apc*. The primers used were based on those used by Shibata et al. (1997) and are shown diagrammatically in Figure 4.1C. A full table of numbers of animals infected with their genotypes and how many animals showed cre-mediated deletion of exon 14 of *Apc* is shown in Figure 4.3. Southern blots were originally used in an attempt to evaluate which infected animals showed cre mediated deletion. The probe used was a 1kb Hind III-Xba I fragment derived from exon 15 of *Apc* (Figure 4.1C).

Period sacrificed post infection	No of mice culled at each stage	Hydrocephalic animals	No. of mice showing cre-mediated deletion	Genotypes
3 days	4	0	3	2 $Apc^{LoxP/LoxP}$ 2 $Apc^{LoxP/+}$
2 weeks	8	0	6	6 $Apc^{LoxP/LoxP}$ 1 $Apc^{LoxP/+}$ 1 $Apc^{+/+}$
3 weeks	6	0	3	3 $Apc^{LoxP/LoxP}$ 1 $Apc^{LoxP/+}$ 2 $Apc^{+/+}$
5 weeks	8	1	5	6 $Apc^{LoxP/LoxP}$ 2 $Apc^{LoxP/+}$ 1 $Apc^{+/+}$
8 weeks	4	3	4	4 $Apc^{LoxP/Lox}$ 1 $Apc^{LoxP/+}$ 2 $Apc^{+/+}$
10 weeks	4	2	4	4 $Apc^{LoxP/LoxP}$ 2 $Apc^{LoxP/+}$
Adult (+12 weeks)	53	1	37	36 $Apc^{LoxP/Lox}$ 7 $Apc^{LoxP/+}$ 11 $Apc^{+/+}$

Figure 4.3: Table of AdCre infected mice. $Apc^{LoxP/LoxP}$ animals were the experimental group, and control mice had a genotype of either $Apc^{+/+}$ or $Apc^{LoxP/+}$

Figure 4.4: Hydrocephalic AdenovirusCre injected brain. Brain removed from an adult mouse exhibiting a swollen head and displaying sluggish movement and lack of appetite. All the ventricles are enlarged, which is characteristic of hydrocephalus. Note the sunken forebrain and midbrain are due to fluid loss when the brain was removed from skull. The cerebellum (CB) is also affected and appears to be filled with fluid. The choroid plexus (CP) also appears distorted in shape, possibly due to increased interventricular pressure.

This is the same probe that was used by Shibata et al. (1997) and the expected band sizes would be 12kb for the floxed *Apc* band, 8kb for the deleted band, and 7kb for the wild-type band. Figure 4.2C shows the only southern blot to produce a positive result. Other Southern blots which were attempted, either produced extremely high background or revealed no bands at all. I proceeded to troubleshoot the protocol by remaking the probes and solutions, used new hybond membrane, increasing the number of wash steps post hybridisation to reduce background, and varied the length of time the film was developed (between 1 and 5 days) to attempt to produce a clearer blot. However, after all of these attempts, I was unable to recreate the results I produced on my first Southern blot.

Figure 4.2C shows some of the same samples as Figure 4.2A with two animals taken 3 days post-infection, and three animals taken 21 days post-infection. Comparing Southern blot results with those from the PCR method for detecting cre-mediated deletion, the Southern blot method is less sensitive as only samples 1 and 4 show a deleted band with sample 5 possibly showing a very faint band.

Our PCR screening for *Apc* deletion showed that AdCre virus must have been infecting cells and mutating *Apc.* We picked brains from mice which showed the strongest floxed-deleted *Apc* band from the PCRs, and cut serial sections sagittally through the cerebellum. However, no evidence of brain abnormalities were evident when comparing brains from mice showing *Apc* deletion when compared to controls (Figure 4.5)

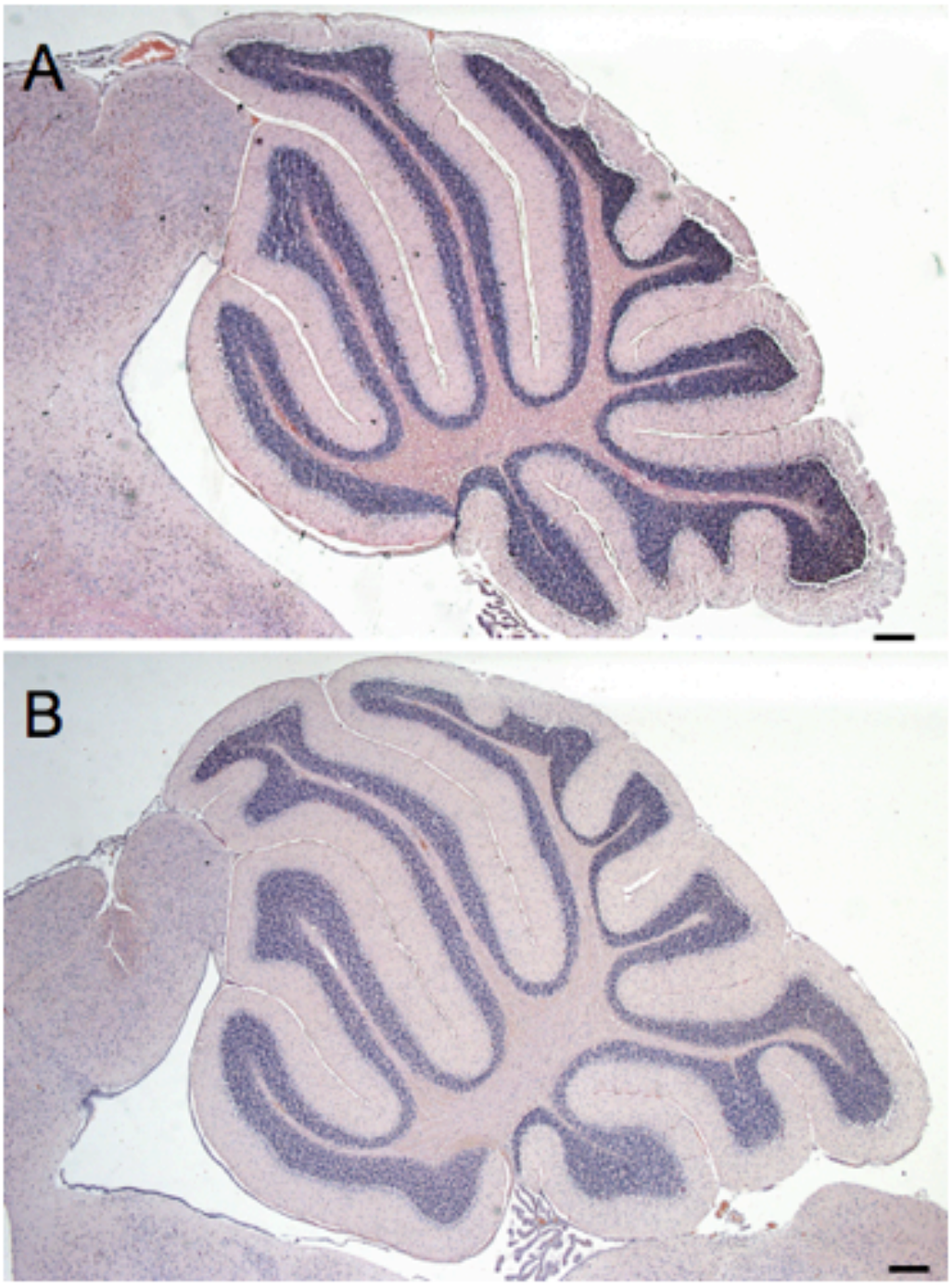

Figure 4.5 Histological analysis of AdCre infected mouse cerebella. A: *Apc* $^{LoxP/LoxP}$ mouse which displayed strong loss of *Apc* by PCR analysis . B=WT (*Apc*$^{+/+}$) control injected animal. Mice showing *Apc* mutation displayed no histological difference to control animals. Scale bar=200um

It was hypothesised that only a very small amount of cre-mediated deletion was occurring. This would also explain why the Southern blot showed such a faint deleted bands as there were so few cells infected, it was probably below the threshold of detection for Southern blots. To test the efficiency of AdCre infection, we infected 8 R26R reporter mice with our AdCre. These R26R mice are a transgenic strain in which a lacZ reporter gene is activated in response to cre-recombinase activity. 5 days after infection, we collected cerebella from infected R26R animals, cut sections and stained for lacZ activity. The results are shown in Figure 4.6. We found that only cells of the choroid plexus epithelium showed evidence of cre-mediated deletion. Since activation of lacZ should have no deleterious consequences for cells, this suggests that the tissue tropism of the virus was not as expected, accounting for the failure of AdCreM2-infected $Apc^{LoxP/LoxP}$ animals to show any abnormalities in the cerebellum.

If more time had allowed, we would have performed Apc and β-catenin immunohistochemistry on these sections to categorically show that there was no loss of Apc expression in the cerebellum and that the Wnt signalling pathway was not abnormally activated as shown by nuclear β-catenin localisation.

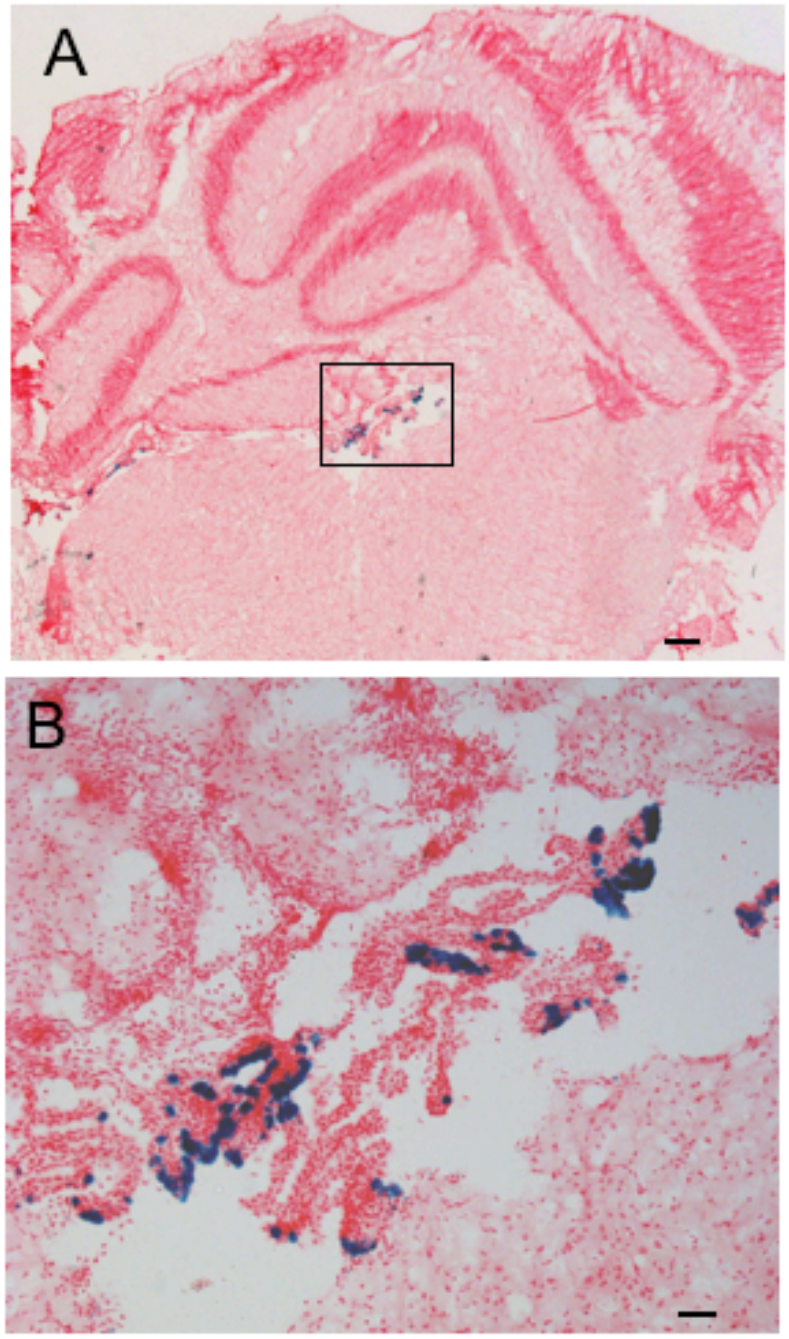

Figure 4.6: AdCre injected R26R mice. Cerebellum of R26R mouse which was infected with AdCre virus directly into the developing CB at P4. Brains were removed 7 days post infection. Figure A is CB cut sagitally at 200μm thickness and stained with alkaline phosphatase. Blue staining is β-galactosidase and indicates cre activity. Staining was observed only in choroid plexus cells. Figure B shows boxed area at higher magnification. Scale bars: A= 200μm, B=50μm

4.3 Discussion

This set of experiments aimed to produce a mouse with an *Apc* mutation specifically in the hindbrain at an early postnatal stage. As with the RCAS-cre experiment, which had the same goals, this was unsuccessful. None of our 87 AdCre infected animals displayed any histological abnormalities with the exception of the seven mice which developed hydrocephalus. Since we have shown that only cells of the choroid plexus were infected by the AdCre, and that defects in the choroid plexus could possibly to lead to hydrocephaly (Shin et al. 2006) the most likely explanation for this result is that *Apc* function was lost in these cells causing overproduction of cerebrospinal fluid (CSF). Since no mice infected with RCAS-cre displayed any sign of hydrocephaly, we ruled out the possibility that hydrocephaly was caused by damage done during the injection procedure. Adenovirus vectors injected into the brain can stimulate an inflammatory response (Cartmell et al. 1999). It is possible that the a localised immune reaction to the adenovirus could lead to cause swelling of the ventricles by immune cells crossing the blood brain barrier and entering the CNS parenchyma or ventricles. Another possibility is that adenovirus material may produce a meningeal irritation (Norrby et al. 1980) causing disturbances of the extraventricular flow or reabsorption of cerebrospinal fluid, leading to hydrocephalus.

After a search of the literature, we decided that the AdCreM2 virus would be a good option for introducing cre-recombinase to the cerebellum. E1-deleted first generation AdCre vectors have been successfully used to mediate loxP – dependent recombination *in vitro* using cultured cells (Kanegae et al. 1995; Kanegae et al. 1996) and *in vivo* targeting cells in the liver (Chang et al. 1999; Wang et al. 1996), in

tumours (Addison et al. 1997; Sato et al. 1998) and in the brain (Wang et al. 1996). In the study by Wang et al. (1996), AdCre was injected into one hemisphere of the forebrain in newborn $Apc^{LoxP/LoxP}$ mice. Mice were sacrificed and genomic DNA was isolated from each hemisphere and subjected to PCR analysis. Cre-mediated recombination was detected in the injected hemispheres at all time points (Wang et al. 1996). Our experiment seemed to fail mainly from the fact that our AdCre virus did not infect cells of the cerebellum, as was the intention, and instead only infected a very small population of cells in the choroid plexus of the 4th ventricle. The Wang et al. (1996) study clearly showed the ability of their AdCre virus to infect various brain regions including the cerebellum in adult mice, however in newborn mice, it is impossible to tell from this study which cell types were infected. This virus is driven by the herpes simplex virus thymidine kinase gene enhancer/promoter, however, our AdCre uses the MCMV gene promoter. This murine CMV was shown to be 5-30% more efficient than the human CMV promoter (in luciferase assays), which is commonly used in Ad vectors (Addison et al. 1997). This study by Addison et al. (1997) however did not directly inject adenovirus into the brain, instead the *in vivo* part of their study only included intratumoral injection. The rest of their study was conducted *in vitro*. Adenoviruses are know to infect some tissues and cell types less efficiently (Badorf et al. 2002), however, we could not have known that our AdCre upon injection into our early postnatal mice would only infect cells of the choroid plexus. In retrospect, it may have been better to try to obtain our AdCre directly from Y. Wang's group as their AdCre has been shown to work, however time constraints made it necessary to obtain our AdCre from a commercial source. It is also of note that Microbix's AdCreM2 virus has not yet been described in the literature at the time of writing.

A technical difficulty which could have contributed to the poor infection rate by the AdCre virus was that when performing the injections, the needle should inserted into the brain, and held still after infection of the adenovirus for as long as possible to allow the viral solution to dissipate, before the needle is removed as slowly as possible. The difficulty was that some viral solution was often drawn out when the needle was removed. A solution to this would be to leave the needle in for longer, however, it is also very important that the mice should not be left chilled for too long, otherwise they would die. However, this is unlikely to be the only reason that cerebellar cells were not infected with AdCre since choroid plexus cells were consistently the only cells infected in each of the brains tested.

To gain a more definitive answer to Apc's role in medulloblastoma, we one could use a different mouse line to mutate *Apc* in the cerebellum postnatally. Two possibilities would be to use a Nestin-CreER mouse such as the one which has recently been produced by Imayoshi et al. (2006). In this mouse, CreER, a fusion of Cre and the mutated ligand-binding domain of the human oestrogen receptor α, is inactive for recombination but becomes activated by administration of tamoxifen (Feil et al. 1997). Expression of CreER is driven by the Nestin promoter and enhancer (Imayoshi et al. 2006). We could cross this Nes-CreER strain to our floxed *Apc* mice and then administer tamoxifen to mice at P4 stage of development. Another option would be to use a Math1-CreER (Machold and Fishell 2005). Similar to Nestin, Math1 is expressed strongly in the cerebellum at postnatal day 4 of mouse development (Machold and Fishell 2005). Using one of these mouse strains, we would carry out the experiment as follows. Firstly, we would cross the cre strain of mouse (eg Nes-

CreER) to the reporter strain R26R. We would then administer tamoxifen and remove the brains for histological analysis. This experiment would indicate whether we are targeting the correct populations of cells efficiently. We would then produce *Nes-CreER*$^{+}$*;Apc*$^{LoxP/LoxP}$ mice and administer tamoxifen to at least 100 animals at P4 of development. 10 animals would then be sacrificed at certain time intervals (eg every 7 days up until 8 weeks post tamoxifen administration). Mice would be examined histologically with haematoxylin and eosin staining, as well as immunohistochemically with Apc and β-catenin staining to look for tumour formation and whether or not Apc has been efficiently mutated and whether the Wnt pathway has been stimulated.

5. Apc's role at the midbrain hindbrain junction during embryonic development

5.1 Background

Medulloblastoma is a tumour which predominantly manifests in childhood. As discussed in Chapter 1, MBs are thought to have neurodevelopmental roots, so understanding the role of Apc in normal cerebellar development would shed light on its possible role in MB.

To study Apc's role in cerebellar development, we used our conditional allele of *Apc* to assess the consequences of losing Apc in a cell population that gives rise to the cerebellum: the midbrain-hindbrain junction. To do this we obtained a line of transgenic mice which expresses cre recombinase under the *Engrailed-1* promoter (*En1-cre* mice) (Gifted from Wolfgang Wurst, Institute of Developmental Genetics, Munich). *Engrailed (En)* is a homologue of the *Drosophila engrailed (en)* gene. Expression of *En1* begins in the mouse at the 1-somite stage in the anterior neuroepithelium (Davidson et al. 1988). Later, expression can be seen more ventrally in band of cells whose population gives rise to the mid-hindbrain region. By E9.5, *En1* expression can be seen in a rostral to caudal progression in two lateral stripes along the hindbrain and spinal cord. By this stage, expression can also be observed in the somites and the ventral extoderm of the limb buds. In the adult mouse brain, *En1* is expressed in groups of motor nuclei in the pons and the substantia nigra (Wurst et

al. 1994). A fate-mapping study by Zinyk et al. (1998) which utilised an En2-cre strain of mouse crossed to a reporter strain which consists of a *loxP* – stop of transcription/translation – *loxP* – *lacZ*, showed that tissues derived from the midbrain-hindbrain region during embryonic days 9 – 12, contributed significantly to the medial cerebellum and colliculi (Zinyk et al. 1998).

En1 is a transcription factor involved early in development, establishing the body plan and in particular, for defining the posterior half of each parasegment (Kornberg 1981). Of note, *En1* is also a known target of Wnt signalling (Danielian & McMahon 1996). Later it determines neuronal identity of, for example, midline serotonergic neurones in *drosophila* (Lundell et al. 1996). *En1* in the mouse is known to play an important role in embryonic development of the brain and limbs (Joyner 1996; Loomis et al. 1998). During early neural development in the mouse, *En1* is thought to be critical for the development and patterning of the mid and hindbrain region (Araki & Nakamura 1999; Wurst et al. 1994).

$En1^{-/-}$ mice have a deletion in the dorsal and ventral parts of the midbrain and rostral hindbrain (Wurst et al. 1994). In contrast, $En2^{-/-}$ mutant mice show only subtle cerebellar defects (Millen et al. 1994). When combined, mice with an $En1^{-/-};En2^{-/-}$ double mutation show a complete deletion of mid-hindbrain region indicating that the *En* genes are involved in the maintenance of a functional mid-hindbrain organiser (MHO).

Since En1 is expressed at the boundary between the embryonic mid- and hindbrain, an area that gives rise to the future anterior part of the cerebellum, creating a line of mice where Apc is mutated in *En1* expressing cells should indicate Apc's role in early cerebellar development. A study by Panhuysen et al. (2004), examining the role of

Wnt1 in the developing mid-hindbrain region, ectopically expressed *Wnt1* under the control of the endogenous *En1* promoter. This approach extended *Wnt1* expression rostrally into the anterior midbrain and caudally into rhombomere 1, causing overproliferation of precursor cells in the caudal midbrain in a gene dosage dependent manner. The authors of this study suggested that Wnt1 primarily acts as a regulator of proliferation of specific precursor populations in the developing mid-hindbrain region, and is secondarily involved in maintenance of the MHO (Panhuysen et al. 2004). This study backed up previous studies using a *Wnt1* null mutant mouse have shown an absence of midbrain and cerebellar structures (McMahon & Bradley 1990), and increased cell death in the metencephalon (Serbedzija et al. 1996), implying that *Wnt1* is necessary for development of the midbrain and cerebellum.

By generating $En1cre^{+};Apc^{LoxP/LoxP}$ mice, we hope to examine Apc's role in midbrain and early cerebellar development. As discussed in chapter 1, the main consequence of the loss of Apc is functionally equivalent to constitutive activation of canonical Wnt signalling, leading to the stabilisation of β-catenin and its translocation to the nucleus. Of note, the *En1cre* mice are knock-in mice where the cre-recombinase gene cassette has been knocked into the *En1* locus (Kimmel et al. 2000). This produces a null mutation in *En1*, therefore all of our *En1cre* mice are heterozygous.

Since Wnt signalling is critical for normal development of the mid-hindbrain region, we hypothesised that our $En1cre^{+};Apc^{LoxP/LoxP}$ mice would have major abnormalities in the midbrain and the anterior cerebellum. In particular we expected a phenotype similar to the one seen by Panhuysen et al. (2004) in their mutant as overexpressing *Wnt1* should have the same effect as reducing *Apc* levels. However, we did not expect

that the phenotype would be identical due to Apc's roles outside the Wnt pathway, which were discussed in Chapter 1.

5.2 Results

5.2.1 Validation of the En1-cre mouse strain

To ensure that our En1-cre mice were expressing cre-recombinase efficiently and in the expected pattern, we crossed it to a ROSA-26 reporter (R26R) strain which expresses β-galactosidase in the presence of cre-recombinase (Soriano 1999). These R26R mice have a loxP-flanked stop cassette followed by lacZ gene in the ROSA-26 locus (Soriano 1999). The resultant progeny were collected at embryonic days 16 and 18, and stained with X-gal to reveal β-galactosidase expression. As shown in Figures 5.1 and 5.2, cre-recombinase was expressed efficiently in the midbrain and the hindbrain following what appears to be the normal expression pattern of En1 (Davis & Joyner 1988; McMahon et al. 1992), with staining in the hindbrain as well as in all but the dorsal layers of the midbrain and cerebellum. This staining was performed on whole mount embryos however, so the cellular resolution is not very high. In conclusion, we believe that the expression pattern of cre looks very close to what we would expect of the expression pattern of *En1*.

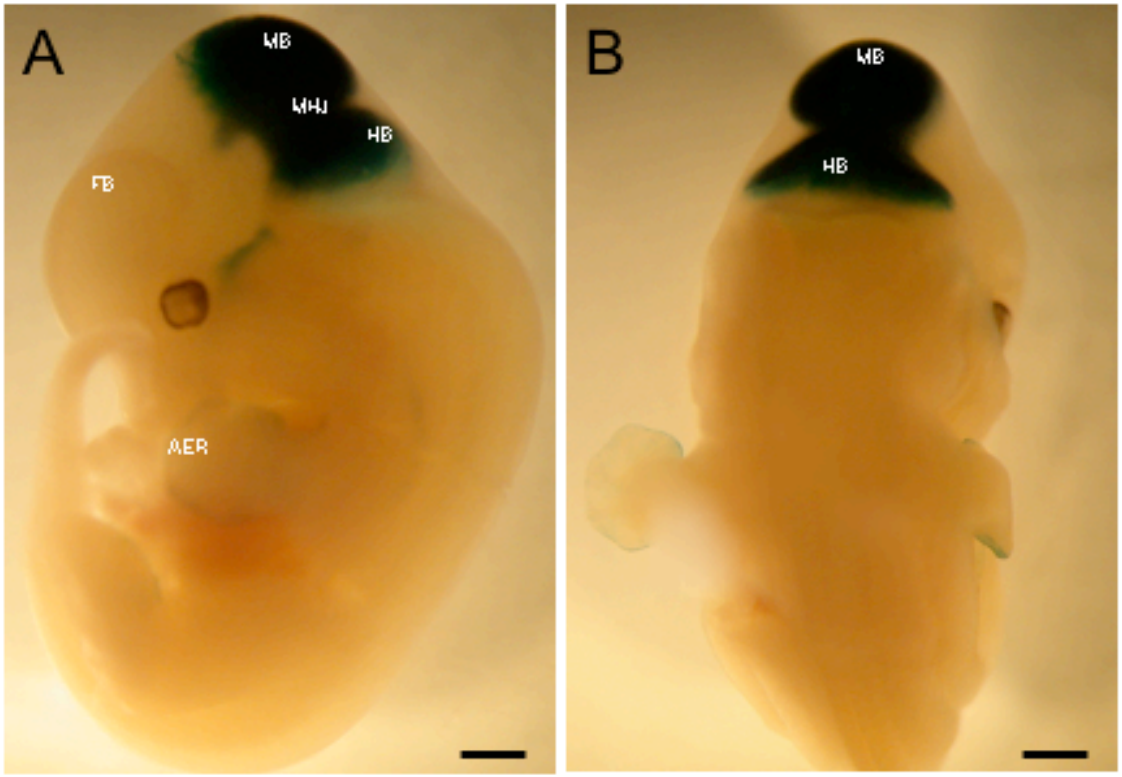

Figure 5.1: β-galactosidase expression in *En1cre*$^{+}$;*R26R*$^{+}$ mice.E16.5 mouse embryo lightly fixed and stained with X-gal to reveal β-galactosidase expression. Expression can be observed in the midbrain and rostral hindbrain. Outside of the brain, expression can be seen in the apical ectodermal ridge (AER) of the developing limb bud. A, lateral view. B, dorsal view. AER, apical ectodermal ridge. FB, forebrain. HB, hindbrain. MHJ, mid-hindbrain junction. MB, midbrain. Scale bar: 2mm

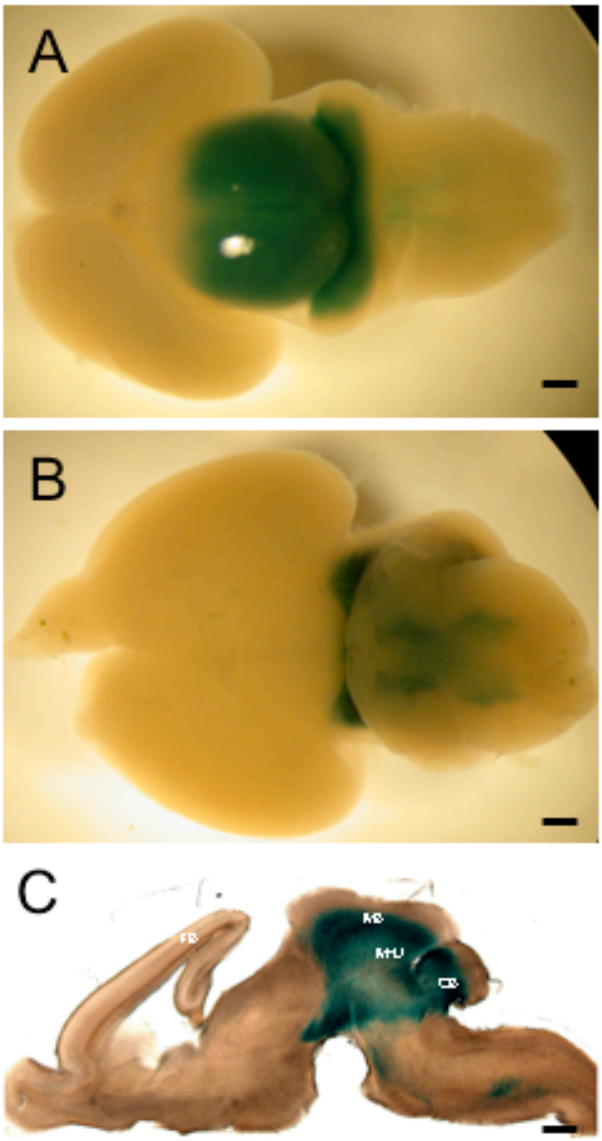

Figure 5.2: β-galactosidase expression in *En1-cre*$^{+}$;*R26R*$^{+}$ mice.E18.5 mouse brain expressing β-galactosidase. Again, En1cre expression extends from midbrain to anterior hindbrain. Of note, strong expression is detected in the anterior part of the cerebellum as shown by figure C, although expression is not seen in dorsal region of midbrain or cerebellum. Panel A, dorsal view. B, ventral view, of whole mount X-gal stained brain. C, sagittally sectioned brain cut to a thickness of 200μm. CB, cerebellum. FB, forebrain. MHJ, mid-hindbrain junction. MB, midbrain. Scale bar, 500μm.

5.2.1 Phenotype of *En1cre^{+};Apc$^{LoxP/LoxP}$* embryos

To begin our study of this mutant mouse, embryos were collected at various stages of development and sectioned sagittally before bein stained with haematoxylin and eosin. The embryos' morphology were then carefully examined. *En1cre^{+};Apc$^{LoxP/LoxP}$* mice at the early developmental stage of E10.5 were discovered to have a relatively subtle phenotype. No obvious abnormalities were noted at low magnification, however upon closer inspection, cells along the ventricular zone of the developing midbrain had a disorganised structure with occasional rosette-like formations, which were absent in the control *En1cre^{+};Apc$^{LoxP/LoxP}$* littermates (Figure 5.3A-D). We looked this early in development for any abnormalities even though the cerebellum has not started to form (and doesn't become apparent until around E15.5), because we wanted to try to identify when the mutation first became apparent, and how severe it is at this very early stage.

At E12.5, one of the *En1cre^{+};Apc$^{LoxP/LoxP}$* mice appears to have enlarged mesencephalic, 3rd and 4th ventricles, which indicates that the mouse is suffering from hydrocephalus (Figure 5.4B). Also of note was a cluster of disorganised cells at the junction between the midbrain and hindbrain (Figure 5.4C) which is absent from control *En1cre^{-};Apc$^{LoxP/LoxP}$* mice (Figure 5.4A). In keeping with this phenotype, another *En1cre^{+};Apc$^{LoxP/LoxP}$* embryo taken at E12.5 displayed enlargement of all vesicles with the exception of the lateral ventricle (Figure 5.4D). This embryo differs from the previous however in that it displays at much larger area of disorganised tissue in the caudal midbrain / mid-hindbrain junction (Figure 5.4E).

A third E12.5 *En1cre*$^{+}$;*Apc*$^{LoxP/LoxP}$ mutant embryo showed another differing phenotype. Hydrocephalus was not as pronounced although the lateral ventricle may be slightly enlarged, however, the most striking phenotype is a very large area of disorganised cells in the midbrain (Figures 5.4F-G). As much care as possible was taken to match these sections although there may be variation due to differences across medio-lateral tissue or variability across embryos. As a rough marker, the size of the telencephalon and size of the lateral ventricle were used to match sections although the latter is not so accurate due to variations in hydrocephalus between animals.

In wild-type mice at E15.5, the ventricles are reduced in size and (as discussed in Chapter 1) the cerebellum should be evident (Figure 5.5A). However, when comparing our *En1cre*$^{+}$;*Apc*$^{LoxP/LoxP}$ mice to the control *En1cre*$^{+}$;*Apc*$^{LoxP/LoxP}$ littermate, one can see that all ventricles are greatly enlarged in both embryos, indicating hydrocephalus. Also, the cerebellums appear under-developed with an arrowhead in Figures 5.5C and E, indicating the location of the presumptive cerebellums.

Once we had established that there was a phenotype in the *En1cre*$^{+}$;*Apc*$^{LoxP/LoxP}$ mice, we expanded our evaluation of the mutants by performing immunohistochemial analysis to characterise the tissue.

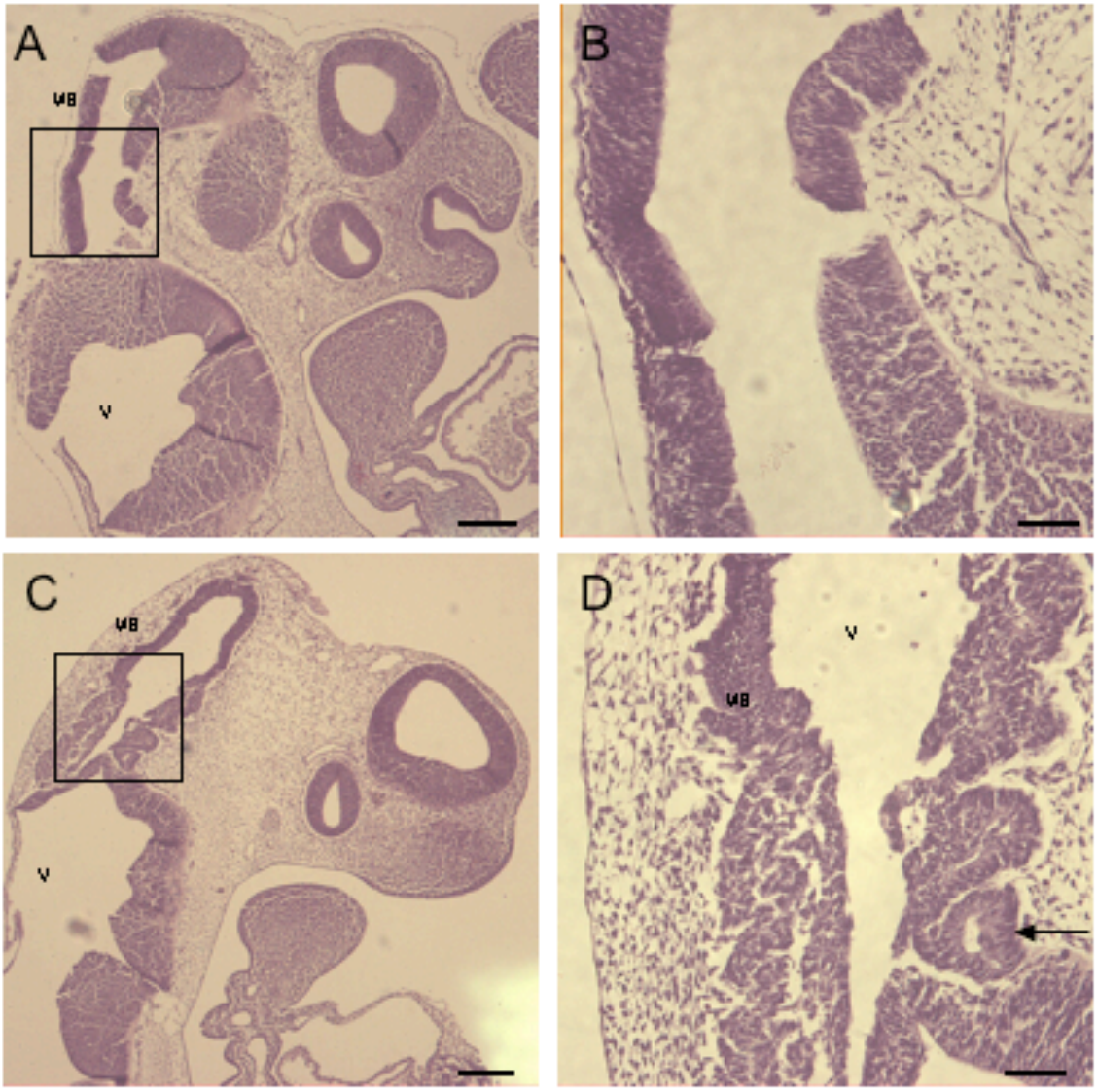

Figure 5.3. Histological analysis of *En1cre*$^{+}$;*Apc*$^{LoxP/LoxP}$ mice at E10.5. A, Control *En1cre*$^{-}$;*Apc*$^{LoxP/LoxP}$ mouse. B, enlarged panel from A showing midbrain area. Panel C shows E10.5 *En1cre*$^{+}$;*Apc*$^{LoxP/LoxP}$ mouse displaying disorganised tissue at caudal midbrain area, with panel D displaying this area at higher magnification. Disorganised groups of cells marked with arrows. All embryos were sectioned sagittally at a 10μm thickness.CP, choroid plexus. MB, midbrain. V, ventricle Scale bars: A and C represent 200μm, B and D, 50μm.

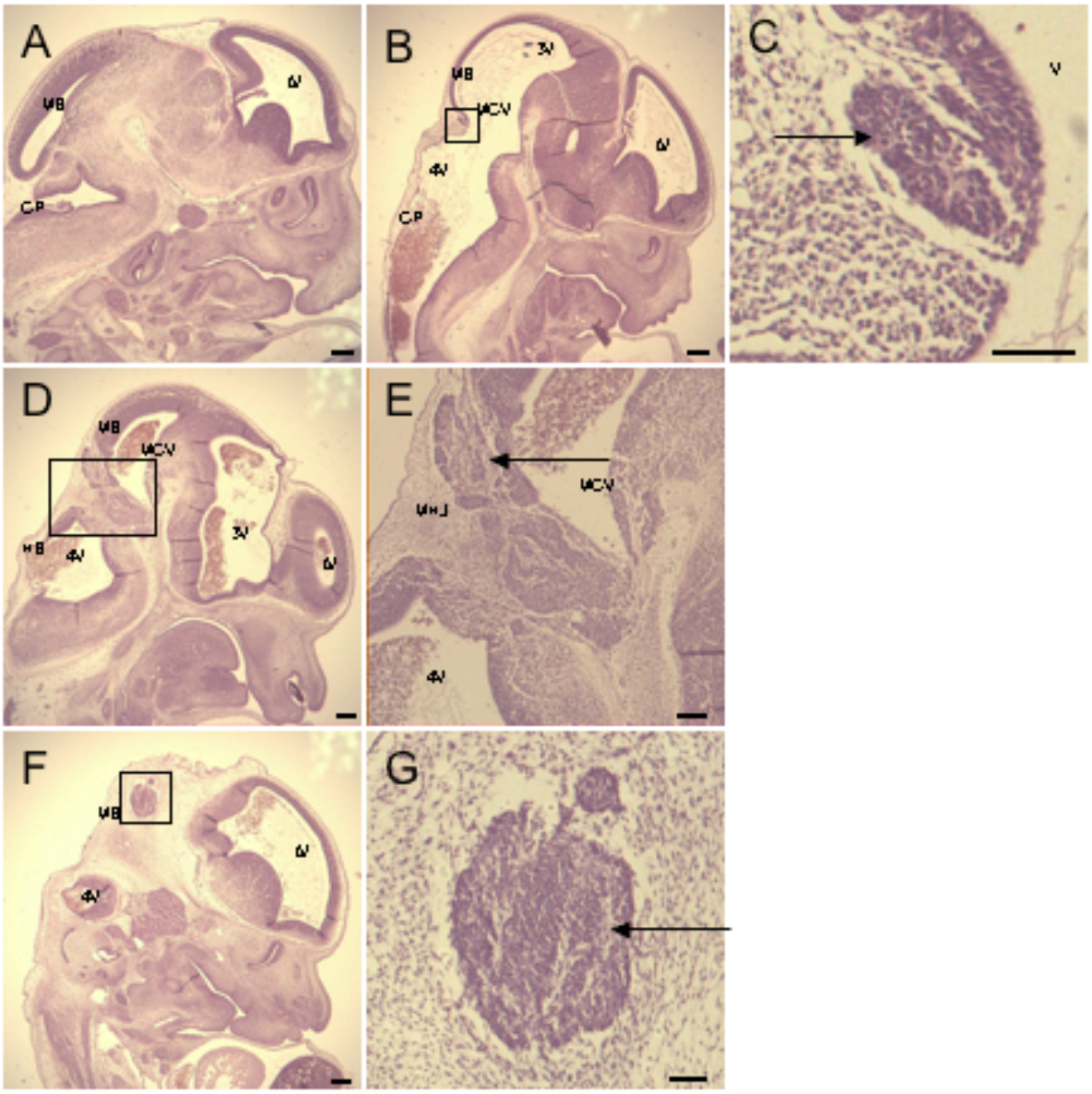

Figure 5.4: Histological analysis of *En1cre⁻;Apc^{LoxPLoxP}* mice at E12.5 A, Control *En1cre⁻;Apc^{LoxPLoxP}* E12.5 mouse. B, *En1cre⁻;Apc^{LoxPLoxP}* E12.5 mouse showing small ball of disorganised cells at the mid-hindbrain junction area. Enlarged 3rd and 4th ventricles. C, high power view of boxed area in panel B. Disorganised group of cells marked with arrow. D, En1cre⁻;Apc^{LoxPLoxP} mouse also showing disorganisation of cells in the midbrain region. All ventricles with the exception of the lateral ventricle appear enlarged, indicating hydrocephalus. Panel E shows boxed area of panel D. Panel F shows a different *En1cre⁻;Apc^{LoxPLoxP}* mouse. Hydrocephalus may be present in this embryo with an enlarged lateral ventricle. Also, a large ball of dysorganised tissue is visible in the midbrain (boxed area). G, boxed area from panel F, enlarged. All embryos were sectioned sagittally at a 10μm thickness. 3V, 3rd ventricle, 4V, 4th ventricle. CP, choroid plexus. LV, Lateral ventricle. MB, midbrain. MCV, mesencephalic vesicle, MHJ, Mid-hindbrain junction. V, ventricle. Scale bars: A, B, D and F represent 200μm. C, E and G represent 50μm.

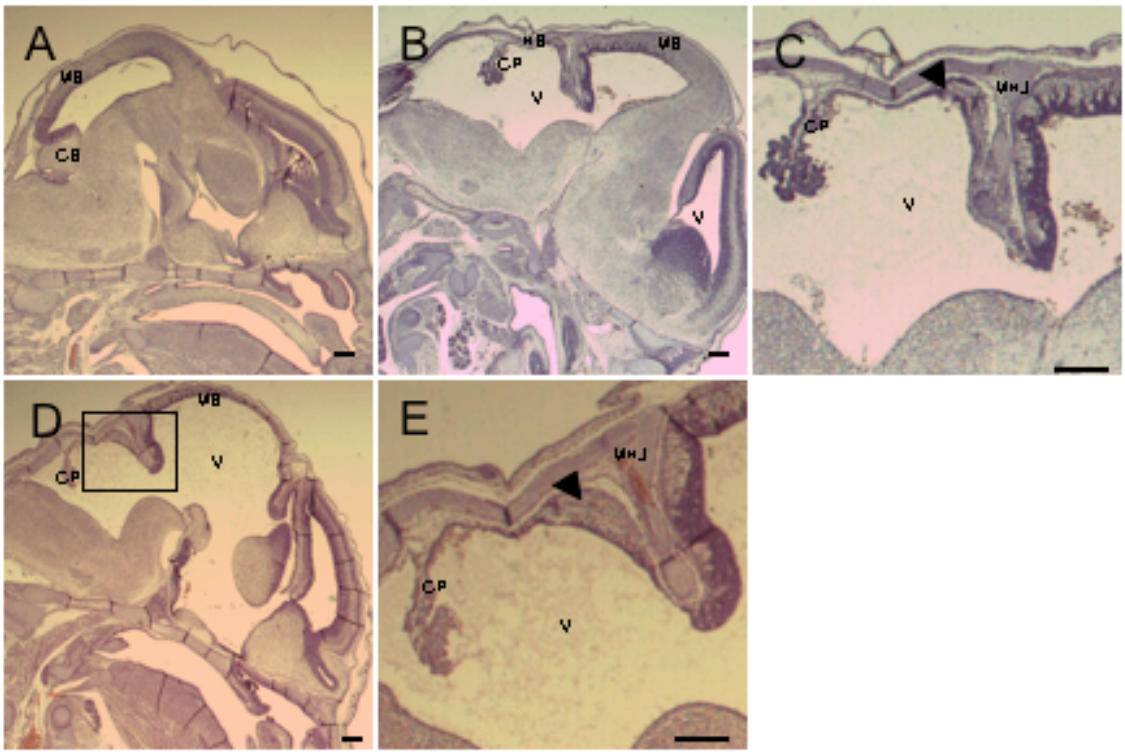

Figure 5.5: Histological analysis of *En1cre*$^{+}$;*APC*$^{LoxP/LoxP}$ mice at E15.5 Panel A displays an E15.5 control *En1cre*$^{-}$;*Apc*$^{LoxP/LoxP}$ embryo. Panel B, shows an E15.5 *En1cre*$^{+}$;*Apc*$^{LoxP/LoxP}$ embryo. Hydrocephalus is evident and cerebellum is under developed. Midbrain appears slightly thicker and shorter compared to controls and hindbrain region appears larger and thinner. Hindbrain appears to be pushing midbrain structures rostrally. C, shows area of disorganised tissue at mid-hindbrain junction, and possible location of cerebellar primordium (arrowhead). D, another E15.5 *En1cre*$^{+}$;*Apc*$^{LoxP/LoxP}$ embryo. This embryo also displays hydrocephalus evidenced by enlarged ventricles, but differs from the embryo in panel B by having a thinner and longer midbrain compared to other control and mutant mice. These anatomical differences are likely caused as a result of hydrocephalus. All embryos were sectioned sagittally at a 10μm thickness.CP, choroid plexus. MB, midbrain. MHJ, mid-hindbrain junction. HB, hindbrain. V, ventricle. Scale bars: A and B represent 200μm, C represents 50μm.

5.2.2 Characterisation of Apc expression in conditional mutant embryos.

We used an anti-Apc antibody (Santa Cruz) that recognises a C-terminal epitope that is absent in the mutated form of Apc due to the frame-shift mutation caused by the deletion of exon 14. Therefore, performing immunohistochemistry with this antibody should accurately indicate where Apc has been deleted.

At E16.5, $En1cre^{+};Apc^{LoxP/LoxP}$ mutant mice show severe hydrocephalus with an enlargement of all ventricles of the brain. In addition to this, mutant mice display an area of abnormal tissue at the mid-hindbrain junction. Apc is expressed strongly throughout the entire CNS at E17.5 including the mid-hindbrain area (Bhat et al 1994) (Figure 5.6A). Although, the exact cell types which express *Apc* is still controversial. However, mid-hindbrain junction in $En1cre^{+};Apc^{LoxP/LoxP}$ mutant mice is now populated with cells which appear to be mesenchymal cells (Figure 5.6B-E). We performed Apc immunohistochemistry and found that these cells do not express Apc protein. Usually situated ventrally to these mesenchymal cells, is an area of disorganised neuroblastic cells, which are also negative for Apc expression (Figure 5.6D-E).

Cells in this area seem to be arranged in a turbulent fashion with small clusters of cells interspersed with other unidentified cell types. The only $En1cre^{+};Apc^{LoxP/LoxP}$ mutant embryo, out of a total of 27, to not display this tumour-like ball of disorganised cells is displayed in Figure 5.6B.

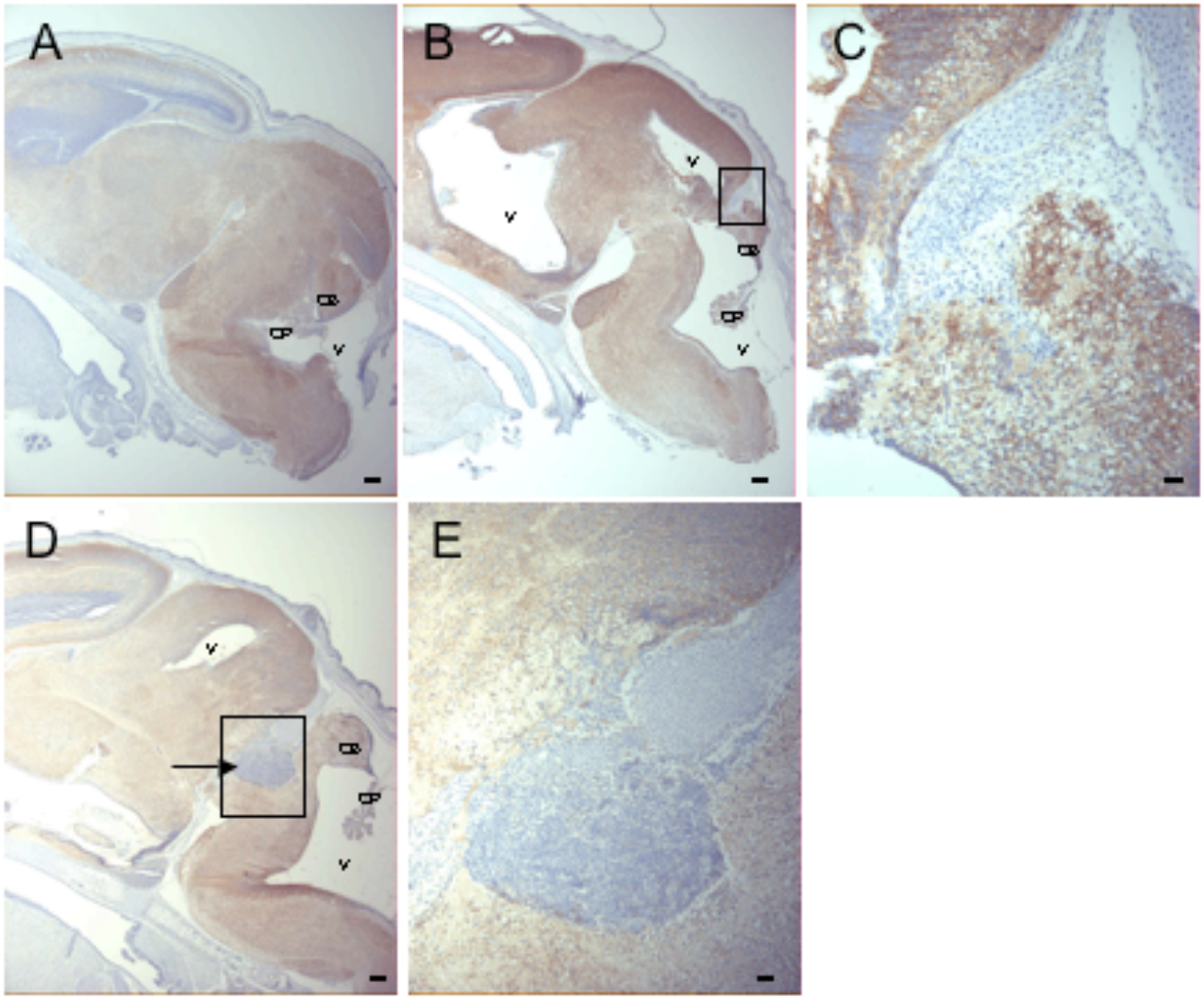

Figure 5.6: Immunohistochemistry using anti-Apc antibody showing loss of Apc and disorganised tissue at the mid-hindbrain junction and hydrocephalus. A, E17.5 control littermate showing normal Apc expression. B, E16.5 *En1cre*$^{+}$;*Apc*$^{LoxP/LoxP}$ mouse displaying hydrocephalus evidenced by hugely enlarged ventricles. Tissue that resembles mesenchymal tissue is invading ventrally at mid-hinbrain junction. C, Boxed area from figure B enlarged showing mesenchymal tissue invading anterior cerebellum. D, E18.5 *En1cre*$^{+}$;*Apc*$^{LoxP/LoxP}$ mouse again showing hydrocephalus and tumour-like area of disorganised tissue (arrow) ventral to mesenchyme tissue displaying no Apc expression. E, Enlargement of boxed area from panel D. All sections were cut sagittally at a thickness of 10μm. Scale bars: A,C,E= 200μm, B,D=50μm. CB=cerebellum, CP=choroid plexus, V=ventricle

5.2.3 Expression of β-catenin in conditional mutant embryos

To further characterise this area of dysregulated tissue, we carried out β-catenin immunohistochemistry on *En1cre*$^{+}$;*Apc*$^{LoxP/LoxP}$ mutants at a range of developmental stages from E13.5 to E18.5. In control *En1cre*$^{-}$;*Apc*$^{LoxP/LoxP}$ mice, β-catenin is expressed strongly throughout the brain (Figure 5.7A). However, situated at the mid-hindbrain junction of mutant *En1cre*$^{+}$;*Apc*$^{LoxP/LoxP}$ mice, we can see a large β-catenin negative area (Figure 5.7E, marked with an asterisk). The cells of this area appear, based on morphology, to be mesenchyme cells which have invaded ventrally into the brain. They express β-catenin at very low levels with some cells showing nuclear localisation (Figure 5.8B). This tissue normally displays β-catenin in some nuclei, and has also been shown not to express Apc in our *En1cre*$^{-}$;*Apc*$^{LoxP/LoxP}$ control mice (Figure 5.7A). In the disorganised mass of neuroblastic cells located ventrally to the mesenchyme cells, nuclear β-catenin staining can be observed indicating that there is loss of functional Apc in these cells (Figures 5.7F, and 5.8D), which has effectively activated the Wnt signalling pathway. Of note, not all cells in this dysregulated area express β-catenin, suggesting that there are at least two types of cells in this area. Also, Homer-Wright rosettes, which are common in human MBs and signify neuronal differentiation (*Prof. Ian Whittle, Pers Comm*), can be observed in this dysregulated area (Figure 5.7F).

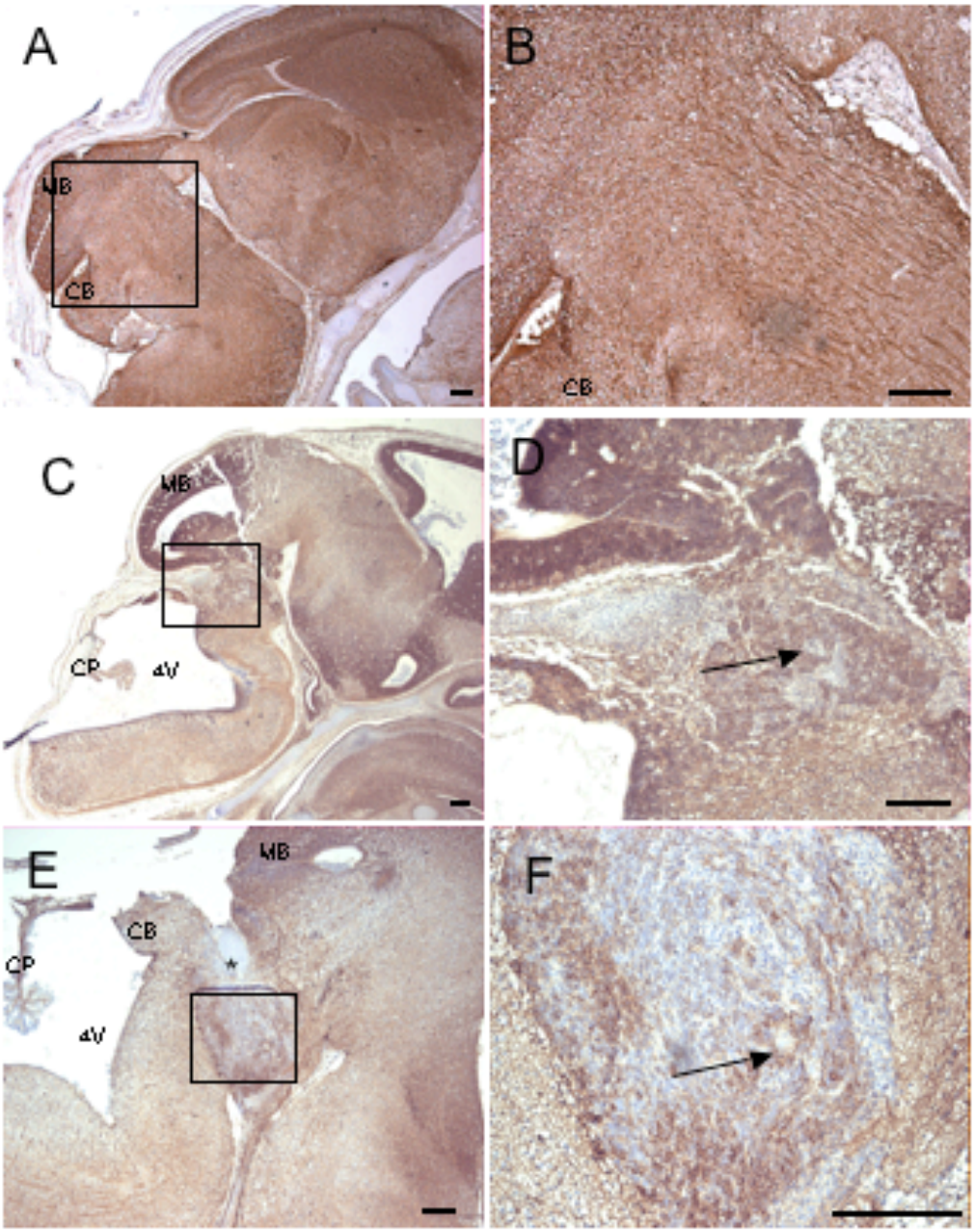

Figure 5.7: Immunohistochemistry using anti-βcatenin antibody showing nuclear localisation of β-catenin in disorganised tissue adjacent to the cerebellum in *En1cre⁻;Apc^{LoxPLoxP}* mice. A, shows normal β-catenin expression in a control mouse at E17.5. B, enlargement of boxed area in panel A showing β-catenin expression in midbrain-hindbrain area. C: E13.5 *En1cre⁻;Apc^{LoxPLoxP}* mouse displaying hydrocephalus evidenced by enlarged ventricles. Mesenchymal tissue as well as disorganised tissue at mid-hindbrain is displaying nuclear β-catenin localisation. D: Boxed area from figure C enlarged showing disorganised tissue at mid-hindbrain junction. Arrow indicates a Homer-Wright rosette. E, E15.5 *En1cre⁻;Apc^{LoxPLoxP}* mouse again showing hydrocephalus and tumour-like area of disorganised tissue at the mid-hindbrain junction. Asterisk denotes area of mesenchyme tissue which is negative for β-catenin. F, Enlargement of boxed area from figure E showing rosette formation in tumour-like structure (arrow). All sections were cut sagittally at a thickness of 10μm. Scale bars: 200μm. CB=cerebellum, CP=choroid plexus, MB= midbrain, 4V= 4th ventricle.

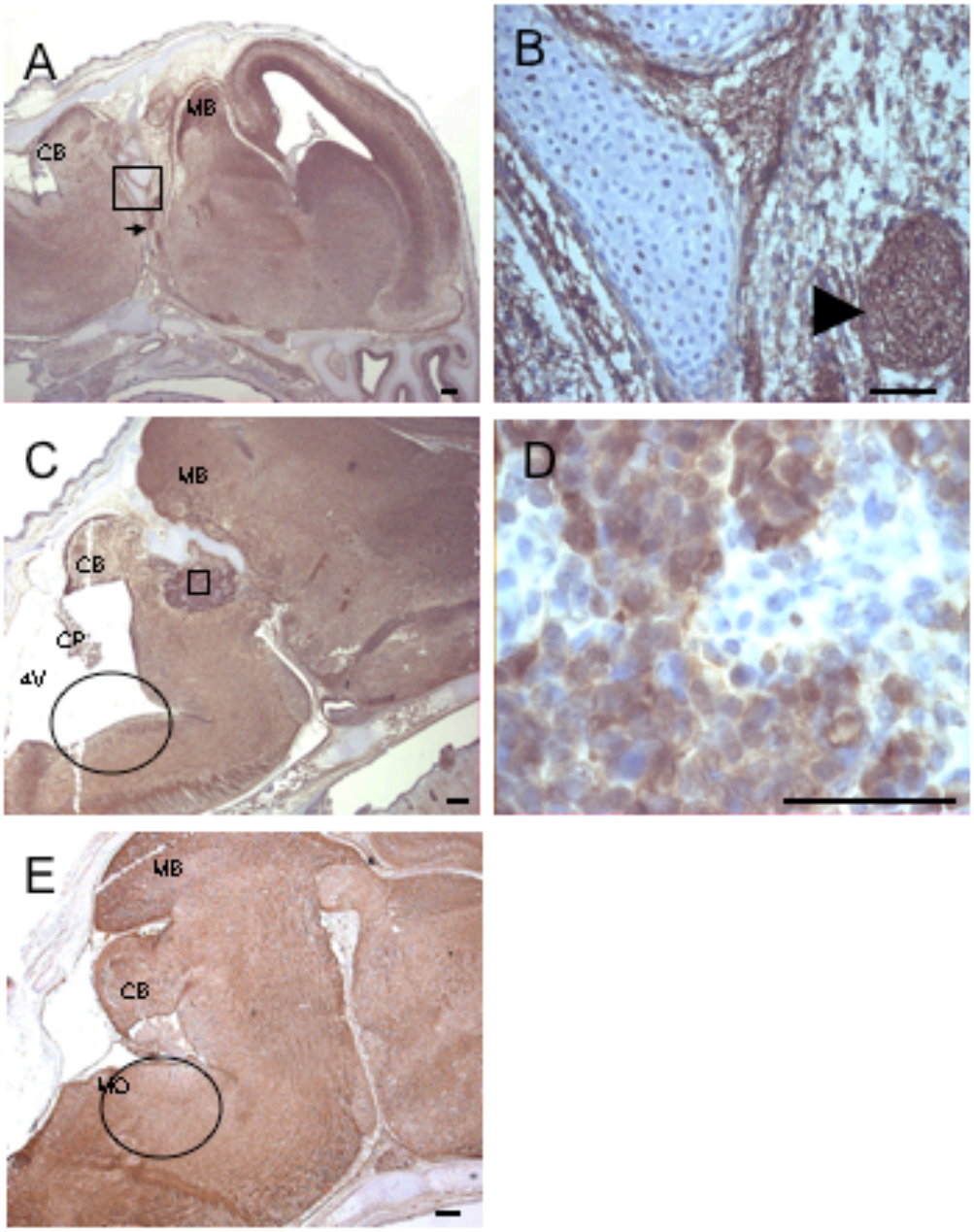

Figure 5.8 Immunohistochemistry using anti-βcatenin antibody showing nuclear localisation of β-catenin in disorganised tissue adjacent to the cerebellum in *En1cre⁻;Apc^{LoxPLoxP}* mice. A, E16.5 *En1cre⁻;Apc^{LoxPLoxP}* mouse showing less pronounced hydrocephalus and smaller patches of disorganised bundles of cells (arrow head). Midbrain seems reduced in size. B, enlarged area from panel A showing small bundle of nuclear β-catenin expressing cells. C shows E18.5 *En1cre⁻;Apc^{LoxPLoxP}* mouse displaying disorganised area with at least 2 different cell types. Panel D shows highly magnified boxed area from panel C. Panel E shows E17.5 *En1cre⁻;Apc^{LoxPLoxP}* control which illustrates that hindbrain tissue appears to have been lost in *En1cre⁻;Apc^{LoxPLoxP}* mutants (circled area of panel C) compared to *En1cre⁻;Apc^{LoxPLoxP}* controls. All sections were cut sagittally at a thickness of 10μm. Scale bars, A and C: 200μm, B and D: 50μm. CB=cerebellum, CP=choroid plexus, MB= midbrain, MO=Medulla Oblongata. 4V=4th ventricle

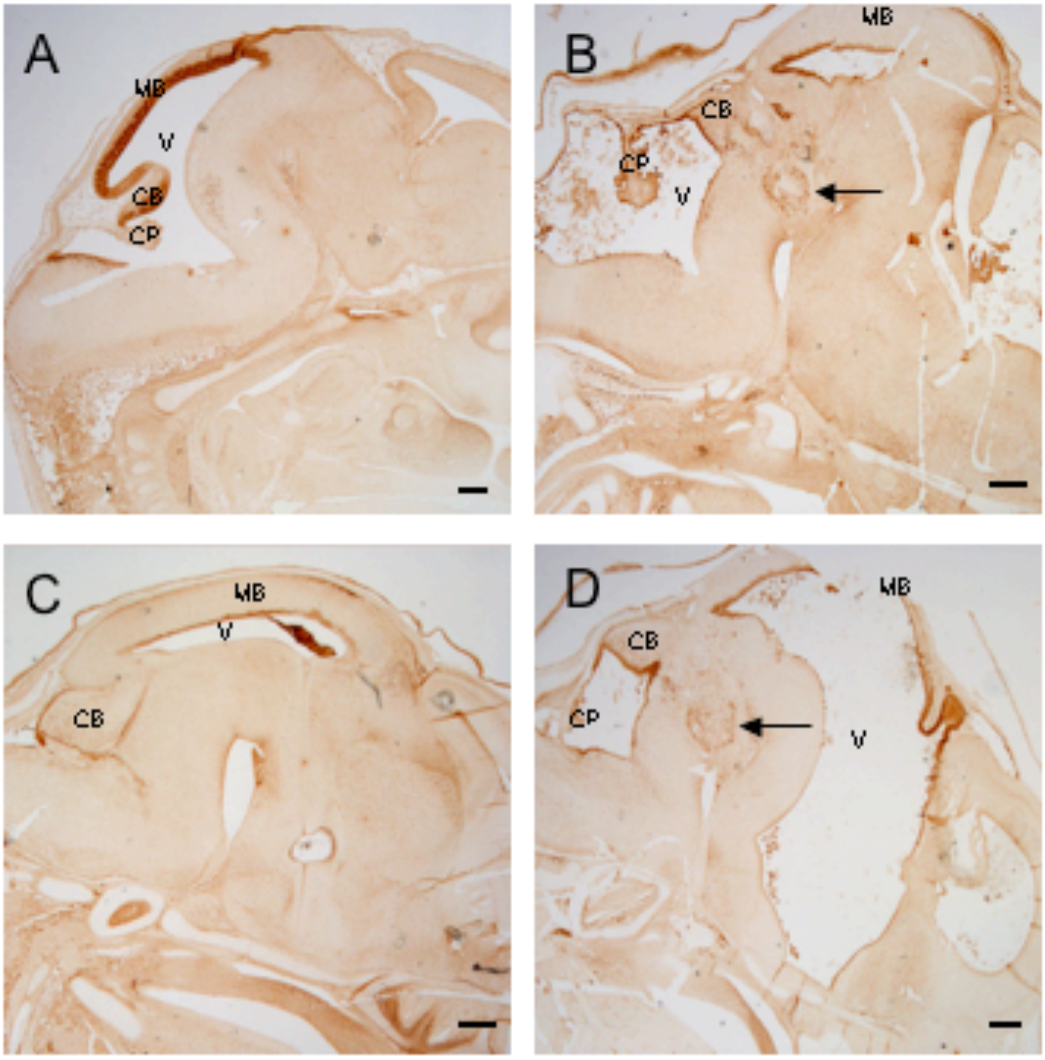

Figure 5.9 Pax3 expression in *En1cre*$^{+}$;*Apc*$^{LoxP/LoxP}$ mice by immunohistochemistry using an anti-Pax3 antibody. A, E13.5 control showing Pax3 expression in ventricular zone of the midbrain. Also in the EGL of developing CB. B, E13.5 *En1cre*$^{+}$;*Apc*$^{LoxP/LoxP}$ mouse again showing expression of Pax3 around ventricluar zone in the midbrain as well as the cerebellum and choroid plexus. Disorganised tissue located at the mid-hindbrain region also expresses Pax3 in some cells (arrow). C, Immunohistochemistry in control E15.5 mouse showing normal expression. D, shows E15.5 *En1cre*$^{+}$;*Apc*$^{LoxP/LoxP}$ littermate. Arrow again indicates disorganised Pax3 expressing tissue. Note: Large gap in dorsal midbrain due to human error and not due to any abnormality caused by mutation. Scale bars: 200μm. CB=cerebellum, CP=choroid plexus, MB= midbrain, V=ventricle

5.2.4 Pax3 expression in conditional mutant embryos

In addition to examining the disorganised area at the mid-hindbrain region, we were interested in examining the effect that mutating Apc in the midbrain and rostral hindbrain had on the development of these areas.

We used an anti-Pax3 antibody which is expressed strongly in the midbrain and EGL of the developing cerebellum to look for possible changes in cell fate. In the area of disorganised tissue, Pax3 expression can be observed in a large proportion of cells (Figure 5.9 B and D). When comparing mutant mice to controls at E13.5 and E15.5, it can be seen that there is still Pax3 staining where we would expect it in the ventricular zone of the midbrain and in the EGL of the CB. This suggests that the midbrain region has not been deleted by mutating Apc in this area. Similarly with the cerebellum, this structure does not seem to be significantly reduced or enlarged in size compared to controls. The histological differences between control mice and mutant mice seem to stem from the effect of hydrocephalus and not due to loss of Apc deleting or expanding mid- or hindbrain structures. Of note, a proportion of cells contained within the disorganised neuroblastic mass express Pax3.

We let a total of seven litters go to full term. The resulting litters were small (with an average size of five pups), and none of the pups had the desired $En1cre^{+};Apc^{LoxP/LoxP}$ genotype. The null hypothesis would state that the resultant progeny were expected to follow Mendelian genetics giving us 1 out of 4 animals of the mutant $En1cre^{+};Apc^{LoxP/LoxP}$ genotype. To test this hypothesis, a chi-squared test was performed to compare the observed results against the expected result. The result of this test showed $p< 0.001$, hence we can reject the null hypothesis that the observed values of our cross are the same as the theoretical distribution of a 3:1 ratio. To recap,

mice survived to at least E18.5, but as no *En1cre*$^{+}$;*Apc*$^{LoxP/LoxP}$ mutants were found after birth, and taking in to account the severity of the brain abnormalities, we believe that mutating *Apc* under control of the *En1* promoter causes an embryonic lethal mutation.

5.3 Discussion

This set of experiments was set up to assess Apc's role in midbrain and early cerebellar development. The reasoning was as follows: Medulloblastoma is thought to stem from dividing neural precursor cells of the outer layer of the cerebellum (Kadin et al. 1970; Marino et al. 2000; Reddy & Packer 1999). A proportion of MBs have lost Apc or otherwise show evidence of dysregulated Wnt siganlling and Wnt signalling is known to be important for the normal development of the cerebellum (McMahon & Bradley 1990). We therefore chose to attempt to address the role of Apc in the early development of the midbrain-hindbrain region in the expectation that it might shed light on the developmental origins of medulloblastoma.

As discussed earlier in this chapter, Panhuysen et al. (2004) ectopically expressed Wnt1 under the control of the En1 promoter. We expected that our *En1cre*$^{+}$;*Apc*$^{LoxP/LoxP}$ mutant mouse would display a similar phenotype as the Panhuysen *En1*$^{+/Wnt1}$ knock-in mutant as the effect of overexpressing Wnt1 has a similar result to deleting Apc by increasing cytoplasmic β-catenin which can in-turn translocate to the nucleus and turn on downstream targets of the Wnt pathway such as *c-myc* and *cyclinD1*. The *En1*$^{+/Wnt1}$ mutant displays an enlarged inferior colliculus

(IC), which is a structure located in the dorso-caudal midbrain. *En1*$^{+/Wnt1}$ mice are viable and fertile, while *En1*$^{Wnt1/Wnt1}$ mice die at P0 and exhibit an even larger IC (Panhuysen et al. 2004). It is thought that *En1*$^{Wnt1/Wnt1}$ mice display an exaggerated phenotype not only due to having additional copies of Wnt1, but also as a consequence of completely losing En1 expression (Panhuysen et al. 2004). Of interest, the phenotype of the *En1*$^{Wnt1/Wnt1}$ mouse differs from the previously published work from the same laboratory which created an *En1*$^{-/-}$ mutant mouse that lacked midbrain and hindbrain structures (Wurst et al. 1994). That implies that the difference in phenotype seen between the *En1*$^{+/Wnt1}$ and the *En1*$^{Wnt1/Wnt1}$ mice is not just attributable to loosing *En1* function in the mid-hindbrain, instead it is probably due to both the loss of *En1* function and the overexpression of *Wnt1*.

In our mutant mice, we saw mesenchyme tissue invading ventrally into the CNS at E13.5 of development. Closely associated with this mesenchyme tissue is a mass of neuroblastic cells which are negative for Apc staining, but do display nuclear β-catenin and Pax3 staining. There are a few possibilities to account for this phenotype. Firstly, it is difficult to know if the neuroblast tissue is giving abnormal signals to make the mesenchyme grow into neural tissue or whether the mesenchyme is causing the abnormal blast tissue to form. Another explanation could be that the loss of *Apc* in the mid-hindbrain region is causing cells to die, thus creating a space for adjacent tissue to grow into. Indeed, a study by Hasegawa et al. (2002) showed a similar result when they conditionally mutated *Apc* in neural crest cells which resulted in massive apoptosis of cephalic and cardiac neural crest cells from E11.5 of development through to birth.

I believe that the hypothesis that loss of *Apc* caused large amounts of cell death leading to surrounding tissue invading the space is unlikely however, because of previous studies suggest that overexpressing *Wnt1* under the control of the *En1* promoter (*En1*$^{+/Wnt1}$) increases cell proliferation in the dorsal midbrain (Panhuysen et al. 2004). Further, if *Wnt1* controls cell proliferation in the early development of the midbrain, it must play a role in its maintenance. Maintenance of the midbrain is in turn necessary to sustain the MHO and subsequently the entire mid-hindbrain region (Panhuysen et al. 2004). To reinforce this, experiments that created Wnt1-null mutants, show a deletion of the entire mid-hindbrain region including the MHO at early stages of gestation (E8.5) (McMahon & Bradley 1990; McMahon et al. 1992; Thomas & Capecchi 1990). In addition to these studies on the effects of Wnt1 in the developing brain, the study by Chen & Walsh (2002) showed that ectopic expression of β-catenin in the brain results in enhanced proliferation of neuronal progenitor cells. This ties in with the theory that canonical Wnt signalling enhances growth of neuronal precursor cells (Chenn & Walsh 2002).

I believe most likely explanation is that the loss of *Apc* causes the disorganised tumour-like region of cells and in these cells, β-catenin is translocated to the nucleus and activates Wnt target genes such as CyclinD1 and matrix metalloproteinase MT1-MMP which are known to stimulate human mesenchymal stem cell (hMSC) proliferation by 40% (Neth et al. 2006). In a study by Neth et al. (2006), hMSCs were stimulated with recombinant Wnt3a and conversely had β-catenin expression knocked-down using RNA interference technology. The results of this study showed that stimulation of hMSCs with recombinant Wnt3a increased by 2-fold their ability to migrate and invade surrounding tissues. Using the reverse approach, by knocking down β-catenin expression (and hence down-regulating cyclinD1 and MT1-MMP),

reduced hMSC proliferation rate and invasion capacity by 64% and 52% respectively (Neth et al. 2006). This study lends weight to the hypothesis that the Apc-negative mass of cells in the mid-hindbrain region is stimulating the mesenchyme tissue to proliferate and invade the neural tissue.

Of note also is that this tumour-like cell cluster ectopically expresses Pax3. This transcription factor and the Pax3 fusion protein PAX3-FKHR (which contains the DNA binding domain of Pax3 and the potent transcriptional activation domain of FKHR), have been implicated in cell transformation and tumourgenesis. Indeed, aberrant Pax3 expression is often found in various tumour types such as melanoma, rhabdomyosarcoma, neuroblastoma and small cell lung cancer (Muratovska et al. 2003; Parker et al. 2004).

The other major phenotype found in all of our $En1cre^{+};Apc^{LoxP/LoxP}$ mutant mice is hydrocephaly. Hydrocephaly can be defined as a brain pathology characterized by increased volume of CSF associated with enlargement of the head, and progressive brain atrophy (Forni et al. 2006). CSF is an important determinant of the extracellular fluid that bathes neurons and glia in the CNS. The choroid plexus maintains the chemical stability of the CSF, and not only continuously produces CSF, but it also is responsible for active transport of metabolites out of the CNS and into the blood. The rest of the CSF which is not secreted by the choroid plexus, is secreted by capillaries in the brain. There are a few factors that could cause an animal to become hydrocephalic. These include, loss of brain tissue causing ventricles to expand, impaired absorption of CSF, or an obstruction in the exit foramina or arachniod villi. Oversecretion of CSF is rare but is thought to occur in some functioning tumours of the choroid plexus (papillomas) (Kandel et al 1996). Although subarachnoid

hemorrhage and high CSF protein content also characterize these tumours which could lead to impaired reabsorption of CSF (Kandel et al 1996). Obstruction of CSF pathways could result from tumours, congenital malformation, or scarring. Lastly, impaired abdorption of CSF could conceivably result from any condition that raises the venous pressure, such as thrombosis or severe congestive heart failure (Kandel et al 1996).

In some *En1cre*$^{+}$;*Apc*$^{LoxP/LoxP}$ mutant embryos there appears to be a loss of hindbrain tissue (shown in Figures 5.8C and E). This loss of tissue could explain an enlargement of the 4th ventricle, however all ventricles are enlarged so this explanation cannot be the main cause of hydrocephalus in these embryos. A more likely explanation is that there is either some form of obstruction, possibly caused by the drainage mechanisms failing to develop properly, or that an excess of CSF is being produced. As far as I am aware, there have been no published studies linking Apc or Wnt signalling with the development of drainage mechanisms such as the exit foramina or the arachnoid villi. There is also no mention in the literature of a role for Wnt signalling in CSF production. The results of this study is reminiscent of the AdCre infected animals, some of which also developed hydrocephalus, indicating that Apc may be involved in regulating fluid balance in the choroid plexus.

As mentioned above, the dorsal midbrain still develops although the phenotype varies between *En1cre*$^{+}$;*Apc*$^{LoxP/LoxP}$ mutants. In some the dorsal midbrain appears shorter and thicker (Figures 5.5B, 5.9B) and in others the dorsal midbrain appears elongated and thin (Figures 5.5 D, 5.9D). These variations in the dorsal midbrain are most likely a secondary consequence of hydrocephalus otherwise we would expect to see a more consistent phenotype. There is one area of the brain where we have consistently

observed a loss of tissue, and that is the rostroventral hindbrain region (Figures 5.8C and E illustrate this). This area of the hindbrain contains the medulla oblongata which controls heart and lung functions.

Given more time, it would have been an interesting side experiment to look at the limbs of our *En1cre*$^{+}$*;Apc*$^{LoxP/LoxP}$ mutants. It is known that Wnt signalling plays a role in limb development at the AER in the chick. During development of the limb, *Fgf8* and *Fgf10* are known to play a key role in the control of limb initiation and in the induction of the AER (reviewed by (Cohn & Tickle 1996). A study by (Kawakami et al. 2001) conducted in chick embryos, showed that several Wnts (*Wnt2b, Wnt3a and Wnt8c*), acting through β-catenin, are as key regulators of *Fgf8* and *Fgf10*. Ectopically expressed *Wnt2b* and *Wnt8c,* acting through *Fgf10* were able to induce ectopic limbs in the embryonic flanks. They also show that the induction of *Fgf8* in the limb ectoderm by *Fgf10* is mediated by the induction of *Wnt3a* (Kawakami et al. 2001). Given the important role that Wnts play in the development of chick limbs, a possible result of loss of Apc in the AER could be an overgrowth of the limbs, a process mediated through *Fgf8* and *Fgf10*.

Other future experiments could try to address in more detail the effect of loss of *Apc* in the mid-hindbrain. Markers of this region such as *Fgf8, Pax2, En1, En2*, *Otx2* and *Gbx2* would allow us to assess more fully the phenotype (ie a shift in *Otx2* and *Gbx2* expression would indicate a shift in the MHO, or the loss of a regional marker would imply that the region in question had been lost). Studying the expression patterns of these genes would also shed more light on the interactions between them and the Wnt pathway.

The area of hindbrain which contained the medulla oblongata appears to have been lost or reduced in size in *En1cre*$^{+}$;*Apc*$^{LoxP/LoxP}$ mutants. A stereological analysis of the midbrain and hindbrain would more accurately tell us how much tissue has been lost. This would also definitively tell us whether the phenotype is due to tissue failing to develop, or cells in this area dying, or whether intercranial pressure caused by hydrocephalus is compressing this area making it appear smaller in size. If cells are being lost in this area, it could be due to either cell death, or a failure of cells to form in the first place. TUNEL (Terminal Deoxynucleotidyltransferase-Mediated dUTP Nick End Labeling) staining is a method for studying apoptosis in cell populations and would give us an indication on the levels of cell death in the hindbrain. An abnormally high level would indicate that cells in this area are dying as a result of losing *Apc* in the midbrain and anterior hindbrain.

We could also study proliferation levels in the mid-hindbrain region of *En1cre*$^{+}$;*Apc*$^{LoxP/LoxP}$ mutants using a BrdU approach. This will label cells which are undergoing s-phase in the cell cycle. It would be interesting to see whether cells within the tumour-like disorganised area of cells at the mid-hindbrain border area proliferating or whether they are differentiated. If this area is behaving as a malignant tumour, we would expect the cells to be actively dividing. Given that a large proportion of cells in this area show nuclear β-catenin localisation, and that an active Wnt signalling pathway often leads to increased proliferation, I would expect that these cells were dividing aggressively. Also, it appears that these tumour-like cells could be associated with the mesenchyme tissue, especially since there is mesenchyme tissue located inside the mass of disorganised cells. Tumours such as gliomas (McComb & Bigner 1985), as well as well as glioblastomas (Tso et al. 2006) have been shown to express mesenchyme immunhistochemical markers. Indeed, a

study by Tso et al. (2006) showed that genes associated with mesenchymal tissue but not to neural lineage such as *TKL-40, TNC, osteonectin, and CD105* were overexpressed in glioblastomas suggesting that these tumours possess mesenchymal properties (Tso et al. 2006). It would be very interesting to test these tumour-like cells for these mesenchymal marker genes by *in situ* hybridisation or test for overexpression of the proteins by immunohistochemistry. If these proteins were overexpressed, then it might suggest that this area had similar characteristics to those of glioblastomas.

This study is not the only one to make use of the Apc^{LoxP} mouse. This mouse was originally created by Shibata et al. (1997) who produced the Apc^{580s} mouse (as it was originally named) to study the effects of conditionally mutating *Apc* in the intestine. It is of note, that the Apc^{LoxP} mouse is a hypomorphic mouse, meaning that it has less than normal expression levels of the wild type *Apc* gene. This is thought to be a consequence of leaving the *neo* cassette in the intron when creating the mouse.

There have however been many studies utilising this mouse and mutating *Apc* in various tissues with severe phenotypic effects. For example, as mentioned earlier, Sansom et al. (2004) used this mouse to mutate *Apc* the gut epithelium. The resulting mutant cells displayed abnormal apoptosis, differentiation, migration and proliferation resulting in *Apc* mutant cells reverting to stem cells and ultimately leading to multiple colorectal adenomcarcinoma formation (Sansom et al. 2004).

Another study used the Apc^{LoxP} mouse in conjunction with an AdCre vector to mutate Apc in the liver. The resulting mice showed a marked phenotype with greatly enlarged hepatocytes and rapid mortality (Colnot et al. 2004). When the adenovirus was administered at a lower dose, 67% of mice developed hepatocellular carcinoma

(HCC), implying that this mouse makes a very good model for studying cancer in the liver.

In the prostate, mutating *Apc* results in hyperplasia after 4.5 weeks of age and adenocacrinoma after 7 months (Bruxvoort et al. 2007), again implying that Apc is a potent tumour suppressor.

Gallagher et al. (2002) looked at the effects of mutating *Apc* specifically in the mammary gland to assess Apc's role in breast tumours. Mutant mice showed a marked delay in mammary duct network growth and during lactation, mice developed multiple metaplastic growths, although these did not progress to neoplasia. It was only when *Tcf-1* was also mutated in these mice, that acanthoma's, a tumour of the epidermis, formed.

As mentioned earlier, a study carried out by Hasegawa et al. (2002), looked at the effects of loss of Apc in the neural crest, leading to severe apoptosis of cardiac and neural crest cells, however there was no sign of tumour formation.

These investigations all point towards the conclusion that conditionally mutating *Apc* in various tissues leads to severe mutations and usually death. It is interesting that not all mutations lead to the same outcome. For instance, deleting *Apc* in the gut leads to formation of multiple adenomas, whereas deleting *Apc* in the prostate leads to growth of a tumour which does not metastasise, and in the breast metaplastic growths form but do not progress to neoplasia. This is could due to regional variation in the function of Apc and also the effects of other signalling factors. The differences in phenotypes could also be due to different potencies of the cre-recombinase used. For instance in Sansom et al.'s (2004) paper, when they reduced the concentration of cre administered, the phenotype reduced in severity.

6. FINAL DISCUSSION

The main aim of this project was to assess the role of Apc in medulloblastoma. Our central hypothesis was that by specifically mutating *Apc* in the hindbrain of early postnatal mice, we could produce a mouse model of medulloblastoma. We took three approaches to this. Firstly, we attemped to specifically inactivate Apc in neural precursor cells in the early postnatal hindbrain using the cre-loxP system. We then, inactivated Apc during embryonic development of the cerebellum, again using cre-loxP tissue-specific gene targeting. This experiment aimed to assess Apc's role in early development of the midbrain and hindbrain and the hypothesised that our $En1cre^{+};Apc^{LoxP/LoxP}$ mice would have major abnormalities in the midbrain and the anterior cerebellum. In particular we expected a phenotype similar to the one seen by Panhuysen et al. (2004) in their mutant as overexpressing *Wnt1* should have the same effect as reducing *Apc* levels.

We sought to produce a mouse model of MB by mutating *Apc* in the early postnatal hindbrain of mice by firstly using the RCAS/*tv-a* system, and then when that proved unsuccessful, we used the AdCre method. From this we hoped to learn whether the loss of *Apc* in the hindbrain could lead to MB formation. However, as we were unable to successfully mutate *Apc* in the granule-cell precursor cells of the cerebellum, we could not produce a suitable mouse model of MB and determine Apc's role in the development of MB in mice. However, we could take these experiments further by using a different mouse line to mutate *Apc* in the cerebellum postnatally. Two possibilities would be to use a Nestin-CreER mouse or the Math1-CreER mouse

(Machold and Fishell 2005). The experiments would be carried out as described in section 4.3.

The final part of this project involved using the En1cre mouse and crossing it to the $Apc^{LoxP/LoxP}$ strain to examine Apc's role in midbrain and early cerebellar development. As discussed earlier, MB is thought of arise from granule cell precursor cells and by an alteration of the normal developmental pathway causing unrestrained cellular growth. Therefore, examining the loss of Apc at the mid-hindbrain junction could shed light on how MBs develop. The resulting $En1cre^{+};Apc^{LoxP/LoxP}$ mutants showed an unexpected and exciting phenotype by displaying hydrocephalus in all ventricles and an in-growth of mesenchyme tissue at the mid-hindbrain border, closely associated with a tumour-like area of cells showing activated Wnt signalling. This mutation was found to be embryonically lethal. Time restrictions limited the current study of this mutant, so future work could again look more closely at the choroid plexus in these mutants and try to assess the role *Apc* in this structure is playing on the hydrocephalic phenotype found in all $En1cre^{+};Apc^{LoxP/LoxP}$ mice. The histology of the choroid plexus could be looked at in more detail, comparing WT mice with $En1cre^{+};Apc^{LoxP/LoxP}$ mutant mice. If this structure was found to be histologically altered in mutant mice, then perhaps the hydrocephaly is being caused by an overproduction of CSF by the choroid plexus. Alternatively drainage structures such as the exit foramen could be studied histologically. If these were found to be blocked, or if they have not formed in the first place, then one could argue that hydrocephaly is being caused by an inability of CSF to drain from the ventricles.

Expression patterns of genes of the mid- and hindbrain such as *Fgf8, Pax2, En1, En2*, *cyclinD1, Otx2* and *Gbx2* could also be studied, which would give more insight into whether or not structures have been lost or shifted in the midbrain and hindbrain regions. For instance, it might shed light on whether structures such as the mid-hindbrain junction have moved because of the effects of hydrocephalus. Also, testing these markers on the tumour-like area of cells at the mid-hindbrain junction might give us more information on the cells in this area. For example, cyclinD1 is a key regulator of G1 to S phase progression in the cell cycle, and promotes proliferation (Shtutman et al. 1999) so if it is highly expressed in this tumour-like area, then it might lend weight to the theory that a loss of *Apc* could lead to increased β-catenin levels may thus promote neoplastic conversion by triggering *cyclinD1* gene expression and, consequently, uncontrolled progression into the cell cycle. Taking this further, examining this area with a BrdU (bromodeoxyuridine) and IddU (iododeoxyuridine) double labelling approach would give us an accurate measure of their cell cycle kinetics. This would tell us how quickly these cells are dividing and give an insight into whether the cells are differentiating or not. Also, immunohistochemistry for proteins such as cyclinD1 and MT1-MMP could give insight on whether this tumour-like area of cells is cauing mesenchyme tissue to invade ventrally into the midbrain.

Further, a stereological analysis of the hindbrain could definitively tell us whether the apparent loss of tissue in this area is due to a loss of cells or an effect of pressure caused by hydrocephalus, compressing the area. TUNEL staining could also be used to shed light on whether large amounts of apoptosis are taking place causing a loss of tissue.

In a study not related to the brain, it would be interesting to look at the limbs of our *En1cre*$^{+}$;*Apc*$^{LoxP/LoxP}$ mutants as is known that Wnt signalling plays a role in limb development at the AER in the chick (Cohn & Tickle 1996). It is very likely that the limbs of these mice are mutated and characterising this mutation would be a novel study.

In conclusion, I believe that components of the Wnt pathway such as Apc play an important role in the development of some MBs. This can be seen through Turcots patients with mutations in *Apc* displaying MBs, as well as studies such as ours who have tested MBs for mutations of components of the Wnt signalling pathway such as β-catenin, Apc and axin and found mutations of proteins in the Wnt pathway occur in around 15% of sporadic MBs (Baeza et al. 2003; Eberhart et al. 2000; Huang et al. 2000; Koch et al. 2001). It is also clear however, that other signalling pathways play at least an equal role in MB development. For instance many studies have looked at the role of Hedgehog signalling in MB, and shown that around 30% of sporadic MB carry mutations in components of the Shh pathway such as *PTCH1, SUFU* and *SMOH* (Pietsch 1997; Raffel et al. 1997; Reifenberger et al. 1998; Taylor et al. 2002; Xie et al. 1997).

7. REFERENCES

Aberle, H., H. Schwartz, and R. Kemler. 1996. Cadherin-catenin complex: protein interactions and their implications for cadherin function. J Cell Biochem **61**:514-523.

Abremski, K., and R. Hoess. 1984. Bacteriophage P1 site-specific recombination. Purification and properties of the Cre recombinase protein. J Biol Chem **259**:1509-1514.

Addison, C. L., M. Hitt, D. Kunsken, and F. L. Graham. 1997. Comparison of the human versus murine cytomegalovirus immediate early gene promoters for transgene expression by adenoviral vectors. J Gen Virol **78 (Pt 7)**:1653-1661.

Adler, P. N. 2002. Planar signaling and morphogenesis in Drosophila. Dev Cell **2**:525-535.

Adler, P. N., and H. Lee. 2001. Frizzled signaling and cell-cell interactions in planar polarity. Curr Opin Cell Biol **13**:635-640.

Adler, P. N., and J. Taylor. 2001. Asymmetric cell division: plane but not simple. Curr Biol **11**:R233-236.

Ahmed, Y., A. Nouri, and E. Wieschaus. 2002. Drosophila Apc1 and Apc2 regulate Wingless transduction throughout development. Development **129**:1751-1762.

Akagi, K., V. Sandig, M. Vooijs, M. Van der Valk, M. Giovannini, M. Strauss, and A. Berns. 1997. Cre-mediated somatic site-specific recombination in mice. Nucleic Acids Res **25**:1766-1773.

Akong, K., B. M. McCartney, and M. Peifer. 2002. Drosophila APC2 and APC1 have overlapping roles in the larval brain despite their distinct intracellular localizations. Dev Biol **250**:71-90.

Amit, S., A. Hatzubai, Y. Birman, J. S. Andersen, E. Ben-Shushan, M. Mann, Y. Ben-Neriah, and I. Alkalay. 2002. Axin-mediated CKI phosphorylation of beta-catenin at Ser 45: a molecular switch for the Wnt pathway. Genes Dev **16**:1066-1076.

Anisimov, V. N., S. V. Ukraintseva, and A. I. Yashin. 2005. Cancer in rodents: does it tell us about cancer in humans? Nat Rev Cancer **5**:807-819.

Araki, I., and H. Nakamura. 1999. Engrailed defines the position of dorsal di-mesencephalic boundary by repressing diencephalic fate. Development **126**:5127-5135.

Askham, J. M., P. Moncur, A. F. Markham, and E. E. Morrison. 2000. Regulation and function of the interaction between the APC tumour suppressor protein and EB1. Oncogene **19**:1950-1958.

Badorf, M., F. Edenhofer, V. Dries, S. Kochanek, and G. Schiedner. 2002. Efficient in vitro and in vivo excision of floxed sequences with a high-capacity adenoviral vector expressing Cre recombinase. Genesis **33**:119-124.

Baeg, G. H., A. Matsumine, T. Kuroda, R. N. Bhattacharjee, I. Miyashiro, K. Toyoshima, and T. Akiyama. 1995. The tumour suppressor gene product APC blocks cell cycle progression from G0/G1 to S phase. Embo J **14**:5618-5625.

Baeza, N., J. Masuoka, P. Kleihues, and H. Ohgaki. 2003. AXIN1 mutations but not deletions in cerebellar medulloblastomas. Oncogene **22**:632-636.

Bailey, P., Cushing, H. 1925. Medulloblastoma cerebelli. Arch Neurol Psychiatry **14**:192-223.

Bardos, J., Z. Sulekova, and W. G. Ballhausen. 1997. Novel exon connections of the brain-specific (BS) exon of the adenomatous polyposis coli gene. Int J Cancer **73**:137-142.

Bates, P., J. A. Young, and H. E. Varmus. 1993. A receptor for subgroup A Rous sarcoma virus is related to the low density lipoprotein receptor. Cell **74**:1043-1051.

Behrens, J., B. A. Jerchow, M. Wurtele, J. Grimm, C. Asbrand, R. Wirtz, M. Kuhl, D. Wedlich, and W. Birchmeier. 1998. Functional interaction of an axin homolog, conductin, with beta-catenin, APC, and GSK3beta. Science **280**:596-599.

Berkner, K. L. 1992. Expression of heterologous sequences in adenoviral vectors. Curr Top Microbiol Immunol **158**:39-66.

Berman, D. M., S. S. Karhadkar, A. R. Hallahan, J. I. Pritchard, C. G. Eberhart, D. N. Watkins, J. K. Chen, M. K. Cooper, J. Taipale, J. M. Olson, and P. A. Beachy. 2002. Medulloblastoma growth inhibition by hedgehog pathway blockade. Science **297**:1559-1561.

Beroud, C., and T. Soussi. 1996. APC gene: database of germline and somatic mutations in human tumors and cell lines. Nucleic Acids Res **24**:121-124.

Berrueta, L., S. K. Kraeft, J. S. Tirnauer, S. C. Schuyler, L. B. Chen, D. E. Hill, D. Pellman, and B. E. Bierer. 1998. The adenomatous polyposis coli-binding protein EB1 is associated with cytoplasmic and spindle microtubules. Proc Natl Acad Sci U S A **95**:10596-10601.

Bhat, R. V., K. J. Axt, J. S. Fosnaugh, K. J. Smith, K. A. Johnson, D. E. Hill, K. W. Kinzler, and J. M. Baraban. 1996. Expression of the APC tumor suppressor protein in oligodendroglia. Glia **17**:169-174.

Bhat, R. V., J. M. Baraban, R. C. Johnson, B. A. Eipper, and R. E. Mains. 1994. High levels of expression of the tumor suppressor gene APC during development of the rat central nervous system. J Neurosci **14**:3059-3071.

Biegel, J. A., L. Tan, F. Zhang, L. Wainwright, P. Russo, and L. B. Rorke. 2002. Alterations of the hSNF5/INI1 gene in central nervous system atypical teratoid/rhabdoid tumors and renal and extrarenal rhabdoid tumors. Clin Cancer Res **8**:3461-3467.

Bisgaard, M. L., K. Fenger, S. Bulow, E. Niebuhr, and J. Mohr. 1994. Familial adenomatous polyposis (FAP): frequency, penetrance, and mutation rate. Hum Mutat **3**:121-125.

Blaker, H., W. J. Hofmann, R. J. Rieker, R. Penzel, M. Graf, and H. F. Otto. 1999. Beta-catenin accumulation and mutation of the CTNNB1 gene in hepatoblastoma. Genes Chromosomes Cancer **25**:399-402.

Boerkoel, C. F., M. J. Federspiel, D. W. Salter, W. Payne, L. B. Crittenden, H. J. Kung, and S. H. Hughes. 1993. A new defective retroviral vector system based on the Bryan strain of Rous sarcoma virus. Virology **195**:669-679.

Bower, J. M. 2002. The organization of cerebellar cortical circuitry revisited: implications for function. Ann N Y Acad Sci **978**:135-155.

Brakeman, J. S., S. H. Gu, X. B. Wang, G. Dolin, and J. M. Baraban. 1999. Neuronal localization of the Adenomatous polyposis coli tumor suppressor protein. Neuroscience **91**:661-672.

Brennan, K., J. M. Gonzalez-Sancho, L. A. Castelo-Soccio, L. R. Howe, and A. M. Brown. 2004. Truncated mutants of the putative Wnt receptor LRP6/Arrow can stabilize beta-catenin independently of Frizzled proteins. Oncogene **23**:4873-4884.

Broccoli, V., E. Boncinelli, and W. Wurst. 1999. The caudal limit of Otx2 expression positions the isthmic organizer. Nature **401**:164-168.

Brown, H. G., J. L. Kepner, E. J. Perlman, H. S. Friedman, D. R. Strother, P. K. Duffner, L. E. Kun, P. T. Goldthwaite, and P. C. Burger. 2000. "Large cell/anaplastic" medulloblastomas: a Pediatric Oncology Group Study. J Neuropathol Exp Neurol **59**:857-865.

Brunner, A., C. Ensinger, M. Christiansen, S. Heiss, I. Verdorfer, G. Mikuz, and A. Tzankov. 2007. Expression and prognostic significance of Tetranectin in invasive and non-invasive bladder cancer. Virchows Arch **450**:659-664.

Brunner, E. C., B. F. Romeike, M. Jung, N. Comtesse, and E. Meese. 2006. Altered expression of beta-catenin/E-cadherin in meningiomas. Histopathology **49**:178-187.

Bruxvoort, K. J., H. M. Charbonneau, T. A. Giambernardi, J. C. Goolsby, C. N. Qian, C. R. Zylstra, D. R. Robinson, P. Roy-Burman, A. K. Shaw, B. D. Buckner-Berghuis, R. E. Sigler, J. H. Resau, R. Sullivan, W. Bushman, and B. O. Williams. 2007. Inactivation of Apc in the mouse prostate causes prostate carcinoma. Cancer Res **67**:2490-2496.

Bryant, P. J., K. L. Watson, R. W. Justice, and D. F. Woods. 1993. Tumor suppressor genes encoding proteins required for cell interactions and signal transduction in Drosophila. Dev Suppl:239-249.

Burger, P. C., I. T. Yu, T. Tihan, H. S. Friedman, D. R. Strother, J. L. Kepner, P. K. Duffner, L. E. Kun, and E. J. Perlman. 1998. Atypical teratoid/rhabdoid tumor of the central nervous system: a highly malignant tumor of infancy and childhood frequently mistaken for medulloblastoma: a Pediatric Oncology Group study. Am J Surg Pathol **22**:1083-1092.

Cabrera, C. V., M. C. Alonso, P. Johnston, R. G. Phillips, and P. A. Lawrence. 1987. Phenocopies induced with antisense RNA identify the wingless gene. Cell **50**:659-663.

Cadigan, K. M., and R. Nusse. 1997. Wnt signaling: a common theme in animal development. Genes Dev **11**:3286-3305.

Cartmell, T., T. Southgate, G. S. Rees, M. G. Castro, P. R. Lowenstein, and G. N. Luheshi. 1999. Interleukin-1 mediates a rapid inflammatory response after injection of adenoviral vectors into the brain. J Neurosci **19**:1517-1523.

Cavenee, W. K. 2000. High-grade gliomas with chromosome 1p loss. J Neurosurg **92**:1080-1081.

Cervoni, L., A. Maleci, M. Salvati, R. Delfini, and G. Cantore. 1994. Medulloblastoma in late adults: report of two cases and critical review of the literature. J Neurooncol **19**:169-173.

Chang, B. H., W. Liao, L. Li, M. Nakamuta, D. Mack, and L. Chan. 1999. Liver-specific inactivation of the abetalipoproteinemia gene completely abrogates very low density lipoprotein/low density lipoprotein production in a viable conditional knockout mouse. J Biol Chem **274**:6051-6055.

Chang, C. H., Houseplan, E.M., Herbert, C. 1969. An operative staging system for a megavoltage radiotherapeutic technique for cerebellar medulloblastomas. Radiology **93**:1351-1359.

Chen, T., I. Yang, R. Irby, K. H. Shain, H. G. Wang, J. Quackenbush, D. Coppola, J. Q. Cheng, and T. J. Yeatman. 2003. Regulation of caspase expression and apoptosis by adenomatous polyposis coli. Cancer Res **63**:4368-4374.

Chenn, A., and C. A. Walsh. 2002. Regulation of cerebral cortical size by control of cell cycle exit in neural precursors. Science **297**:365-369.

Cholley, B., M. Wassef, L. Arsenio-Nunes, A. Brehier, and C. Sotelo. 1989. Proximal trajectory of the brachium conjunctivum in rat fetuses and its early association with the parabrachial nucleus. A study combining in vitro HRP anterograde axonal tracing and immunocytochemistry. Brain Res Dev Brain Res **45**:185-202.

Ciani, L., and P. C. Salinas. 2005. WNTs in the vertebrate nervous system: from patterning to neuronal connectivity. Nat Rev Neurosci **6**:351-362.

Ciemerych, M. A., A. M. Kenney, E. Sicinska, I. Kalaszczynska, R. T. Bronson, D. H. Rowitch, H. Gardner, and P. Sicinski. 2002. Development of mice expressing a single D-type cyclin. Genes Dev **16**:3277-3289.

Clements, W. M., J. Wang, A. Sarnaik, O. J. Kim, J. MacDonald, C. Fenoglio-Preiser, J. Groden, and A. M. Lowy. 2002. beta-Catenin mutation is a frequent cause of Wnt pathway activation in gastric cancer. Cancer Res **62**:3503-3506.

Cohn, M. J., and C. Tickle. 1996. Limbs: a model for pattern formation within the vertebrate body plan. Trends Genet **12**:253-257.

Colnot, S., T. Decaens, M. Niwa-Kawakita, C. Godard, G. Hamard, A. Kahn, M. Giovannini, and C. Perret. 2004. Liver-targeted disruption of Apc in mice activates beta-catenin signaling and leads to hepatocellular carcinomas. Proc Natl Acad Sci U S A **101**:17216-17221.

Dahlstrand, J., M. Lardelli, and U. Lendahl. 1995. Nestin mRNA expression correlates with the central nervous system progenitor cell state in many, but not all, regions of developing central nervous system. Brain Res Dev Brain Res **84**:109-129.

Dahmane, N., and A. Ruiz i Altaba. 1999. Sonic hedgehog regulates the growth and patterning of the cerebellum. Development **126**:3089-3100.

Dameron, K. M., O. V. Volpert, M. A. Tainsky, and N. Bouck. 1994. Control of angiogenesis in fibroblasts by p53 regulation of thrombospondin-1. Science **265**:1582-1584.

Danielian, P. S., and A. P. McMahon. 1996. Engrailed-1 as a target of the Wnt-1 signalling pathway in vertebrate midbrain development. Nature **383**:332-334.

Danthinne, X., and M. J. Imperiale. 2000. Production of first generation adenovirus vectors: a review. Gene Ther **7**:1707-1714.

Davidson, D., E. Graham, C. Sime, and R. Hill. 1988. A gene with sequence similarity to Drosophila engrailed is expressed during the development of the neural tube and vertebrae in the mouse. Development **104**:305-316.

Davis, C. A., and A. L. Joyner. 1988. Expression patterns of the homeo box-containing genes En-1 and En-2 and the proto-oncogene int-1 diverge during mouse development. Genes Dev **2**:1736-1744.

Dikovskaya, D., I. P. Newton, and I. S. Nathke. 2004. The adenomatous polyposis coli protein is required for the formation of robust spindles formed in CSF Xenopus extracts. Mol Biol Cell **15**:2978-2991.

Dolman, C. L. 1988. Melanotic medulloblastoma. A case report with immunohistochemical and ultrastructural examination. Acta Neuropathol (Berl) **76**:528-531.

Eberhart, C. G., K. J. Cohen, T. Tihan, P. T. Goldthwaite, and P. C. Burger. 2003. Medulloblastomas with systemic metastases: evaluation of tumor histopathology and clinical behavior in 23 patients. J Pediatr Hematol Oncol **25**:198-203.

Eberhart, C. G., T. Tihan, and P. C. Burger. 2000. Nuclear localization and mutation of beta-catenin in medulloblastomas. J Neuropathol Exp Neurol **59**:333-337.

Ellison, D. 2002. Classifying the medulloblastoma: insights from morphology and molecular genetics. Neuropathol Appl Neurobiol **28**:257-282.

Evans, A. E., R. D. Jenkin, R. Sposto, J. A. Ortega, C. B. Wilson, W. Wara, I. J. Ertel, S. Kramer, C. H. Chang, S. L. Leikin, and et al. 1990. The treatment of medulloblastoma. Results of a prospective randomized trial of radiation therapy with and without CCNU, vincristine, and prednisone. J Neurosurg **72**:572-582.

Fan, H., and P. A. Khavari. 1999. Sonic hedgehog opposes epithelial cell cycle arrest. J Cell Biol **147**:71-76.

Favor, J., R. Sandulache, A. Neuhauser-Klaus, W. Pretsch, B. Chatterjee, E. Senft, W. Wurst, V. Blanquet, P. Grimes, R. Sporle, and K. Schughart. 1996. The mouse Pax2(1Neu) mutation is identical to a human PAX2 mutation in a family with renal-coloboma syndrome and results in developmental defects of the brain, ear, eye, and kidney. Proc Natl Acad Sci U S A **93**:13870-13875.

Fearnhead, N. S., M. P. Britton, and W. F. Bodmer. 2001. The ABC of APC. Hum Mol Genet **10**:721-733.

Feil, R., J. Wagner, D. Metzger, and P. Chambon. 1997. Regulation of Cre recombinase activity by mutated estrogen receptor ligand-binding domains. Biochem Biophys Res Commun **237**:752-757.

Fodde, R. 2002. The APC gene in colorectal cancer. Eur J Cancer **38**:867-871.

Forni, P. E., C. Scuoppo, I. Imayoshi, R. Taulli, W. Dastru, V. Sala, U. A. Betz, P. Muzzi, D. Martinuzzi, A. E. Vercelli, R. Kageyama, and C. Ponzetto. 2006. High levels of Cre expression in neuronal progenitors cause defects in brain development leading to microencephaly and hydrocephaly. J Neurosci **26**:9593-9602.

Fukumura, D., R. Xavier, T. Sugiura, Y. Chen, E. C. Park, N. Lu, M. Selig, G. Nielsen, T. Taksir, R. K. Jain, and B. Seed. 1998. Tumor induction of VEGF promoter activity in stromal cells. Cell **94**:715-725.

Galiatsatos, P., and W. D. Foulkes. 2006. Familial adenomatous polyposis. Am J Gastroenterol **101**:385-398.

Gallagher, R. C., T. Hay, V. Meniel, C. Naughton, T. J. Anderson, H. Shibata, M. Ito, H. Clevers, T. Noda, O. J. Sansom, J. O. Mason, and A. R. Clarke. 2002. Inactivation of Apc perturbs mammary development, but only directly results in acanthoma in the context of Tcf-1 deficiency. Oncogene **21**:6446-6457.

Gao, C., H. Guo, Z. Mi, M. J. Grusby, and P. C. Kuo. 2007. Osteopontin induces ubiquitin-dependent degradation of STAT1 in RAW264.7 murine macrophages. J Immunol **178**:1870-1881.

Garcia-Castro, M. I., C. Marcelle, and M. Bronner-Fraser. 2002. Ectodermal Wnt function as a neural crest inducer. Science **297**:848-851.

Gilbertson, R. J. 2004. Medulloblastoma: signalling a change in treatment. Lancet Oncol **5**:209-218.

Giles, R. H., J. H. van Es, and H. Clevers. 2003. Caught up in a Wnt storm: Wnt signaling in cancer. Biochim Biophys Acta **1653**:1-24.

Giordana, M. T., P. Cavalla, A. Dutto, L. Borsotti, A. Chio, and D. Schiffer. 1997. Is medulloblastoma the same tumor in children and adults? J Neurooncol **35**:169-176.

Goodrich, L. V., L. Milenkovic, K. M. Higgins, and M. P. Scott. 1997. Altered neural cell fates and medulloblastoma in mouse patched mutants. Science **277**:1109-1113.

Graham, F. L. 2000. Adenovirus vectors for high-efficiency gene transfer into mammalian cells. Immunol Today **21**:426-428.
Greenhouse, J. J., C. J. Petropoulos, L. B. Crittenden, and S. H. Hughes. 1988. Helper-independent retrovirus vectors with Rous-associated virus type O long terminal repeats. J Virol **62**:4809-4812.
Groden, J., A. Thliveris, W. Samowitz, M. Carlson, L. Gelbert, H. Albertsen, G. Joslyn, J. Stevens, L. Spirio, M. Robertson, and et al. 1991. Identification and characterization of the familial adenomatous polyposis coli gene. Cell **66**:589-600.
Hahn, H., L. Wojnowski, A. M. Zimmer, J. Hall, G. Miller, and A. Zimmer. 1998. Rhabdomyosarcomas and radiation hypersensitivity in a mouse model of Gorlin syndrome. Nat Med **4**:619-622.
Hahn, W. C., and R. A. Weinberg. 2002. Modelling the molecular circuitry of cancer. Nat Rev Cancer **2**:331-341.
Hall, A. C., F. R. Lucas, and P. C. Salinas. 2000. Axonal remodeling and synaptic differentiation in the cerebellum is regulated by WNT-7a signaling. Cell **100**:525-535.
Hamada, F., and M. Bienz. 2002. A Drosophila APC tumour suppressor homologue functions in cellular adhesion. Nat Cell Biol **4**:208-213.
Hamilton, S. R., B. Liu, R. E. Parsons, N. Papadopoulos, J. Jen, S. M. Powell, A. J. Krush, T. Berk, Z. Cohen, B. Tetu, and et al. 1995. The molecular basis of Turcot's syndrome. N Engl J Med **332**:839-847.
Hart, M. J., R. de los Santos, I. N. Albert, B. Rubinfeld, and P. Polakis. 1998. Downregulation of beta-catenin by human Axin and its association with the APC tumor suppressor, beta-catenin and GSK3 beta. Curr Biol **8**:573-581.
Hasegawa, S., T. Sato, H. Akazawa, H. Okada, A. Maeno, M. Ito, Y. Sugitani, H. Shibata, J. Miyazaki Ji, M. Katsuki, Y. Yamauchi, K. Yamamura Ki, S. Katamine, and T. Noda. 2002. Apoptosis in neural crest cells by functional loss of APC tumor suppressor gene. Proc Natl Acad Sci U S A **99**:297-302.
Hayashi, S., B. Rubinfeld, B. Souza, P. Polakis, E. Wieschaus, and A. J. Levine. 1997. A Drosophila homolog of the tumor suppressor gene adenomatous polyposis coli down-regulates beta-catenin but its zygotic expression is not essential for the regulation of Armadillo. Proc Natl Acad Sci U S A **94**:242-247.
Henderson, B. R. 2000. Nuclear-cytoplasmic shuttling of APC regulates beta-catenin subcellular localization and turnover. Nat Cell Biol **2**:653-660.
Henderson, B. R., and F. Fagotto. 2002. The ins and outs of APC and beta-catenin nuclear transport. EMBO Rep **3**:834-839.
Houart, C., L. Caneparo, C. Heisenberg, K. Barth, M. Take-Uchi, and S. Wilson. 2002. Establishment of the telencephalon during gastrulation by local antagonism of Wnt signaling. Neuron **35**:255-265.
Hsu, W., L. Zeng, and F. Costantini. 1999. Identification of a domain of Axin that binds to the serine/threonine protein phosphatase 2A and a self-binding domain. J Biol Chem **274**:3439-3445.
Huang, H., B. M. Mahler-Araujo, A. Sankila, L. Chimelli, Y. Yonekawa, P. Kleihues, and H. Ohgaki. 2000. APC mutations in sporadic medulloblastomas. Am J Pathol **156**:433-437.
Huard, J. M., C. C. Forster, M. L. Carter, P. Sicinski, and M. E. Ross. 1999. Cerebellar histogenesis is disturbed in mice lacking cyclin D2. Development **126**:1927-1935.

Huelsken, J., and J. Behrens. 2002. The Wnt signalling pathway. J Cell Sci **115**:3977-3978.

Hulsken, J., W. Birchmeier, and J. Behrens. 1994. E-cadherin and APC compete for the interaction with beta-catenin and the cytoskeleton. J Cell Biol **127**:2061-2069.

IARC. 2001. The International Agency for Research on Cancer. IARC monographs on the evaluation of carcinogenic risks to humans. **1-78**.

Ikeda, S., S. Kishida, H. Yamamoto, H. Murai, S. Koyama, and A. Kikuchi. 1998. Axin, a negative regulator of the Wnt signaling pathway, forms a complex with GSK-3beta and beta-catenin and promotes GSK-3beta-dependent phosphorylation of beta-catenin. Embo J **17**:1371-1384.

Ikeya, M., S. M. Lee, J. E. Johnson, A. P. McMahon, and S. Takada. 1997. Wnt signalling required for expansion of neural crest and CNS progenitors. Nature **389**:966-970.

Imayoshi, I., T. Ohtsuka, D. Metzger, P. Chambon, and R. Kageyama. 2006. Temporal regulation of Cre recombinase activity in neural stem cells. Genesis **44**:233-238.

Ishidate, T., A. Matsumine, K. Toyoshima, and T. Akiyama. 2000. The APC-hDLG complex negatively regulates cell cycle progression from the G0/G1 to S phase. Oncogene **19**:365-372.

Jarrett, C. R., J. Blancato, T. Cao, D. S. Bressette, M. Cepeda, P. E. Young, C. R. King, and S. W. Byers. 2001. Human APC2 localization and allelic imbalance. Cancer Res **61**:7978-7984.

Jeng, Y. M., M. Z. Wu, T. L. Mao, M. H. Chang, and H. C. Hsu. 2000. Somatic mutations of beta-catenin play a crucial role in the tumorigenesis of sporadic hepatoblastoma. Cancer Lett **152**:45-51.

Johnson, R. L., A. L. Rothman, J. Xie, L. V. Goodrich, J. W. Bare, J. M. Bonifas, A. G. Quinn, R. M. Myers, D. R. Cox, E. H. Epstein, Jr., and M. P. Scott. 1996. Human homolog of patched, a candidate gene for the basal cell nevus syndrome. Science **272**:1668-1671.

Joyner, A. L. 1996. Engrailed, Wnt and Pax genes regulate midbrain--hindbrain development. Trends Genet **12**:15-20.

Kadin, M. E., L. J. Rubinstein, and J. S. Nelson. 1970. Neonatal cerebellar medulloblastoma originating from the fetal external granular layer. J Neuropathol Exp Neurol **29**:583-600.

Kandel, E.R., Schwartz, J.H., Jessell, T.M. 1996. Principles of neural science. Appleton and Lange; 3rd edition.

Kanegae, Y., G. Lee, Y. Sato, M. Tanaka, M. Nakai, T. Sakaki, S. Sugano, and I. Saito. 1995. Efficient gene activation in mammalian cells by using recombinant adenovirus expressing site-specific Cre recombinase. Nucleic Acids Res **23**:3816-3821.

Kanegae, Y., K. Takamori, Y. Sato, G. Lee, M. Nakai, and I. Saito. 1996. Efficient gene activation system on mammalian cell chromosomes using recombinant adenovirus producing Cre recombinase. Gene **181**:207-212.

Kawakami, Y., J. Capdevila, D. Buscher, T. Itoh, C. Rodriguez Esteban, and J. C. Izpisua Belmonte. 2001. WNT signals control FGF-dependent limb initiation and AER induction in the chick embryo. Cell **104**:891-900.

Kenney, A. M., and D. H. Rowitch. 2000. Sonic hedgehog promotes G(1) cyclin expression and sustained cell cycle progression in mammalian neuronal precursors. Mol Cell Biol **20**:9055-9067.

Kerbel, R., and J. Folkman. 2002. Clinical translation of angiogenesis inhibitors. Nat Rev Cancer **2**:727-739.

Kiecker, C., and C. Niehrs. 2001. A morphogen gradient of Wnt/beta-catenin signalling regulates anteroposterior neural patterning in Xenopus. Development **128**:4189-4201.

Kimmel, R. A., D. H. Turnbull, V. Blanquet, W. Wurst, C. A. Loomis, and A. L. Joyner. 2000. Two lineage boundaries coordinate vertebrate apical ectodermal ridge formation. Genes Dev **14**:1377-1389.

Kinoshita, N., H. Iioka, A. Miyakoshi, and N. Ueno. 2003. PKC delta is essential for Dishevelled function in a noncanonical Wnt pathway that regulates Xenopus convergent extension movements. Genes Dev **17**:1663-1676.

Kinzler, K. W., M. C. Nilbert, L. K. Su, B. Vogelstein, T. M. Bryan, D. B. Levy, K. J. Smith, A. C. Preisinger, P. Hedge, D. McKechnie, and et al. 1991. Identification of FAP locus genes from chromosome 5q21. Science **253**:661-665.

Kita, K., T. Wittmann, I. S. Nathke, and C. M. Waterman-Storer. 2006. Adenomatous polyposis coli on microtubule plus ends in cell extensions can promote microtubule net growth with or without EB1. Mol Biol Cell **17**:2331-2345.

Kleihues, P., D. N. Louis, B. W. Scheithauer, L. B. Rorke, G. Reifenberger, P. C. Burger, and W. K. Cavenee. 2002. The WHO classification of tumors of the nervous system. J Neuropathol Exp Neurol **61**:215-225; discussion 226-219.

Knoepfler, P. S., P. F. Cheng, and R. N. Eisenman. 2002. N-myc is essential during neurogenesis for the rapid expansion of progenitor cell populations and the inhibition of neuronal differentiation. Genes Dev **16**:2699-2712.

Koch, A., D. Denkhaus, S. Albrecht, I. Leuschner, D. von Schweinitz, and T. Pietsch. 1999. Childhood hepatoblastomas frequently carry a mutated degradation targeting box of the beta-catenin gene. Cancer Res **59**:269-273.

Koch, A., A. Waha, J. C. Tonn, N. Sorensen, F. Berthold, M. Wolter, J. Reifenberger, W. Hartmann, W. Friedl, G. Reifenberger, O. D. Wiestler, and T. Pietsch. 2001. Somatic mutations of WNT/wingless signaling pathway components in primitive neuroectodermal tumors. Int J Cancer **93**:445-449.

Kornberg, T. 1981. Engrailed: a gene controlling compartment and segment formation in Drosophila. Proc Natl Acad Sci U S A **78**:1095-1099.

Kuhl, M., K. Geis, L. C. Sheldahl, T. Pukrop, R. T. Moon, and D. Wedlich. 2001. Antagonistic regulation of convergent extension movements in Xenopus by Wnt/beta-catenin and Wnt/Ca2+ signaling. Mech Dev **106**:61-76.

Lagutin, B. M., I. D. Petrov, V. L. Sukhorukov, S. Kammer, S. Mickat, R. Schill, K. H. Schartner, A. Ehresmann, Y. A. Shutov, and H. Schmoranzer. 2003. Raman regime energy dependence of alignment and orientation of KrII states populated by resonant Auger effect. Phys Rev Lett **90**:073001.

Lee, Y., H. L. Miller, P. Jensen, R. Hernan, M. Connelly, C. Wetmore, F. Zindy, M. F. Roussel, T. Curran, R. J. Gilbertson, and P. J. McKinnon. 2003. A molecular fingerprint for medulloblastoma. Cancer Res **63**:5428-5437.

Liu, C., Y. Li, M. Semenov, C. Han, G. H. Baeg, Y. Tan, Z. Zhang, X. Lin, and X. He. 2002. Control of beta-catenin phosphorylation/degradation by a dual-kinase mechanism. Cell **108**:837-847.

Liu, H., Z. Wu, and B. Liu. 2001. [Effects of retinoic acid on secretion of apolipoproteins A I, A II, B100, C III and E by cultured HepG2 cells]. Hua Xi Yi Ke Da Xue Xue Bao **32**:52-54.

Loomis, C. A., R. A. Kimmel, C. X. Tong, J. Michaud, and A. L. Joyner. 1998. Analysis of the genetic pathway leading to formation of ectopic apical ectodermal ridges in mouse Engrailed-1 mutant limbs. Development **125**:1137-1148.

Louie, R. K., S. Bahmanyar, K. A. Siemers, V. Votin, P. Chang, T. Stearns, W. J. Nelson, and A. I. Barth. 2004. Adenomatous polyposis coli and EB1 localize in close proximity of the mother centriole and EB1 is a functional component of centrosomes. J Cell Sci **117**:1117-1128.

Lundell, M. J., Q. Chu-LaGraff, C. Q. Doe, and J. Hirsh. 1996. The engrailed and huckebein genes are essential for development of serotonin neurons in the Drosophila CNS. Mol Cell Neurosci **7**:46-61.

Mahmoud, N. N., S. K. Boolbol, R. T. Bilinski, C. Martucci, A. Chadburn, and M. M. Bertagnolli. 1997. Apc gene mutation is associated with a dominant-negative effect upon intestinal cell migration. Cancer Res **57**:5045-5050.

Mahmoud, N. N., A. J. Dannenberg, R. T. Bilinski, J. R. Mestre, A. Chadburn, M. Churchill, C. Martucci, and M. M. Bertagnolli. 1999. Administration of an unconjugated bile acid increases duodenal tumors in a murine model of familial adenomatous polyposis. Carcinogenesis **20**:299-303.

Mao, J., J. Wang, B. Liu, W. Pan, G. H. Farr, 3rd, C. Flynn, H. Yuan, S. Takada, D. Kimelman, L. Li, and D. Wu. 2001. Low-density lipoprotein receptor-related protein-5 binds to Axin and regulates the canonical Wnt signaling pathway. Mol Cell **7**:801-809.

Marino, S. 2005. Medulloblastoma: developmental mechanisms out of control. Trends Mol Med **11**:17-22.

Marino, S., M. Vooijs, H. van Der Gulden, J. Jonkers, and A. Berns. 2000. Induction of medulloblastomas in p53-null mutant mice by somatic inactivation of Rb in the external granular layer cells of the cerebellum. Genes Dev **14**:994-1004.

Maronpot, R. R., G. Flake, and J. Huff. 2004. Relevance of animal carcinogenesis findings to human cancer predictions and prevention. Toxicol Pathol **32 Suppl 1**:40-48.

Matsumine, A., A. Ogai, T. Senda, N. Okumura, K. Satoh, G. H. Baeg, T. Kawahara, S. Kobayashi, M. Okada, K. Toyoshima, and T. Akiyama. 1996. Binding of APC to the human homolog of the Drosophila discs large tumor suppressor protein. Science **272**:1020-1023.

McCartney, B. M., H. A. Dierick, C. Kirkpatrick, M. M. Moline, A. Baas, M. Peifer, and A. Bejsovec. 1999. Drosophila APC2 is a cytoskeletally-associated protein that regulates wingless signaling in the embryonic epidermis. J Cell Biol **146**:1303-1318.

McComb, R. D., and D. D. Bigner. 1985. Immunolocalization of monoclonal antibody-defined extracellular matrix antigens in human brain tumors. J Neurooncol **3**:181-186.

McMahon, A. P., and A. Bradley. 1990. The Wnt-1 (int-1) proto-oncogene is required for development of a large region of the mouse brain. Cell **62**:1073-1085.

McMahon, A. P., P. W. Ingham, and C. J. Tabin. 2003. Developmental roles and clinical significance of hedgehog signaling. Curr Top Dev Biol **53**:1-114.

McMahon, A. P., A. L. Joyner, A. Bradley, and J. A. McMahon. 1992. The midbrain-hindbrain phenotype of Wnt-1-/Wnt-1- mice results from stepwise deletion of engrailed-expressing cells by 9.5 days postcoitum. Cell **69**:581-595.

Meyers, E. N., M. Lewandoski, and G. R. Martin. 1998. An Fgf8 mutant allelic series generated by Cre- and Flp-mediated recombination. Nat Genet **18**:136-141.

Millen, K. J., W. Wurst, K. Herrup, and A. L. Joyner. 1994. Abnormal embryonic cerebellar development and patterning of postnatal foliation in two mouse Engrailed-2 mutants. Development **120**:695-706.
Miller, J. R., A. M. Hocking, J. D. Brown, and R. T. Moon. 1999. Mechanism and function of signal transduction by the Wnt/beta-catenin and Wnt/Ca2+ pathways. Oncogene **18**:7860-7872.
Mogensen, M. M., J. B. Tucker, J. B. Mackie, A. R. Prescott, and I. S. Nathke. 2002. The adenomatous polyposis coli protein unambiguously localizes to microtubule plus ends and is involved in establishing parallel arrays of microtubule bundles in highly polarized epithelial cells. J Cell Biol **157**:1041-1048.
Morin, P. J., B. Vogelstein, and K. W. Kinzler. 1996. Apoptosis and APC in colorectal tumorigenesis. Proc Natl Acad Sci U S A **93**:7950-7954.
Morrison, E. E., B. N. Wardleworth, J. M. Askham, A. F. Markham, and D. M. Meredith. 1998. EB1, a protein which interacts with the APC tumour suppressor, is associated with the microtubule cytoskeleton throughout the cell cycle. Oncogene **17**:3471-3477.
Moseley, J. B., F. Bartolini, K. Okada, Y. Wen, G. G. Gundersen, and B. L. Goode. 2007. Regulated binding of adenomatous polyposis coli protein to actin. J Biol Chem **282**:12661-12668.
Muenke, M., Beachy, P. A. 2001. The Metabolic and Molecular Bases of Inherited Disease (eds Scriver, C., Beaudet, A., Sly, W. & Valle, D.) (McGraw-Hill, New York).6203–6230.
Muncan, V., O. J. Sansom, L. Tertoolen, T. J. Phesse, H. Begthel, E. Sancho, A. M. Cole, A. Gregorieff, I. M. de Alboran, H. Clevers, and A. R. Clarke. 2006. Rapid loss of intestinal crypts upon conditional deletion of the Wnt/Tcf-4 target gene c-Myc. Mol Cell Biol **26**:8418-8426.
Munemitsu, S., I. Albert, B. Souza, B. Rubinfeld, and P. Polakis. 1995. Regulation of intracellular beta-catenin levels by the adenomatous polyposis coli (APC) tumor-suppressor protein. Proc Natl Acad Sci U S A **92**:3046-3050.
Munemitsu, S., B. Souza, O. Muller, I. Albert, B. Rubinfeld, and P. Polakis. 1994. The APC gene product associates with microtubules in vivo and promotes their assembly in vitro. Cancer Res **54**:3676-3681.
Muratovska, A., C. Zhou, S. He, P. Goodyer, and M. R. Eccles. 2003. Paired-Box genes are frequently expressed in cancer and often required for cancer cell survival. Oncogene **22**:7989-7997.
Nakagawa, H., Y. Murata, K. Koyama, A. Fujiyama, Y. Miyoshi, M. Monden, T. Akiyama, and Y. Nakamura. 1998. Identification of a brain-specific APC homologue, APCL, and its interaction with beta-catenin. Cancer Res **58**:5176-5181.
Nathke, I. S. 1999. The adenomatous polyposis coli protein. Mol Pathol **52**:169-173.
Nathke, I. S. 2004. The adenomatous polyposis coli protein: the Achilles heel of the gut epithelium. Annu Rev Cell Dev Biol **20**:337-366.
Nathke, I. S., C. L. Adams, P. Polakis, J. H. Sellin, and W. J. Nelson. 1996. The adenomatous polyposis coli tumor suppressor protein localizes to plasma membrane sites involved in active cell migration. J Cell Biol **134**:165-179.
Neth, P., M. Ciccarella, V. Egea, J. Hoelters, M. Jochum, and C. Ries. 2006. Wnt signaling regulates the invasion capacity of human mesenchymal stem cells. Stem Cells **24**:1892-1903.

Norrby, E., P. Swoveland, K. Kristensson, and K. P. Johnson. 1980. Further studies on subacute encephalitis and hydrocephalus in hamsters caused by measles virus from persistently infected cell cultures. J Med Virol **5**:109-116.

Nusse, R., and H. E. Varmus. 1982. Many tumors induced by the mouse mammary tumor virus contain a provirus integrated in the same region of the host genome. Cell **31**:99-109.

Orsulic, S. 2002. An RCAS-TVA-based approach to designer mouse models. Mamm Genome **13**:543-547.

Palay, S. L., S. Billings-Gagliardi, and V. Chan-Palay. 1974. Neuronal perikarya with dispersed, single ribosomes in the visual cortex of Macaca mulatta. J Cell Biol **63**:1074-1089.

Panhuysen, M., D. M. Vogt Weisenhorn, V. Blanquet, C. Brodski, U. Heinzmann, W. Beisker, and W. Wurst. 2004. Effects of Wnt1 signaling on proliferation in the developing mid-/hindbrain region. Mol Cell Neurosci **26**:101-111.

Park, W. S., R. R. Oh, J. Y. Park, P. J. Kim, M. S. Shin, J. H. Lee, H. S. Kim, S. H. Lee, S. Y. Kim, Y. G. Park, W. G. An, H. S. Kim, J. J. Jang, N. J. Yoo, and J. Y. Lee. 2001. Nuclear localization of beta-catenin is an important prognostic factor in hepatoblastoma. J Pathol **193**:483-490.

Parker, C. J., S. G. Shawcross, H. Li, Q. Y. Wang, C. S. Herrington, S. Kumar, R. M. MacKie, W. Prime, I. G. Rennie, K. Sisley, and P. Kumar. 2004. Expression of PAX 3 alternatively spliced transcripts and identification of two new isoforms in human tumors of neural crest origin. Int J Cancer **108**:314-320.

Parks, R. J., L. Chen, M. Anton, U. Sankar, M. A. Rudnicki, and F. L. Graham. 1996. A helper-dependent adenovirus vector system: removal of helper virus by Cre-mediated excision of the viral packaging signal. Proc Natl Acad Sci U S A **93**:13565-13570.

Pietsch, M. 1997. [The "Wittlich Vaccination Study" as a model for improving specific immunoprotection of the population]. Gesundheitswesen **59**:707-709.

Pietsch, T., and O. D. Wiestler. 1997. Molecular neuropathology of astrocytic brain tumors. J Neurooncol **35**:211-222.

Pili, R., Y. Guo, J. Chang, H. Nakanishi, G. R. Martin, and A. Passaniti. 1994. Altered angiogenesis underlying age-dependent changes in tumor growth. J Natl Cancer Inst **86**:1303-1314.

Pinto, V. B., S. Prasad, J. Yewdell, J. Bennink, and S. H. Hughes. 2000. Restricting expression prolongs expression of foreign genes introduced into animals by retroviruses. J Virol **74**:10202-10206.

Polakis, P. 1997. The adenomatous polyposis coli (APC) tumor suppressor. Biochim Biophys Acta **1332**:F127-147.

Polakis, P. 2000. Wnt signaling and cancer. Genes Dev **14**:1837-1851.

Pomeroy, S. L., P. Tamayo, M. Gaasenbeek, L. M. Sturla, M. Angelo, M. E. McLaughlin, J. Y. Kim, L. C. Goumnerova, P. M. Black, C. Lau, J. C. Allen, D. Zagzag, J. M. Olson, T. Curran, C. Wetmore, J. A. Biegel, T. Poggio, S. Mukherjee, R. Rifkin, A. Califano, G. Stolovitzky, D. N. Louis, J. P. Mesirov, E. S. Lander, and T. R. Golub. 2002. Prediction of central nervous system embryonal tumour outcome based on gene expression. Nature **415**:436-442.

Prevec, L., B. S. Christie, K. E. Laurie, M. M. Bailey, F. L. Graham, and K. L. Rosenthal. 1991. Immune response to HIV-1 gag antigens induced by recombinant adenovirus vectors in mice and rhesus macaque monkeys. J Acquir Immune Defic Syndr **4**:568-576.

Raffel, B. 1997a. Random-pattern lower leg fasciocutaneous flap. Plast Reconstr Surg **99**:269.
Raffel, C. 1997b. Recombinant DNA technology. Pediatr Neurosurg **26**:170-179.
Raffel, C. 2004. Medulloblastoma: molecular genetics and animal models. Neoplasia **6**:310-322.
Raffel, C., R. B. Jenkins, L. Frederick, D. Hebrink, B. Alderete, D. W. Fults, and C. D. James. 1997. Sporadic medulloblastomas contain PTCH mutations. Cancer Res **57**:842-845.
Reddy, A. T., and R. J. Packer. 1999. Medulloblastoma. Curr Opin Neurol **12**:681-685.
Reifenberger, J., M. Wolter, R. G. Weber, M. Megahed, T. Ruzicka, P. Lichter, and G. Reifenberger. 1998. Missense mutations in SMOH in sporadic basal cell carcinomas of the skin and primitive neuroectodermal tumors of the central nervous system. Cancer Res **58**:1798-1803.
Relf, M., S. LeJeune, P. A. Scott, S. Fox, K. Smith, R. Leek, A. Moghaddam, R. Whitehouse, R. Bicknell, and A. L. Harris. 1997. Expression of the angiogenic factors vascular endothelial cell growth factor, acidic and basic fibroblast growth factor, tumor growth factor beta-1, platelet-derived endothelial cell growth factor, placenta growth factor, and pleiotrophin in human primary breast cancer and its relation to angiogenesis. Cancer Res **57**:963-969.
Rijsewijk, F., M. Schuermann, E. Wagenaar, P. Parren, D. Weigel, and R. Nusse. 1987. The Drosophila homolog of the mouse mammary oncogene int-1 is identical to the segment polarity gene wingless. Cell **50**:649-657.
Robertson, C. P., M. M. Braun, and H. Roelink. 2004. Sonic hedgehog patterning in chick neural plate is antagonized by a Wnt3-like signal. Dev Dyn **229**:510-519.
Robertson, P. L. 2006. Advances in treatment of pediatric brain tumors. NeuroRx **3**:276-291.
Rodriguez, C. I., and S. M. Dymecki. 2000. Origin of the precerebellar system. Neuron **27**:475-486.
Romer, J. T., H. Kimura, S. Magdaleno, K. Sasai, C. Fuller, H. Baines, M. Connelly, C. F. Stewart, S. Gould, L. L. Rubin, and T. Curran. 2004. Suppression of the Shh pathway using a small molecule inhibitor eliminates medulloblastoma in Ptc1(+/-)p53(-/-) mice. Cancer Cell **6**:229-240.
Roose, J., and H. Clevers. 1999. TCF transcription factors: molecular switches in carcinogenesis. Biochim Biophys Acta **1424**:M23-37.
Rorke, L. B. 1994. Experimental production of primitive neuroectodermal tumors and its relevance to human neuro-oncology. Am J Pathol **144**:444-448.
Rorke, L. B., R. J. Packer, and J. A. Biegel. 1996. Central nervous system atypical teratoid/rhabdoid tumors of infancy and childhood: definition of an entity. J Neurosurg **85**:56-65.
Rubinfeld, B., I. Albert, E. Porfiri, C. Fiol, S. Munemitsu, and P. Polakis. 1996. Binding of GSK3beta to the APC-beta-catenin complex and regulation of complex assembly. Science **272**:1023-1026.
Rubinfeld, B., P. Robbins, M. El-Gamil, I. Albert, E. Porfiri, and P. Polakis. 1997. Stabilization of beta-catenin by genetic defects in melanoma cell lines. Science **275**:1790-1792.
Sansom, O. J., V. S. Meniel, V. Muncan, T. J. Phesse, J. A. Wilkins, K. R. Reed, J. K. Vass, D. Athineos, H. Clevers, and A. R. Clarke. 2007. Myc deletion rescues Apc deficiency in the small intestine. Nature **446**:676-679.

Sansom, O. J., K. R. Reed, A. J. Hayes, H. Ireland, H. Brinkmann, I. P. Newton, E. Batlle, P. Simon-Assmann, H. Clevers, I. S. Nathke, A. R. Clarke, and D. J. Winton. 2004. Loss of Apc in vivo immediately perturbs Wnt signaling, differentiation, and migration. Genes Dev **18**:1385-1390.

Santoro, I. M., and J. Groden. 1997. Alternative splicing of the APC gene and its association with terminal differentiation. Cancer Res **57**:488-494.

Sato, Y., K. Tanaka, G. Lee, Y. Kanegae, Y. Sakai, S. Kaneko, H. Nakabayashi, T. Tamaoki, and I. Saito. 1998. Enhanced and specific gene expression via tissue-specific production of Cre recombinase using adenovirus vector. Biochem Biophys Res Commun **244**:455-462.

Sauer, B., and N. Henderson. 1988. Site-specific DNA recombination in mammalian cells by the Cre recombinase of bacteriophage P1. Proc Natl Acad Sci U S A **85**:5166-5170.

Schmidt, E. V., G. Christoph, R. Zeller, and P. Leder. 1990. The cytomegalovirus enhancer: a pan-active control element in transgenic mice. Mol Cell Biol **10**:4406-4411.

Seeling, J. M., J. R. Miller, R. Gil, R. T. Moon, R. White, and D. M. Virshup. 1999. Regulation of beta-catenin signaling by the B56 subunit of protein phosphatase 2A. Science **283**:2089-2091.

Senda, T., S. Iino, K. Matsushita, A. Matsumine, S. Kobayashi, and T. Akiyama. 1998. Localization of the adenomatous polyposis coli tumour suppressor protein in the mouse central nervous system. Neuroscience **83**:857-866.

Serbedzija, G. N., M. Dickinson, and A. P. McMahon. 1996. Cell death in the CNS of the Wnt-1 mutant mouse. J Neurobiol **31**:275-282.

Shi, Q., S. Rafii, M. H. Wu, E. S. Wijelath, C. Yu, A. Ishida, Y. Fujita, S. Kothari, R. Mohle, L. R. Sauvage, M. A. Moore, R. F. Storb, and W. P. Hammond. 1998. Evidence for circulating bone marrow-derived endothelial cells. Blood **92**:362-367.

Shibata, H., K. Toyama, H. Shioya, M. Ito, M. Hirota, S. Hasegawa, H. Matsumoto, H. Takano, T. Akiyama, K. Toyoshima, R. Kanamaru, Y. Kanegae, I. Saito, Y. Nakamura, K. Shiba, and T. Noda. 1997. Rapid colorectal adenoma formation initiated by conditional targeting of the Apc gene. Science **278**:120-123.

Shin, I., H. J. Kim, J. E. Lee, and M. C. Gye. 2006. Aquaporin7 expression during perinatal development of mouse brain. Neurosci Lett **409**:106-111.

Shtutman, M., J. Zhurinsky, I. Simcha, C. Albanese, M. D'Amico, R. Pestell, and A. Ben-Ze'ev. 1999. The cyclin D1 gene is a target of the beta-catenin/LEF-1 pathway. Proc Natl Acad Sci U S A **96**:5522-5527.

Simeone, A. 2000. Positioning the isthmic organizer where Otx2 and Gbx2meet. Trends Genet **16**:237-240.

Sloan, D. A., D. M. Fleiszer, G. K. Richards, D. Murray, and R. A. Brown. 1983. Increased incidence of experimental colon cancer associated with long-term metronidazole therapy. Am J Surg **145**:66-70.

Smith, A. J., H. S. Stern, M. Penner, K. Hay, A. Mitri, B. V. Bapat, and S. Gallinger. 1994a. Somatic APC and K-ras codon 12 mutations in aberrant crypt foci from human colons. Cancer Res **54**:5527-5530.

Smith, D. W. 1996. Cancer mortality at very old ages. Cancer **77**:1367-1372.

Smith, K. J., D. B. Levy, P. Maupin, T. D. Pollard, B. Vogelstein, and K. W. Kinzler. 1994b. Wild-type but not mutant APC associates with the microtubule cytoskeleton. Cancer Res **54**:3672-3675.

Smith, T. W., and R. I. Davidson. 1984. Medullomyoblastoma. A histologic, immunohistochemical, and ultrastructural study. Cancer **54**:323-332.
Soriano, P. 1999. Generalized lacZ expression with the ROSA26 Cre reporter strain. Nat Genet **21**:70-71.
Stec, D. E., R. L. Davisson, R. E. Haskell, B. L. Davidson, and C. D. Sigmund. 1999. Efficient liver-specific deletion of a floxed human angiotensinogen transgene by adenoviral delivery of Cre recombinase in vivo. J Biol Chem **274**:21285-21290.
Stern, H. S., S. Viertelhausen, A. G. Hunter, K. O'Rourke, M. Cappelli, H. Perras, K. Serfas, A. Blumenthall, D. Dewar, E. Baumann, and A. E. Lagarde. 2001. APC I1307K increases risk of transition from polyp to colorectal carcinoma in Ashkenazi Jews. Gastroenterology **120**:392-400.
Stricklett, P. K., R. D. Nelson, and D. E. Kohan. 1999. The Cre/loxP system and gene targeting in the kidney. Am J Physiol **276**:F651-657.
Su, L. K., K. A. Johnson, K. J. Smith, D. E. Hill, B. Vogelstein, and K. W. Kinzler. 1993. Association between wild type and mutant APC gene products. Cancer Res **53**:2728-2731.
Tada, M., and J. C. Smith. 2000. Xwnt11 is a target of Xenopus Brachyury: regulation of gastrulation movements via Dishevelled, but not through the canonical Wnt pathway. Development **127**:2227-2238.
Tait, D. M., H. Thornton-Jones, H. J. Bloom, J. Lemerle, and P. Morris-Jones. 1990. Adjuvant chemotherapy for medulloblastoma: the first multi-centre control trial of the International Society of Paediatric Oncology (SIOP I). Eur J Cancer **26**:464-469.
Taniguchi, K., L. R. Roberts, I. N. Aderca, X. Dong, C. Qian, L. M. Murphy, D. M. Nagorney, L. J. Burgart, P. C. Roche, D. I. Smith, J. A. Ross, and W. Liu. 2002. Mutational spectrum of beta-catenin, AXIN1, and AXIN2 in hepatocellular carcinomas and hepatoblastomas. Oncogene **21**:4863-4871.
Taylor, M. D., L. Liu, C. Raffel, C. C. Hui, T. G. Mainprize, X. Zhang, R. Agatep, S. Chiappa, L. Gao, A. Lowrance, A. Hao, A. M. Goldstein, T. Stavrou, S. W. Scherer, W. T. Dura, B. Wainwright, J. A. Squire, J. T. Rutka, and D. Hogg. 2002. Mutations in SUFU predispose to medulloblastoma. Nat Genet **31**:306-310.
Teune, T. M., J. van der Burg, J. van der Moer, J. Voogd, and T. J. Ruigrok. 2000. Topography of cerebellar nuclear projections to the brain stem in the rat. Prog Brain Res **124**:141-172.
Thliveris, A., H. Albertsen, T. Tuohy, M. Carlson, J. Groden, G. Joslyn, L. Gelbert, W. Samowitz, L. Spirio, and R. White. 1996. Long-range physical map and deletion characterization of the 1100-kb NotI restriction fragment harboring the APC gene. Genomics **34**:268-270.
Thomas, K. R., and M. R. Capecchi. 1990. Targeted disruption of the murine int-1 proto-oncogene resulting in severe abnormalities in midbrain and cerebellar development. Nature **346**:847-850.
Townsley, F. M., and M. Bienz. 2000. Actin-dependent membrane association of a Drosophila epithelial APC protein and its effect on junctional Armadillo. Curr Biol **10**:1339-1348.
Tso, C. L., P. Shintaku, J. Chen, Q. Liu, J. Liu, Z. Chen, K. Yoshimoto, P. S. Mischel, T. F. Cloughesy, L. M. Liau, and S. F. Nelson. 2006. Primary glioblastomas express mesenchymal stem-like properties. Mol Cancer Res **4**:607-619.

Urbanek, P., I. Fetka, M. H. Meisler, and M. Busslinger. 1997. Cooperation of Pax2 and Pax5 in midbrain and cerebellum development. Proc Natl Acad Sci U S A **94**:5703-5708.

Utsuki, S., H. Oka, Y. Sato, B. Tsutiya, K. Kondo, Y. Tanizaki, S. Tanaka, and K. Fujii. 2004. E, N-cadherins and beta-catenin expression in medulloblastoma and atypical teratoid/rhabdoid tumor. Neurol Med Chir (Tokyo) **44**:402-406; discussion 407.

van de Wetering, M., E. Sancho, C. Verweij, W. de Lau, I. Oving, A. Hurlstone, K. van der Horn, E. Batlle, D. Coudreuse, A. P. Haramis, M. Tjon-Pon-Fong, P. Moerer, M. van den Born, G. Soete, S. Pals, M. Eilers, R. Medema, and H. Clevers. 2002. The beta-catenin/TCF-4 complex imposes a crypt progenitor phenotype on colorectal cancer cells. Cell **111**:241-250.

Wallingford, J. B., and R. M. Harland. 2001. Xenopus Dishevelled signaling regulates both neural and mesodermal convergent extension: parallel forces elongating the body axis. Development **128**:2581-2592.

Wang, V. Y., and H. Y. Zoghbi. 2001. Genetic regulation of cerebellar development. Nat Rev Neurosci **2**:484-491.

Wang, Y., L. A. Krushel, and G. M. Edelman. 1996. Targeted DNA recombination in vivo using an adenovirus carrying the cre recombinase gene. Proc Natl Acad Sci U S A **93**:3932-3936.

Wassarman, K. M., M. Lewandoski, K. Campbell, A. L. Joyner, J. L. Rubenstein, S. Martinez, and G. R. Martin. 1997. Specification of the anterior hindbrain and establishment of a normal mid/hindbrain organizer is dependent on Gbx2 gene function. Development **124**:2923-2934.

Wechsler-Reya, R., and M. P. Scott. 2001. The developmental biology of brain tumors. Annu Rev Neurosci **24**:385-428.

Wei, Y., M. Fabre, S. Branchereau, F. Gauthier, G. Perilongo, and M. A. Buendia. 2000. Activation of beta-catenin in epithelial and mesenchymal hepatoblastomas. Oncogene **19**:498-504.

Wetmore, C., D. E. Eberhart, and T. Curran. 2000. The normal patched allele is expressed in medulloblastomas from mice with heterozygous germ-line mutation of patched. Cancer Res **60**:2239-2246.

Wingate, R. 2005. Math-Map(ic)s. Neuron **48**:1-4.

Wingate, R. J. 2001. The rhombic lip and early cerebellar development. Curr Opin Neurobiol **11**:82-88.

Wodarz, A., and R. Nusse. 1998. Mechanisms of Wnt signaling in development. Annu Rev Cell Dev Biol **14**:59-88.

Wong, M. H., M. L. Hermiston, A. J. Syder, and J. I. Gordon. 1996. Forced expression of the tumor suppressor adenomatosis polyposis coli protein induces disordered cell migration in the intestinal epithelium. Proc Natl Acad Sci U S A **93**:9588-9593.

Wurst, W., A. B. Auerbach, and A. L. Joyner. 1994. Multiple developmental defects in Engrailed-1 mutant mice: an early mid-hindbrain deletion and patterning defects in forelimbs and sternum. Development **120**:2065-2075.

Xia, L., K. A. St Denis, and B. Bapat. 1995. Evidence for a novel exon in the coding region of the adenomatous polyposis coli (APC) gene. Genomics **28**:589-591.

Xiao, J. H., C. Ghosn, C. Hinchman, C. Forbes, J. Wang, N. Snider, A. Cordrey, Y. Zhao, and R. A. Chandraratna. 2003. Adenomatous polyposis coli (APC)-independent regulation of beta-catenin degradation via a retinoid X receptor-mediated pathway. J Biol Chem **278**:29954-29962.

Xie, J., R. L. Johnson, X. Zhang, J. W. Bare, F. M. Waldman, P. H. Cogen, A. G. Menon, R. S. Warren, L. C. Chen, M. P. Scott, and E. H. Epstein, Jr. 1997. Mutations of the PATCHED gene in several types of sporadic extracutaneous tumors. Cancer Res **57**:2369-2372.

Yamanaka, H., N. Hashimoto, K. Koyama, H. Nakagawa, Y. Nakamura, and K. Noguchi. 2002. Expression of Apc2 during mouse development. Brain Res Gene Expr Patterns **1**:107-114.

Yamanaka, R., S. A. Zullo, R. Tanaka, M. Blaese, and K. G. Xanthopoulos. 2001. Enhancement of antitumor immune response in glioma models in mice by genetically modified dendritic cells pulsed with Semliki forest virus-mediated complementary DNA. J Neurosurg **94**:474-481.

Yanagawa, S., Y. Matsuda, J. S. Lee, H. Matsubayashi, S. Sese, T. Kadowaki, and A. Ishimoto. 2002. Casein kinase I phosphorylates the Armadillo protein and induces its degradation in Drosophila. Embo J **21**:1733-1742.

Yokota, N., S. Nishizawa, S. Ohta, H. Date, H. Sugimura, H. Namba, and M. Maekawa. 2002. Role of Wnt pathway in medulloblastoma oncogenesis. Int J Cancer **101**:198-201.

Yu, X., L. Waltzer, and M. Bienz. 1999. A new Drosophila APC homologue associated with adhesive zones of epithelial cells. Nat Cell Biol **1**:144-151.

Zeltzer, P. M., J. M. Boyett, J. L. Finlay, A. L. Albright, L. B. Rorke, J. M. Milstein, J. C. Allen, K. R. Stevens, P. Stanley, H. Li, J. H. Wisoff, J. R. Geyer, P. McGuire-Cullen, J. A. Stehbens, S. B. Shurin, and R. J. Packer. 1999. Metastasis stage, adjuvant treatment, and residual tumor are prognostic factors for medulloblastoma in children: conclusions from the Children's Cancer Group 921 randomized phase III study. J Clin Oncol **17**:832-845.

Zeng, L., F. Fagotto, T. Zhang, W. Hsu, T. J. Vasicek, W. L. Perry, 3rd, J. J. Lee, S. M. Tilghman, B. M. Gumbiner, and F. Costantini. 1997. The mouse Fused locus encodes Axin, an inhibitor of the Wnt signaling pathway that regulates embryonic axis formation. Cell **90**:181-192.

Zinyk, D. L., E. H. Mercer, E. Harris, D. J. Anderson, and A. L. Joyner. 1998. Fate mapping of the mouse midbrain-hindbrain constriction using a site-specific recombination system. Curr Biol **8**:665-668.

Zumbrunn, J., K. Kinoshita, A. A. Hyman, and I. S. Nathke. 2001. Binding of the adenomatous polyposis coli protein to microtubules increases microtubule stability and is regulated by GSK3 beta phosphorylation. Curr Biol **11**:44-49.

Zurawel, R. H., S. A. Chiappa, C. Allen, and C. Raffel. 1998. Sporadic medulloblastomas contain oncogenic beta-catenin mutations. Cancer Res **58**:896-899.

8. Appendix

8.1 Solutions and Reagents

Ampicillin (Amp)
0.5g Ampicillin (Sigma A-9518)
dH_2O to 100ml, filter-sterilise and store at -20°C (100μg/ml working concentration)

Buffer QBT (Equilibration buffer)
750mM NaCl
50mM MOPS (pH 7.0)
15% isopropanol
0.15% Triton® X-100.

Buffer QC (wash buffer)
1.0M NaCl
50mM MOPS (pH 7.0)
15% isopropanol.

Buffer QF (Elution buffer)
1.25M NaCl
50mM Tris (pH 8.5)
15% isopropanol

Church Hybridisation Buffer
5g BSA (Bovine Serum Albumin)
Dissolve in 75 ml of water, then add
250ml 1M Na_2HPO_4 (pH 7.2)
175ml 20% SDS
1ml 0.5M EDTA

Church Wash
40ml 1M Na_2HPO_4 (pH 7.2)
50ml 20% SDS
2ml 0.5M EDTA

DNase-free RNase A
200mg RNase A (Sigma R-5500)
3.3μl 3M NaOAc, pH 4.5
dH_2O to 10ml
boil for 10minutes (aliquot and store at –20°C)

0.5 M EDTA, pH 8.0 (disodium ethylenediamine tetraacetate)
186.1g Na_2EDTA
Dissolve in approx. 400ml dH_2O, adjust pH to 8.0 with 10 N NaOH, and adjust to 1 litre final volume with water.

100 mM EDTA

20ml 0.5 M EDTA
80ml dH_2O

5mg/ml ethidium bromide (EtBr)
500mg EtBr (Sigma H-3375)
dH_2O to 100ml

Filter denaturing solution
1.5M NaCl
0.5M NaOH

Filter neutralising solution
1.5M NaCl
1mM EDTA
0.5M Tris-HCL (pH=7.2)

LB Medium
10g Bacto-Tryptone
5g Bacto-yeast extract
10g NaCl
dH_2O to 950ml, adjust pH to 7.0 with 5M NaOH, and adjust volume to 1L with distilled water, aliquot into 250ml bottles and autoclave to sterilize.

LB plates
10g Bacto-Tryptone
10g NaCl
15g Bacto-agar
dH_2O to 1 litre, autoclave to sterilize, cool to 55ºC, add antibiotic if desired, and pour into sterile petri dishes (approx. 20ml/plate).

Lysis/Solution P2
200mM NaOH
1% SDS
Stored at room temperature

PCR 10x reaction buffer
100mM Tris-HCL (pH 8.3)
15mM $MgCl_2$
500mM KCL

Phenol/chloroform/isoamyl alcohol (25:25:1)
100ml TE-saturated phenol
100ml chloroform
4ml isoamyl alcohol

Phosphate –Buffered Saline (PBS)
8g NaCl
0.2g KCL
1.44g Na_2HPO_4
0.24g KH_2PO_4
dH_2O to 800ml, adjust pH to 7.4 with 1N HCL and adjust volume to 1L with distilled water.

4% Paraformaldyhide (PFA)
4g PFA powder
Make up to 100ml with PBS

10% SDS (sodium dodecyl sulfate)
10g SDS (Fisher S529-3)
dH_2O to 100ml

SOC Media
2% w/v Bacto- tryptone
0.5% w/v Bacto-yeast extract
0.05% NaCl
Autoclave and add the following filter sterilised reagents. 1% (v/v) 1M $MgCl_2$, 1% (v/v) 1M $MgS0_4$ and 0.1% (v/v) 2M glucose solution.

3M NaOAc, pH 4.5
408.24g $NaOAc\text{-}3H_2O$
Dissolve in approx. 800ml dH_2O, adjust pH to 4.5 with glacial acetic acid and bring to a final volume of 1 L with dH_2O.

10M NaOH (sodium hydroxide)
40g NaOH dissolved
dH_2O to 100ml

Southern denaturing solution
0.4M NaOH
0.6M NaCL

Southern neutralisation solution
1.5M NaCL
0.5M Tris-HCL (pH=7.5)

SSC (20X) (standard saline-citrate)
88.3g sodium citrate
175.3g NaCl
Dissolved in approximately 900ml water, adjust pH to 7.0 with 1N HCL and bring final volume to 1L.

1X SSC
5ml 20X SSC
95ml dH_20

10 X TBE
109g Tris base
55g boric acid
9.3g EDTA
dH_2O to 1L

TE buffer
10ml 1 M Tris-HCl (pH 7.6)
2ml 0.5 M EDTA
dH_2O to 1L

Tissue Lysis Buffer (TTLB)
100mM Tris HCL (pH 8.5)
5mM EDTA
200mM NaCl
0.2% SDS
Proteinase K added to final concentration of 100μg /ml prior to use.

Transfer Buffer
1.45g Tris buffer
7.2g Glycine
200ml methanol
dH_2O to 1L

Tris-Buffered Saline (TBS)
8g NaCl
0.2g KCL
3g Tris base
dH_2O to 800ml, adjust pH to 7.4 with 1N HCL and bring final volume to 1L.

TBS-Tx
100ml 10x TBS
1ml 0.1% Triton-X100
dH_2O to 1L

1M Tris-HCl, pH 7.6, 8.0, 8.5, 9.0, 9.5
121.1g Tris base
dH_2O to 800ml
Adjust pH with concentrated HCl and then add dH_2O to 1 L.

Type III loading buffer
0.25% bromophenol blue
0.25% xylene cyanol
30% glycerol

2XTY medium
16g Bacto- tryptone
10g Bacto-yeast extract
5g NaCl
dH_2O to 1L

8.2 Protocols

8.2.1 Apc Immunohistochemistry

A. Dewaxing:

-Xylene	2 x 10 mins
-100% EtOH	2 x 5 mins
-95% EtOH	1 x 5 mins
-90% EtOH	1 x 5 mins
-70% EtOH	1 x 5 mins
-50% EtOH	1 x 5 mins
-PBS	1 x 5 mins

B. Antigen Retrieval:

-10mM Na Citrate (pH6)	4 x 5 mins at full power
-Cool slides	20 mins on ice
-PBS	1 x 5 mins

C. Primary Antibody:

-Block slides in PBSTx (0.1% Tx), 10% NGS	15-30mins @ RT
-Apply 1^0 Ab (at 1:500 conc. in PSBTx/NGS)	O/N @ 4^0C

Next day:

-Wash in PBSTx	2 x 5 mins
-Apply Peroxidase block	1 x 5 mins
-Wash in PBSTx	2 x 5 mins

D. Secondary Antibody

-Apply 150µl HRP 2^0 Ab	30 mins

[At this stage, make up DAB solution: 2ml substrate + 2 drops (40µl) DAB]

-Wash in PBSTx	3 x 5 mins

E. Colour Development

-Apply >200µl DAB mix and incubate in dark
-Observe every 2 mins (colour normally develops within 3 – 10 mins)

F. Counterstain (optional)

-(Fresh filtered) Haematoxylin	5 secs (for light stain)
- Water	1 min
-STWS	1 min
-Water	1 min

G. Mounting

-70% EtOH	1 min
-90% EtOH	1 min
-100% EtOH	2 x 2 min
-Xylene	2 x 5 min
-Mount with DPX	Leave O/N @ RT to set

NOTES:
APC antibody is from Santa Cruz. It's a rabbit polyclonal and works on wax sections. It's a C terminal Ab, so should should not bind in areas of APC floxed deletion.
Order: Insight Biotechnology Limited. PO Box 520, Wembley, Middlesex, HA9 7YN, UK. Tel: +44 20 8385 0303. Cat # sc-896. Rabbit anti-Human APC (C-20).
NGS = Normal Goat Serum

Envision Kit: Dako envision plus HRP rabbit kit. Cat # K4010.

8.2.2 β-catenin Immunohistochemistry

A. Dewaxing:

-2 x 7 mins in xylene
-5 mins in each alcohol (100% > 90% > 70%)
-Rinse in dH_2O

B. Antigen Retrieval:

-Microwave 3 x 5 mins in 10mM Na-Citrate buffer (pH6)
-Leave for ~30 mins to cool

-Wash in water

-Apply 150µl peroxidase block (bottle 1)
-Incubate 5 mins
-Rinse with water
-Place in TBS

C. Primary Antibody:

-Apply 350µl Antibody buffer (TBS/20% rabbit serum)
-Leave for ~10 mins to equilibriate
-Apply 200µl 1^0 antibody (between 1/50 - 1/200 dilution in Ab buffer)
-Incubate for 45 mins at room temp
-Rinse with water
-Place in TBS

-Make up DAB solution (needs to sit for ~10 mins)
-1.5 ml buffered substrate (bottle 3a) + 30µl DAB (bottle 3b)
-Mix solution

D. Secondary Antibody

-Apply 150µl HRP anti-mouse (bottle 2) per slide
-Leave for 30 mins
-Put slides back into TBS
-Change the TBS

E. Colour Development

-Apply 150µl pre-prepared DAB solution per slide

-Do this quickly as the colour comes up very quickly
-Will probably only take a maximum of 10 mins

-Rinse twice in water (pour contaminated water into DAB jug)

F. Counterstain (optional)

-Approx 10-20 sec haematoxylin and ~1 min eosin counterstain

G. Mounting

-Dehydrate through alcohol series for ~2 mins in each
-2 x 10 mins in xylene
-Mount with DPX

Citrate buffer (10mM sodium citrate pH6.0) – Na3Citrate.2H2O: 294.1g/mole
-10x (100mM): 29.4g/l + 2.9ml conc. HCl gives pH6.0
-Dilute to 10mM (ie 100ml of 10xbuffer and 900ml ddH2O)
-Will also need to pH again (add ~150µl conc. HCl to give pH6)

Antibodies
-β-Catenin: BD Transduction labs cat no: 610153

TBS
-8g NaCl
-0.2g KCl
-6g Tris-base
-ddH2O to 800ml, adjust pH to 7.5 with conc. HCL and bring final volume to 1L.

Antibody buffer (TBS/20% Rabbit serum)
-4.8ml TBS
-1.2ml serum

Antibody solution (Per slide)

Conc.	µl Ab	µl Ab buffer
1:50	4µl	196µl
1:100	2µl	198µl
1:200	1µl	199µl

8.2.3 Southern Blot Protocol

A. Making Probe

Set up restriction digest
-40ul midi DNA
-5ul buffer H
-5ul EcoR1

-Run 1ul DNA on a gel to make sure it has cut properly, then run the rest on a gel
-Cut band out of gel and gel purify

B. Making Southern Quality DNA

-Tissue (eg half cerebellum) – 0.5ml TTLB + proteinase K (O/N @55^0C)
-Equal vol Phenol Cholorform (eg 500µl) mix by inverting (10mins)
-Take aqueous phase into clean tube
-Add 1/10 vol 3M NaOAc pH 5.5 (50µl) and top up with 100% EtOH (800µl)
-Shake hard
-Can see DNA as white precipitate
-Pick up with yellow tip
-Dip into next epp containing 70% EtOH to wash
-Transfer intoclean empty labelled epp
-Leave open ~2-3h to allow EtOH to evaporate
-Add ~200µl TE buffer (depends on how much DNA there is)
-Resuspend by shaking (O/N @ 37^0C)

C. Cutting DNA

	If using SacI (HC) enzyme (80U/µl)
40µl DNA	*41µl DNA*
5µl 10x Buffer	*5µl 10x Buffer*
2µl Spermidine	*2µl Spermidine*
2µl Enzyme (≥50U)	*1µl Enzyme (80U)*

O/N @ 37^0C

-Then run ~2µl on 0.8% minigel to check it cut properly
-If it cut properly, run 50µl on a maxi gel

D. Maxi gel

300ml of 0.8%
- -300ml 1xTBE
- -2.4g Saekem LE agarose
- -*NO ETHIDIUM*

-Leave to set for 1h
- ~2.5L buffer to fill tank (add this in gel room) and leave for further 30mins
-Add 10µl Loading Buffer to each 50µl sample and load gel
-Run for ~16h (O/N) @ 40V

Next day

-Remove gel from box and put in square container
-Add some of the running buffer and to this add ~100µl ethidium
-Shake for 20mins
-While this is happening, make up HCl solution for the acid nic step
    -500ml H_20 + 12.5ml conc HCl
-Cut off extra lanes and take a picture of gel (with fluorescent ruler next to ladder)
-Remove gel from holder, and GENTLY place in square box
-Pour over ~ 250ml HCl mix and shake for 30mins
-Denat solution (2 x 30mins)
-Neut solution (2 x 30mins)

E. Transfer

-Fill the bottom of the transfer dish with 20xSSC
-Place gel on the wick paper (wick paper is Whatman 3mm paper)
-We want a water tight seal so need to use saran wrap and cut tightly around gel
-Dampen the surface of the gel with 20xSSC
-Cut hybond paper to the exact size of the gel (in cupboard with maxi tank)
-Cut 4 pieces of Whatman (3mm) paper to the exact size of the gel
-Identify the hybond paper using a sharpie pen
-Dip the hybond paper into 2xSSC and put face (writing) side down on the gel
    -Use Millipore tweezers to do this
-Wet 2 pieces of whatman paper and put them on top
-*important* Break a 10ml pipette and roll it across the paper to ensure all the air bubbles are out
-Put 1 roll of Kleenex tissues on top and place a tray with a full 1L bottle for weight
-Leave for ~2h and replace Whatman paper and Kleenex towels and leave O/N

F. Fix DNA to hybond paper

-Take off all the layers of paper
-Put a little 2xSSC on saran wrap, then wrap hybond paper in that
    -crosslinking works better if the membrane is wet
-Cross link in machine (run on automatic program)
-Remove excess water with Whatman paper and allow to air dry
-Make a holder with Whatman paper, place hybond inside and tape the edges closed
-Bake in oven @120^0C for 15mins
-The DNA will be fixed on the membrane now and stable for years at room temp.

G. Radioactive part:

-Fill out radioactivity forms
-Heat 2 water baths (37 and 100^0C) and monitor all surfaces and sign in
-Denature DNA (want to label 25ng DNA per southern) and Salmon Sperm (SS)
    -Make up 45µl (eg 44.5µl buffer TE, 0.5µl DNA proble, if probe conc is 50ng/µl)

-100^0C for 5'
-straight onto ice for 1 min
-spin DNA down briefly

-Add the 45µl ontop of the labelling mix (don't mix at this stage)
-Then add 5µl ^{32}P (pipette up and down ~12 times to mix)
-37^0C for 10 mins (put lead top over tubes)
-Add 5µl 0.2M EDTA (to stop the reaction)
-Use Selfadex column (little porus beads in buffer) Protocol for this is on the fridge on left of centrifuge
-snap bottom off column, then put in screw tube and spin buffer 1 min
-Discard buffer and add the pink ^{32}P mix to the centre of gel in new tube
-spin for 2mins you should be left with the clear labelled probe in tube. This should register off the scale at about 6cm from the Geiger counter if the probe has labelled well.
-Put in lead pot (or Perspex slide rack) then into freezer

[monitor work area]

H. Prehybridise the Filter
-Wet membrane and filter and roll filter in membrane
-Unroll this inside the hyb tube
-Add 20ml buffer and 200µl SS (at 100µg/ml)
-seal lid and put in hyb oven (60^0C) for ~3h
-Put SS back in freezer

I. Hybridisation stage
-After 3h, put SS and probe into 100^0C H_2O bath for 10mins (from frozen)
-then straight onto ice again so the DNA can not re-anneal
-Pour away prehyb buffer and add 10ml Hyb buffer with 100µl SS and all the probe
-Put back in the oven O/N

Next day
-Pour radioactive probe down sink (make sure water is running)
-Give 1 quick wash with wash buffer (Church wash)
-Then 30' washes @65^0C until you see a big fall in radiation levels
-when this happens, stop washes
-Put filter face down on saran wrap and wrap it up
-Wash nylon mesh and bottle and lid to eliminate the radioactive waste
-Estimate how much radiation went down the sink (approx 80%) and how much went into solid bin (approx 20%)
-Need to fill out 3 sheets with this info
-Put filter in cassette and place in -80^0C freezer O/N

Next day
-Turn processor on (takes 30mins to heat up), and take cassette out of freezer to warm up
-Process the film

<u>Isotope paperwork</u>
-Note the stock number (DB number) and mark this on pot of isotope
-We use 5µl ^{32}P per probe

-When you dispose of isotope, you have to record that
-We estimate 80% goes down sink and 20% goes into solid waste
-There are 2 green books in hot room for this information
-There is also a sheet on solid waste bin for amounts of waste

Southern Denaturing solution

	Mol wt.	Per litre	5 litres
0.5M NaOH	40	20g	100g
1.5M NaCl	58.44	87.66g	438.3g

Southern Neutralising solution

	Mol wt.	Per litre	5 litres
0.5M Tris pH 7.0	121.14	60.57g	302.85g
3M NaCl	58.44	175.32g	876.6g

20xSSC

	Mol wt.	Per litre	5 litres
3M NaCl	58.44	175.32g	876.6g
0.3M Na-citrate	294.10	88.23g	441.15g

Church and Gilbert Hybridisation Solutions

Church Hybridisation Mix

250ml 0.5M $NaPO_4$ pH 7.2	0.5M PO_4
175ml 20% SDS (or 350ml 10% SDS)	7% SDS
1ml 0.5M EDTA	1mM EDTA
5g BSA	1% BSA

Top up to 500ml
[For BSA, dissolve the 5g in 75ml ddH_2O before adding to rest of mix]

Church Wash

50ml 20% SDS (or 100ml 10% SDS)	1% SDS
2ml 0.5M EDTA	1mM EDTA
40ml 0.5M $NaPO_4$ pH 7.2	40mM PO_4

Top up to 1 litre

0.5M $NaPO_4$ pH 7.2

134g $Na_2HPO_4.7H_2O$	or 71g anhydrous Na_2HPO_4
4ml H_3PO_4	or 89g dihydrate

Top up to 1 litre

Anhydrous Na_2HPO_4 Mwt = 141.96
Heptahydrate Mwt = 267.96
Dihydrate Mwt = 177.99

Denatured Salmon Sperm DNA
100mg Deoxyribonucleic acid sodium salt (S.S.) [*ICN biomedicals Inc. Cat.#152275*]
10ml H_2O

-Pass vigorously through a 17-G needle 20 times to shear DNA (unless presheared)
-Place in boiling water bath for 10mins then straight onto ice
-If stored at -20^{o}C, reheat to 100^{o}C for 5mins then straight onto ice before using

Labelling Kits:

Amersham Biosciences (http://www4.amershambiosciences.com)
-Probe Quant G50 Micro Columns (Catalogue #27-5335-01 cost £130 in Jan 06)
-Rediprime II Random Prome Labelling System (Cat #RPN1663 cost £256 in Jan 06)

8.2.4 Virus Preparation for the TVA System

Select a vector, either RCASBP(A) or other ALV-A vector

Clone your gene of interest into the selected vector

Purify the plasmid DNA using a method that will yield pure DNA (Cesium chloride gradients, Qiagen Maxiprep, etc.)

Prepare either chicken embryo fibroblast cells or DF1 chicken fibroblasts for transfection. The protocol below is for DF 1 cells.

Maintain DF1 cells in growth medium (DMEM with high glucose, 10% fetal bovine serum, 2 mM L-glutamine, 10 units/ ml penicillin, 10 ug/ml streptomycin) at 37oC and 5% CO2.

Transfection Protocol using GeneJuice (for 35mm dish)

DAY 1

-Seed cells at appropriate density (50-80%) – depends of cell type and protocol etc
-Seed into Penicillin/Streptomycin (pen/strep) free media

DAY 2

-Change medium=> -aspirate
-wash once in PBS
-cover cells in 3ml media (pen/strep free DMEM can work with or without serum)

Transfection Mix

*For most cell lines the optimal ratio of genejuice to DNA is 3µl genejuice to 1µl DNA, but the ratio can be varied from 2-6µl per µg DNA during optimisation

-100µl serum free DMEM + 3µl genejuice
-mix thoroughly
-Incubate at RT for 5 mins
-For each 35mm dish to be transfected, add 1µg to the GJ/serum-free mix. Gently pipette up and down
-Incubate the mixture at RT for 5-15mins
-Add the mixture dropwise (evenly over the plate) to the cells in complete growth medium. Gently rock the dish, as swirling concentrates the transfection mix in the centre of the plate.
-Remove the transfection mix after 2-8 hrs incubation and replace with complete growth medium – this is an optional step
-Incubate the cells for 24-72 hrs at 37^0C (5% CO_2)

-Check cells every day

Virus Collection

To obtain high titer viruses for stocks, collect virus from cultures grown in minimum amounts of medium (5 ml/100 mm tissue culture dish) and approximately 24 hours after cells become confluent. Harvests can be done every 12 hours, adding 5 ml of medium each time. Typically, plates can be passed from 1 to 2 plates, resuming virus collection 18-24 hours after passage.

Remove cell debris by low-speed centrifugation and store supernatant aliquots at –80oC. There is a typical loss of up to one log of viral titer after one cycle of freezing and thawing.

ALV-derived viruses mutate frequently and mutant viruses that have lost the gene of interest commonly show a growth advantage. Following multiple rounds of infections, culture supernatants may have many mutant viruses but due to viral interference, only a limited number of new infections occur in producer cells. Viral mutations can be minimized by passing/propagating the producer cells. New producer cells can be generated by infecting DF1 cells with stocks from frozen culture supernatants collected from early passages following transfection.

Concentrating Viruses

Expand virus-producer cells into 5-10 15-cm dishes depending up the amount of virus needed.

When they are confluent, switch to DMEM/1% FBS, 20 ml/dish; grow overnight.

Collect supernatant. Remove cell debris by a low speed spin (3000 rpm,10 minutes, 4^0C).

Spin in a ultracentrifuge for 1.5 hr. at 26K (50,000 g), 4^oC.

Discard all but 1/100 of the supernatant. Resuspend the pellet by vortexing for 2 min at a medium speed.

Preparing RCAS containing DF-1 cells for injection into mice

On day of experiment, RCAS containing DF-1 cells where trypsinised from T75 flask and a cell count was carried out to determine the number of cells in the flask. The cells were then resuspended in an appropriate volume of DMEM (lacking antibiotics) so that 1µl contained 1x104 RCAS containing DF-1 cells. This virus preparation was then aliquoted into eppendorfs.